X-552-69-332
PREPRINT

NASA TM X-63809

NUMERICAL INTEGRATION ORBITS AND BROUWER AND MODIFIED BROUWER ORBITS

HANS G. HERTZ

AUGUST 1969

GSFC

GODDARD SPACE FLIGHT CENTER
GREENBELT, MARYLAND

X-552-69-332
Preprint

NUMERICAL INTEGRATION ORBITS AND BROUWER AND MODIFIED BROUWER ORBITS

Hans G. Hertz

August 1969

Goddard Space Flight Center
Greenbelt, Maryland

PRECEDING PAGE BLANK NOT FILMED

ACKNOWLEDGMENT

I wish to acknowledge help received from D. Fisher, W. F. Cahill, F. Lerch, and H. Anderson.

NUMERICAL INTEGRATION ORBITS AND BROUWER AND MODIFIED BROUWER ORBITS

By

Hans G. Hertz

ABSTRACT

An orbit constructed by means of Brouwer's theory (AJ 64.378.1959) was compared with a numerical integration orbit started with the same initial conditions and values for the coefficients of the earth's potential.

Two sets of comparisons were made: one every 2 minutes for a 10-day arc, and one every 4 hours for a 60-day arc.

The differences 'Brouwer-Integration' were appreciable but could be greatly reduced by modifying the computation of the short-period terms and by applying second order short-period terms to Brouwer's expression for the semi-major axis as derived from Kozai's theory (AJ 67.446.1962). A further reduction was obtained by basing the mean motion of the mean anomaly on Kozai.

The differences 'Modified Brouwer-Integration' were represented as sums of polynomials of degree zero or one and Fourier series. These analyses resulted in further corrections to Brouwer. New comparisons after the application of these corrections which are empirical were made.

CONTENTS

NUMERICAL INTEGRATION ORBITS AND BROUWER AND MODIFIED BROUWER ORBITS

1. INTRODUCTION

There are two fundamentally different methods of arriving at the quantitative description of the motion of an artificial satellite, i.e., at finding the position of the satellite at any given time.

One approach is by using the method of numerical integration whereas an alternative is a representation of the motion by an analytical theory. The advantages and disadvantages of these two alternatives are well known and need not be discussed here. But I feel there has been less discussion of the relative accuracy of these two methods.

Also to the answer of this question two approaches may be considered.

A set of observations could be represented by an orbit obtained by a numerical integration with subsequent differential correction and, alternately, by an orbit derived from an analytical theory with an adjustment of the parameters of the theory to the observations included. The accuracy of the representation of the observations by the two orbits could then be compared. Because of errors of observations some theoretical shortcomings in either orbit may not always be easily recognizable.

This criticism would not apply to the second approach which is the one selected here and which has, however, shortcomings of its own to be mentioned below.

In view of the 'highest accuracy' of the numerical integration since it is subject to fewer approximations and inaccuracies than a general theory when carried out with a suitable interval a numerical integration orbit constructed with a certain set of initial conditions and a set of values for the coefficients of the earth's potential will be taken as a 'standard orbit.' An orbit will then be constructed with the help of a specific analytical theory, namely Brouwer's theory (Brouwer 1959) corresponding to the same initial conditions and the same values of the earth's potential as used in the numerical integration orbit. The deviation of the Brouwer orbit from the numerical integration orbit, the standard orbit, then gives a measure of the accuracy of the Brouwer orbit with the numerical integration as standard. The disadvantage of this method is that it is not obvious whether any discrepancies which might show up are due to errors in the Brouwer theory or in the numerical integration or in both. Additional tests will be necessary to reduce or increase the probability for one or the other possibility.

It will be seen that the results of the comparison may be varied by using modifications of the Brouwer theory.

2. MATHEMATICAL MODELS

As indicated in the introduction two mathematical models to represent satellite motion will be used in this investigation.

The first model is a numerical integration. It is carried out by means of a computer program using the Cowell scheme. The nucleus of the program has been designed by Juergensmeyer (1962) but I have made many peripheral modifications and additions which, however, do not affect the mathematical model.

The second model is based on the Brouwer theory (Brouwer 1959) which computes secular terms to the second order and periodic terms to the first order. A program to compute satellite positions according to Brouwer has been assembled by Repass and Chaplick (1964). I have again modified this program (Hertz 1969). The modified program allows the computation of satellite positions according to Brouwer as published by him with optional modifications and options to be included or excluded. Details as to the modifications and options have been described (Hertz 1969) but will be briefly stated here.

The long-period terms can be omitted or included. The same applies to the short-period terms. If they are to be included they may be either computed from the secular portions e'', I'' as suggested by Brouwer or they may be computed from the long-period portions e', I' as would be more accurate on theoretical grounds. The lowest order terms in a neglected by Brouwer are the second-order short-period terms there being no long-period terms in a. Those short-period terms may affect the mean motion of the mean anomaly and thus the mean anomaly itself. The program has an option to include them. They are based on expressions given by Kozai (1962) in his second order theory. If desired, the mean motion of the mean anomaly may be computed according to Brouwer or a reduction may be added which would bring it closer to the value based on the Kozai theory. Finally, specified Fourier series may be added to the osculating values of the Keplerian elements $a, e, I, \Omega, \omega, M$ at each data point before being used to compute a position-velocity vector for the data point. These Fourier series will be referred to as supplementary perturbations.

Other options not being used need not be discussed here. The expression for the final value at a time t of an element σ for use in computing the satellite's position and velocity is of the form

$$\sigma = \sigma_0 + \delta_p \sigma + \delta_s \sigma$$

where σ_0 is the secular portion, $\delta_p \sigma$ the periodic portion, and $\delta_s \sigma$ the value of the sum of the optional supplementary perturbations. In case of $\sigma =$ a, e, or I the secular portions are constants and in the case of $\sigma = \Omega$, ω, or M they are linear functions of the time with constant coefficients.

3. ORBITS CONSIDERED IN THIS INVESTIGATION

For the purposes of this investigation we understand an orbit to be a set of orbital data generated in a computer run for a certain set of data points constructed from a specified set of coefficients of the earth's potential, a specified mathematical model, and a specified position-velocity at a specified epoch.

The orbital data considered here for each data point are 12 quantities, viz the rectangular equatorial coordinates and velocity components, and the osculating elements at the data point:

a = semi-major axis

e = eccentricity

I = inclination

Ω = right ascension of the ascending node

(I and Ω: with respect to equator and equinox)

ω = argument of perigee

M = mean anomaly

Two orbits constructed with the same set of coefficients of the earth's potential, the same mathematical model, and the same position-velocity vector for the same epoch but with different sets of data points are considered to be different orbits but are, of course, expected to have the same values for the orbital data for any data point in common.

For all orbits considered here we use with one exception one of two sets of data points: one consists of all 2^m points from the epoch to 10^d from the epoch, i.e. 7201 points; the other consists of all 4^h points from the epoch to 60^d from the epoch, i.e. 361 points. In one case to be pointed out below the set of data points consists of all 40^m points from the epoch to 60^d from the epoch, i.e. 2161 points.

Since we are interested in different mathematical models and two sets of data points we must consider several orbits between which comparisons are to be made. Altogether we consider eighteen orbits of which six are numerical integration orbits and twelve Brouwer or modified Brouwer orbits. They are described in Tables 4 and 5 and the text below.

The same coefficients GM, J_2, J_3, J_4, J_5 of the earth's potential (see Hertz 1969, p. 1)

$$U = \frac{\mu}{r}\left[1 - \sum_{n=1}^{\infty} J_n \left(\frac{R}{r}\right)^n P_n(\sin\beta)\right], \qquad J_1 = 0,$$

namely those given in Table 1 are used for all orbits except for orbits 5, 6, 17, and 18. However, also in these orbits the same value of GM as in the other fourteen orbits is used. The four orbits 5, 6, 17, and 18 have been constructed for a special purpose discussed in section 8 which requires the use of different sets of values for J_3 and J_4.

All eighteen orbits use the same epoch and are constructed with the same position-velocity vector defined by the data in Table 2. Since in addition the same value of GM is used for all eighteen orbits the values of the osculating elements a, e, I, Ω, ω, M at the epoch are the same for all the orbits. The values are given in Table 3.

The fourteen orbits for which all coefficients in Table 1 are used consist of seven pairs, viz. orbits 1,2; 3,4; 7,8; 9,10; 11,12; 13,14; 15,16. Both orbits of each pair except in the case of orbits 1,2, and 3,4 have been constructed with the same mathematical model but one orbit uses the 2^m data points and runs for 10^d whereas the other one uses the 4^h points and runs for 60^d. Also orbits 1, 2, and 3,4 have been constructed with the same mathematical model but the 2^m and 40^m data points were used. Orbits 1 and 3 run for 10^d and orbits 2 and 4 for 60^d.

Table 4 describes the numerical integration orbits.

Orbits 1 and 2 use the same mathematical model since they are both 1^m integrations. They will be used as the 'standard orbits' for the 2^m and 4^h points and should, of course, be in complete agreement for any data points common to the 2^m and 4^h set.

Orbits 3 and 4 being $0^m.5$ integrations use the same mathematical model and will be used to test the reasonableness of the assumption to consider orbits 1 and 2 as standard orbits.

Orbits 5 and 6 are used for a special investigation in section 8.

From the coordinates and velocity components obtained in all numerical integration orbits values for the osculating elements a, e, I, Ω, ω, M were obtained.

Table 5 describes the Brouwer and modified Brouwer orbits used. They consist of the five pairs 7,8; 9,10; 11,12; 13,14; 15,16 to which the statements made above apply, and orbits 17 and 18 used in the discussion of section 8.

For orbits 7 and 8 the short-period terms have been computed with e", I" as suggested by Brouwer. No second-order short-period terms in a, no reduction to Kozai's mean motion, and no supplementary perturbations have been included. In view of what was said concerning this mode (Hertz 1969, p. 8) it would not be realistic to consider orbits with the short-period perturbations computed with e", I", with second-order short-period terms in a or the reduction to Kozai's mean motion included.

In orbits 9-18 the short-period terms have been computed with e', I' which is the correct way on theoretical grounds (Hertz 1969, pp. 7, 8).

In orbits 9-10 no second-order short period terms in a have been included, in orbits 11-18 they are present. The reduction to Kozai's mean motion has been omitted in orbits 9-12 and 17-18 and included in orbits 13-16. The amount is +0°000 000 268 727 per hour for orbits 13 and 14 and +0°000 000 268 730 per hour for orbits 15 and 16. Supplementary perturbations have been included only in orbits 15,16 which will be discussed in section 7.

Since the values of the osculating elements at the epoch are to be the values given in Table 3 it is these values which determine for each orbit and each σ the value of σ_0 at the epoch, i.e. the integration constant corresponding to σ, i.e. the mean value of σ. Its value is given by

$$\sigma_0 = \sigma_{osc} - (\delta_p \sigma)_{epoch} - (\delta_s \sigma)_{epoch}$$

where σ_{osc} is the appropriate value from Table 3 and where $(\delta_p \sigma)_{epoch}$ and $(\delta_s \sigma)_{epoch}$ are the values of $\delta_p \sigma$ and $\delta_s \sigma$ at the epoch. The value of σ_0 therefore changes with the mathematical model used. It therefore will have different values according to whether the short-period terms are computed with e", I" or e', I' or whether the 2nd order short-period terms in a are included or not. The inclusion or non-inclusion of the reduction to the Kozai mean motion, on the other hand, has no effect on σ_0. If the change from one mathematical model to another causes the change of $d\sigma$ in $(\delta_p \sigma)_{epoch} + (\delta_s \sigma)_{epoch}$ then the value of σ_0 will be changed by $-d\sigma$.

4. ORBIT COMPARISONS

An orbit comparison is understood in this investigation to be the formation of differences of the form

$$\Delta q = q_2(t) - q_1(t)$$

where q_1 and q_2 are the values of the same orbital quantity q in orbits O_1 and O_2 respectively for the same time or data point t.

These differences are formed for all data points common to both orbits. They are formed for the twelve quantities listed on p. 3 and are denoted by

$$\Delta x, \Delta y, \Delta z, \Delta \dot{x}, \Delta \dot{y}, \Delta \dot{z}, \Delta a, \Delta e, \Delta I, \Delta \Omega, \Delta \omega, \Delta M,$$

and are said to have been formed in the sense 'Orbit O_2 minus Orbit O_1.' They are functions of the time.

These orbit comparisons will be made for various pairs among the eighteen orbits. The results of some of the comparisons will be used for further analyses to be discussed in section 7.

For each orbit comparison made we will tabulate in Tables 6-9 twelve values one corresponding to each of the twelve quantities involved in the orbit comparison. If $q_1(t)$ and $q_2(t)$ are the values of q, where q is one of the twelve quantities, at time t in orbits O_1 and O_2 respectively then we list the maximum value of $|q_2(t) - q_1(t)|$ as t assumes all data points common to the two orbits. This value will be briefly called the maximum absolute value of the differences of q in the comparison of orbits O_1 and O_2 and will also be denoted by Δq.

Tables 6-9 contain the maximum absolute values of the differences of the twelve orbital quantities in all orbit comparisons. They will be discussed in sections 6 and 8.

5. THE NUMERICAL INTEGRATION ORBITS

The numerical integration orbits 1 and 2 are the standard orbits for the 2^m and 4^h data points. Since they have been constructed with the same mathematical model they should be in complete agreement for all data points in common for the two orbits. Thus orbits 1 and 2 should agree for all 4^h points in the first 10 days. The comparison, actually made for every 40^m, showed complete agreement except in the inclination where the largest discrepancy is about 10^{-12} degrees.

No analytical determination of probable or maximum errors of the coordinates at the data points in the two standard orbits 1 and 2 has been made. In order to obtain some idea of the accuracy of the coordinates and the other nine orbital quantities in these orbits they have been compared with orbits 3 and 4 which are orbits with a $0^m\!.5$ integration interval. The results are given in Table 6 and will be partially used in section 6. Graphs are presented in Figures 1a-f and 2a-f.

6. COMPARISON OF THE BROUWER AND MODIFIED BROUWER ORBITS WITH THE NUMERICAL INTEGRATION ORBITS

The results of the comparisons of the Brouwer and modified Brouwer orbits with the standard numerical integration orbits 1 and 2 are shown in Tables 7 and 8 and Figures 3-12. The results in Table 7 and Figures 3-7 concern the 2^m data points while those in Table 8 and Figures 8-12 refer to the 4^h data points.

The deviations of the unmodified Brouwer orbits 7 and 8 from the respective standard numerical integration orbits 1 and 2 are appreciable. They may be due to any one of the following four causes:

1. an appreciable truncation error in the numerical integration program used in this investigation
2. other types of errors in the numerical integration program
3. an appreciable truncation error in the Brouwer theory
4. errors in the compu‿ r program implementing the Brouwer theory and used in this investigation.

Since the values given in Tables 7 and 8 for orbits 7 and 8 are very much larger than the maximum values of the differences between the $1^m\!.0$ and $0^m\!.5$ numerical integration orbits 1 and 3 and 2 and 4 given in Table 6 the first two of the possible causes for the discrepancies appear to be less likely than the other two although they are not completely ruled out. No effort will be presented in this paper to determine the actual cause of the discrepancies. However, in section 7 we will consider the implications of the third cause.

It is very puzzling that the maximum deviations from the standard orbits 1 and 2 become larger as the computation of the short-period terms with e", I" is replaced by that with e', I' although the latter mode appears to be more preferable on theoretical grounds (Hertz, 1969, pp. 7, 8). No explanation can be offered here.

However, if the computation of the short-period terms with e', I' is adopted then the introduction of the second-order short-period terms in a greatly reduces the discrepancies, i.e. deviations from the standard orbits 1 and 2 in case of most of the twelve orbital variables. A further reduction is observed if the reduction to Kozai's value for the mean motion of the mean anomaly is included, at least if 60 days are considered. Finally, an additional reduction except in the case of the eccentricity for the 60^d run is achieved if the empirical orbits 15 and 16 to be discussed in section 7 are used. The slight increase in case of the eccentricity does not seem to be significant.

7. ANALYSIS OF THE DEVIATIONS OF ORBIT 14 FROM ORBIT 2

Although we are not deciding which of the four causes stated on p. 7 are actually responsible for the deviations of orbit 8 from orbit 2 we shall investigate what the implication would be if the actual cause is No. 3 listed.

The differences between these two orbits and also those between orbits 14 and 2 would then be expected to be Fourier series in case of a, e, I and the sum of a linear function of the time and a Fourier series in case of Ω, ω, and M. The arguments in these Fourier series would be linear combinations with integral coefficients of M and ω where M and ω are the secular portions of M and ω as obtained in the modified Brouwer orbit 14. If such Fourier series and sums of linear functions of the time and Fourier series would be applied to orbit 14 with the proper signs we would expect to obtain an orbit which would be much closer to orbit 2 than orbit 14 and orbit 8 are.

An attempt was made to find the stated representations for the differences between orbits 2 and 14. For this purpose a computer program which cannot be described in detail here has been used. This program has the following capabilities:

The values of a function of a single variable t given for a set of equidistant values of t are represented by the sum of a polynomial in t of specified degree and a Fourier series. The arguments are linear functions of t. The program determines the number of arguments to be used, the coefficient λ of t for each argument and the coefficients of the terms $\cos \lambda t$ and $\sin \lambda t$ the presence of which are implied by the selection of the value λ by the program. The λ's will be called the free frequencies in the analysis. If desired the function can be assumed also to have Fourier terms with specified or prescribed frequencies. The program will determine the coefficients of the associated cosine and sine terms.

For the investigation on hand there would be required six analyses: one each for the differences of a, e, I, Ω, ω, M in orbits 2 and 14 for every 4^h from the epoch to 60^d after the epoch. Ideally, the frequencies of all arguments of the form $iM + j\omega$ where i, j assume all combinations of integers which could reasonably be expected, would be taken as prescribed frequencies. However, the program allows the use of only twelve prescribed frequencies, which would not always provide enough frequencies since it was not a priori known which frequencies would actually occur. The difficulty was circumvented in the following way: in a first iteration only the frequencies $\dot{\omega}$, $2\dot{\omega}$, . . . , $6\dot{\omega}$ were prescribed since they were expected to belong to important long-period arguments on theoretical grounds. If λ is any free frequency found then a term with $\cos\lambda t$ or $\sin\lambda t$ has at the points $t = m\Delta t$* the same values as the term $\cos\beta t$ or $\sin\beta t$ with the same coefficients and with $\beta = \lambda + 2\pi k/\Delta t$, k being an integer. In other words, the actual frequency of the term could be $\beta = \lambda + 2\pi k/\Delta t$ instead of λ with some integral value of k which cannot be determined from the data. But in all cases a reasonably small integer k could be found such that β is close to an integral multiple of $\dot{M}$. Therefore, since $\dot{\omega}$ is small compared with $\dot{M}$ two integers i and j can be found such that

$$|\beta - (i\dot{M} + j\dot{\omega})| < \frac{1}{2}|\dot{\omega}|$$

The analysis now was repeated with introducing prescribed frequencies $i\dot{M} + j\dot{\omega}$ corresponding to each free frequency. Because of differences up to $(1/2)|\dot{\omega}|$ between the free and corresponding prescribed frequencies slightly different coefficients might result in the new analysis. The new analysis might generate new free frequencies. The procedure was repeated until no more free frequencies arose. Seldom more than twelve prescribed frequencies were required. If it happened it was possible to drop one or two frequencies $j\dot{\omega}$ with small coefficients to accommodate the extra frequencies. In view of the higher level iteration procedure described below this is not expected to introduce any serious error.

The results of such analyses led to Fourier series or sums of linear functions of the time and Fourier series which, when applied with the proper signs to a, e, I, Ω, ω, M of orbit 14 would give an orbit which might be expected to be closer to orbit 2 than orbit 14 is. A slight modification must be mentioned. The constant terms obtained in the analyses were not used. The equation on p. 5 shows that changes within certain bounds in the constant terms of the supplementary perturbations have no effect on the values of the supplementary perturbations for any t since such changes are accompanied by opposite changes in the values of the corresponding mean elements. Therefore the constant terms in the supplementary perturbations for Ω, ω, M have been put equal to 0. In case of a, e, I they may uniquely be determined in such a way that the changes in the motions of Ω, ω, M as required by the analyses may be realized.

* m = 0, 1, ...

With the new orbit thus obtained we repeat the cycle. Altogether four such cycles were passed through. The final orbit, orbit 16, was considered to be as close as possible to orbit 2. For reason of shortage of time no further cycles were carried out but it is believed that orbits resulting from additional cycles would change the deviations from orbit 2 only insignificantly. Orbit 15 is then the orbit computed with the same position-velocity vector and the same supplementary perturbations for the 2^m data points. It was already stated on page 8 that the deviations of orbits 15 and 16 from orbits 1 and 2 were smaller than those for orbits 13 and 14, and, of course, smaller than for orbits 7 and 8.

Table 10 shows the supplementary perturbations which must be applied to both orbits 13 and 14 in order to obtain orbits 15 and 16. To obtain orbit 16 from orbit 8 we have to replace the computation of the short-period terms with e'', I'' by that with e', I', add the second-order short-period terms in a, the reduction to Kozai's mean motion, and the supplementary perturbations of Table 10. The total of these reductions then would represent the truncation error of the Brouwer theory if it were actually the cause of the deviations of the unmodified Brouwer orbit 8 from the numerical integration orbit 2.

The hypothesis could be tested if a more accurate theory such as Kozai's theory (Kozai 1962) would be compared with a numerical integration orbit as has been done here.

We shall conclude this section with two remarks.

The supplementary perturbations in Table 10 for a contain terms with arguments $j\dot{\omega}$, i.e. long-period terms. Such terms are not present in Brouwer's and Kozai's theories. It has not been determined whether there could be higher order terms of this type. Possibly the analyses should have been repeated without using $\dot{\omega}$, $2\dot{\omega}$, . . . $6\dot{\omega}$ as prescribed frequencies.

Orbit 16 is closer to the integration than orbit 8. Orbit 14 is also closer but not as close as orbit 16. But orbit 14 can be constructed by 'analytical' means whereas orbit 16 is an empirical orbit and moreover requires the knowledge of the numerical integration orbit. The advantages of analytical orbits would be defeated if one were to try to improve on unmodified Brouwer orbits by applying all corrections which in our case have led to orbit 16. If we want to adhere strictly to analytical processes we can short of introducing a more accurate theory improve the unmodified Brouwer theory by:

1. Replace the computation of the short-period terms with e'', I'' by the computation with e', I'
2. add the second-order short-period terms in "a"
3. add the reduction to Kozai's mean motion of the mean anomaly.

It is hoped to present a more through interpretation of the orbit comparisons in a future report.

8. COMPARISON OF ORBITS WITH SOME ZERO HARMONICS

The numerical integration orbits 5 and 6 are identical with numerical integration orbit 2 except that in orbit 5 J_4 and in orbit 6 J_3 and J_4 have been put equal to zero. The modified Brouwer orbits 17 and 18 are related similarly to modified Brouwer orbit 12. The results of the comparison of orbits 17 and 18 with orbits 5 and 6 are shown in Table 9. These values should be compared with the results of the comparison of orbits 12 and 2 shown in Table 8. The elimination of non-zero values of J_4 and J_3 brought some reductions in the differences 'Brouwer-Integration' but also some increases. It is thus hard to say whether the discrepancies for orbit 12 are due to J_2 or the higher harmonics.

REFERENCES

Brouwer, Dirk, Solution of the Problem of Artificial Satellite Theory Without Drag, AJ (Astronomical Journal) 64,378. 1959

Hertz, Hans G., A Computer Program Version of the Brouwer Orbital Theory with Optional Modifications, August 1969, GSFC X-552-69-338

Juergensmeyer, Charles H., A Double Precision Cowell Integration Program, July 1962, GSFC X-542-63-139

Kozai, Yoshihide, Second-Order Solution of Artificial Satellite Theory Without Air Drag, AJ (Astronomical Journal) 67,446. 1962

Repass, G. D., Chaplick, R. G., A Mutual Visibility Computer Program for Communication Satellites, May 1965, GSFC X-547-65-222

Table 1
Coefficients of the Earth's Potential and Equatorial Radius of the Earth Used in Orbits 1-18*

GM	$3.98603200 \cdot 10^5$ km^3 $seconds^{-2}$
J_2	$+1.0823 \cdot 10^{-3}$
J_3	$-2.3 \cdot 10^{-6}$
J_4	$-1.8 \cdot 10^{-6}$
J_5	0.0
R	6378.165 km

*in orbits 5, 6, 17, 18 $J_4 = 0$
in orbits 6, 18 $J_3 = 0$

Table 2
Epoch and Position-Velocity Vectors Used for all Orbits

Epoch 1966 November 29 $0^h 00^m 00^s$ ET

Position-velocity vector with respect to the equator system

$$\left.\begin{array}{r} +4\ 529\ 467.000000 \\ +5\ 724\ 243.000000 \\ -3\ 803\ 180.000000 \end{array}\right\}\ \text{meters}$$

$$\left.\begin{array}{r} -18\ 438\ 869.000000 \\ +14\ 616\ 528.000000 \\ -\ 8\ 988\ 297.000000 \end{array}\right\}\ \text{meters per hour}$$

Table 3
Osculating Elements at Epoch
for all Orbits

Epoch 1966 November 29 $0^h00^m00^s$ ET

a	8 321 016.341040682	meters
e	0.1659571587412389	
I	32°8537259317278	
Ω	177°8618891421345	
ω	142°5592123598749	
M	76°7687107985003	

In the actual runs there may be values different from those given here by a few units of the last place given.

Table 4
Numerical Integration Orbits

Epoch and position-velocity vector at epoch from Table 2

Ser. No.	Coefficients of the Earth's Potential	Integration Interval	Total Length	Ephemeris Interval
1	Table 1	1^m0	10^d	2^m
2	Table 1	1.0	60	40
3	Table 1	0.5	10	2
4	Table 1	0.5	60	40
5	GM, J_2, J_3 from Table 1 $J_4 = J_5 = 0$	1.0	60	240
6	GM, J_2 from Table 1 $J_3 = J_4 = J_5 = 0$	1.0	60	240

Table 5

Brouwer and Modified Brouwer Orbits

Epoch and position-velocity vector at epoch from Table 2

Ser. No.	Mode of Comput. of Short-per. terms	2^{nd} order Short-per. terms in a included	Reduction to Kozai's mean motion included	Suppl. pert. included	Coeff. of earth's potential	Total Length	Ephem. Int.
7	e'', I''	no	no	no	Table 1	10^d	2^m
8	e'', I''	no	no	no	Table 1	60	240
9	e', I'	no	no	no	Table 1	10	2
10	e', I'	no	no	no	Table 1	60	240
11	e', I'	yes	no	no	Table 1	10	2
12	e', I'	yes	no	no	Table 1	60	240
13	e', I'	yes	yes	no	Table 1	10	2
14	e', I'	yes	yes	no	Table 1	60	240
15	e', I'	yes	yes	yes	Table 1	10	2
16	e', I'	yes	yes	yes	Table 1	60	240
17	e', I'	yes	no	no	GM, J_2, J_3 from Table 1 $J_4 = J_5 = 0$	60	240
18	e', I'	yes	no	no	GM, J_2 from Table 1 $J_3 = J_4 = J_5 = 0$	60	240

Table 6
Maximum Absolute Values of Differences in Comparison of the $0^m\!.5$ numerical integration orbits (orbits 3 and 4) with the $1^m\!.0$ numerical integration orbits (orbits 1 and 2)

		Orbit 3 − Orbit 1	Orbit 4 − Orbit 2
Δx	in meters	0.09	2.88
Δy	in meters	0.09	2.49
Δz	in meters	0.06	1.45
$\Delta \dot{x}$	in meters per hour	0.4	8.9
$\Delta \dot{y}$	in meters per hour	0.3	9.4
$\Delta \dot{z}$	in meters per hour	0.2	6.0
Δa	in meters	0.04	0.04
Δe	in units of 10^{-7}	0.04	0.04
ΔI	in units of $0^\circ\!.00001$	0.000	0.001
$\Delta \Omega$	in units of $0^\circ\!.00001$	0.000	0.006
$\Delta \omega$	in units of $0^\circ\!.00001$	0.089	0.089
ΔM	in units of $0^\circ\!.00001$	0.134	1.817
		2^m points	40^m points

Table 7

Maximum Absolute Values of Differences in Comparison of Brouwer and Modified Brouwer Orbits with 1^m Numerical Integration Orbit using 2^m Points

Orbit n – Orbit 1

n		7	9	11	13	15
Mode of comp. of short-per. terms		e'',I''	e',I'	e',I'	e',I'	e',I'
inclusion of 2nd order short-per. terms in a		no	no	yes	yes	yes
inclusion of reduction to Kozai mean motion		no	no	no	yes	yes
inclusion of suppl. pert.		no	no	no	no	yes
Δx	in meters	4148.5	7023.0	38.6	30.3	24.4
Δy	in meters	4374.3	7382.9	70.6	60.9	31.3
Δz	in meters	2650.6	4481.5	45.7	41.4	22.0
$\Delta \dot{x}$	in meters per hour	16776	28330	197	160	90
$\Delta \dot{y}$	in meters per hour	14051	23790	124	111	52
$\Delta \dot{z}$	in meters per hour	8156	13766	149	132	28
Δa	in meters	25.3	21.9	0.1	0.1	0.1
Δe	in units of 10^{-7}	29	27	29	29	22
ΔI	in units of $0.^\circ 00001$	11	11	11	11	1
$\Delta \Omega$	in units of $0.^\circ 00001$	36	50	37	37	7
$\Delta \omega$	in units of $0.^\circ 00001$	128	143	144	144	35
ΔM	in units of $0.^\circ 00001$	2966	4964	127	127	39

Table 8

Maximum Absolute Values of Differences in Comparison of Brouwer and Modified Brouwer Orbits with 1^m Numerical Integration Orbit using 4^h Points

Orbit n – Orbit 2

		8	10	12	14	16
Mode of comp. of short-per. terms		e'', I''	e', I'	e', I'	e', I'	e', I'
inclusion of 2nd order short-per. terms in a		no	no	yes	yes	yes
inclusion of reduction to Kozai mean motion		no	no	no	yes	yes
inclusion of suppl. pert.		no	no	no	no	yes
Δx	in meters	26840.3	45289.9	177.5	121.1	22.7
Δy	in meters	23378.1	39503.3	125.8	75.5	30.0
Δz	in meters	13869.7	23327.4	191.7	160.9	19.0
$\Delta \dot{x}$	in meters per hour	86391	145944	587	423	94
$\Delta \dot{y}$	in meters per hour	83850	141572	503	373	75
$\Delta \dot{z}$	in meters per hour	58325	98243	706	576	51
Δa	in meters	43.3	64.6	0.4	0.3	0.1
Δe	in units of 10^{-7}	63	86	30	30	32
ΔI	in units of $0\overset{\circ}{.}00001$	19	27	11	11	2
$\Delta \Omega$	in units of $0\overset{\circ}{.}00001$	209	260	153	153	8
$\Delta \omega$	in units of $0\overset{\circ}{.}00001$	387	503	213	213	33
ΔM	in units of $0\overset{\circ}{.}00001$	17284	29279	180	144	36

Table 9

Maximum Absolute Values of Differences in Comparison of Modified Brouwer Orbits and $1^m.0$ Numerical Integration Orbits with Some Zero Harmonics Using 4^h points.

Orbit m – Orbit n

Orbits m are modified Brouwer orbits with the short period terms computed with e', I' and second order short-period terms in a included. No reduction to Kozai's mean motion and no supplementary perturbations were included.

J_2 is taken from Table 1

	m	17	18
	n	5	6
		$J_4 = J_5 = 0$	$J_3 = J_4 = J_5 = 0$
Δx	in meters	212.6	124.5
Δy	in meters	176.2	101.7
Δz	in meters	150.8	109.3
$\Delta \dot{x}$	in meters per hour	676	378
$\Delta \dot{y}$	in meters per hour	597	391
$\Delta \dot{z}$	in meters per hour	590	370
Δa	in meters	0.3	0.2
Δe	in units of 10^{-7}	25	16
ΔI	in units of $0^\circ.00001$	10	4
$\Delta \Omega$	in units of $0^\circ.00001$	63	46
$\Delta \omega$	in units of $0^\circ.00001$	139	128
ΔM	in units of $0^\circ.00001$	213	114

Table 10

Supplementary Perturbations to be Applied to Orbits 13 and 14
Arguments are 0 at JD 2439488.5
Motions of arguments are of the form $i\dot{M} + j\dot{\omega}$, where $\dot{M}$ and $\dot{\omega}$ are secular motions of M and ω in orbit 13 or 14 respectively

No.	i j	Motion per hr.	Δa meters		$\Delta e \cdot 10^7$		$\Delta I \cdot 10^5$		$\Delta\Omega \cdot 10^5$		$\Delta\omega \cdot 10^5$		$\Delta M \cdot 10^5$	
									degrees					
			cos	sin	cos	sin	cos	sin	cos	sin	cos	sin	cos	sin
1	0 0	0°.00000	+0.0245	0.0000	-112.21	0.00	-13.459	0.000	0	0	0	0	0	0
2	0+1	+ 0.21915	+0.0039	-0.0013	+ 5.00	0.00	- 0.807	+0.094	+3	+1	-15	- 4	+10	+ 2
3	0+2	+ 0.43831	-0.0017	+0.0006	- 1.00	0.00	+ 0.024	+0.203	0	+2	+11	- 4	-10	+ 1
4	0+3	+ 0.65746	0.0000	0.0000	0.00	+1.00	- 0.043	-0.102	0	-1	- 2	+ 6	+ 1	- 4
5	0+4	+ 0.87662	0.0000	0.0000	+ 0.01	-0.45	+ 0.035	+0.053	0	+1	0	- 3	0	+ 2
6	0+5	+ 1.09577	0.0000	0.0000	0.00	0.00	- 0.026	-0.030	0	0	0	+ 2	0	- 1
7	0+6	+ 1.31492	0.0000	0.0000	0.00	0.00	+ 0.017	+0.015	0	0	0	- 1	0	+ 1
8	+1-2	+171.18854	0.0000	0.0000	0.00	0.00	0.000	0.000	0	0	+ 3	- 1	- 3	+ 1
9	+1-1	+171.40770	0.0000	0.0000	0.00	0.00	0.000	0.000	0	0	+ 6	- 7	- 6	+ 7
10	+1 0	+171.62685	+0.0877	+0.0220	- 10.00	-2.00	0.000	0.000	-1	+8	+ 7	-34	- 5	+25
11	+1+1	+171.84600	0.0000	0.0000	0.00	0.00	- 4.849	+1.581	0	+1	- 5	-14	- 1	- 3
12	+1+2	+172.06516	0.0000	0.0000	0.00	0.00	- 0.440	+0.560	-1	-1	+ 4	+ 3	- 3	- 3
13	+2 0	+343.25370	-0.0425	-0.0185	0.00	0.00	0.000	0.000	+1	-1	+ 9	-21	-10	+22
14	+2+1	+343.47285	0.0000	0.0000	0.00	0.00	+ 1.202	-0.164	0	0	+ 3	+29	- 3	-25
15	+2+2	+343.69201	-0.0095	+0.0111	0.00	0.00	- 1.129	+0.855	-1	-1	+ 4	+ 6	- 5	- 7
16	+2+3	+343.91116	0.0000	0.0000	0.00	0.00	+ 0.070	-0.230	0	0	0	0	0	0
17	+3 0	+514.88055	0.0000	0.0000	0.00	0.00	0.000	0.000	0	0	- 8	+12	+ 8	-12
18	+3+1	+515.09970	0.0000	0.0000	0.00	0.00	- 0.281	-0.028	0	0	0	-16	0	+14
19	+3+2	+515.31886	-0.0699	+0.0270	0.00	0.00	+ 1.336	-0.642	+1	+2	+ 5	+10	- 5	-10
20	+3+3	+515.53801	0.0000	0.0000	0.00	0.00	+ 0.489	-0.643	0	0	- 3	- 2	+ 3	+ 2
21	+4+1	+686.72655	0.0000	0.0000	0.00	0.00	+ 0.074	+0.011	0	0	0	0	0	0
22	+4+2	+686.94571	+0.0611	-0.0120	0.00	0.00	- 0.705	+0.205	0	0	0	0	0	0
23	+4+3	+687.16486	0.0000	0.0000	0.00	0.00	- 0.364	+0.338	0	0	0	0	0	0
24	+5+2	+858.57255	0.0000	0.0000	0.00	0.00	+ 0.254	-0.027	0	0	0	0	0	0

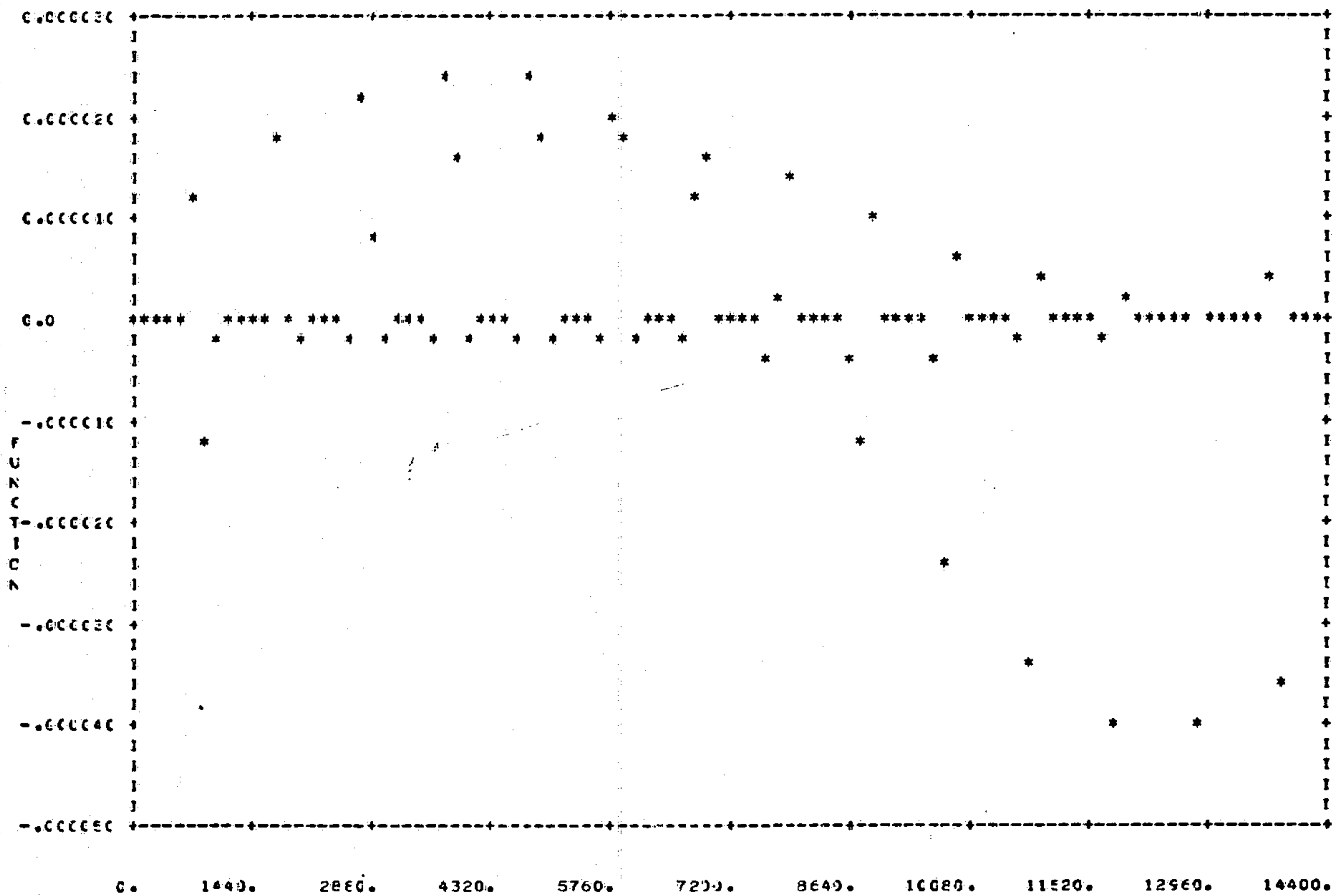

Figure 1a--Plot of Data from Comparison of Orbit 3 Minus Orbit 1 Semi Major Axis.

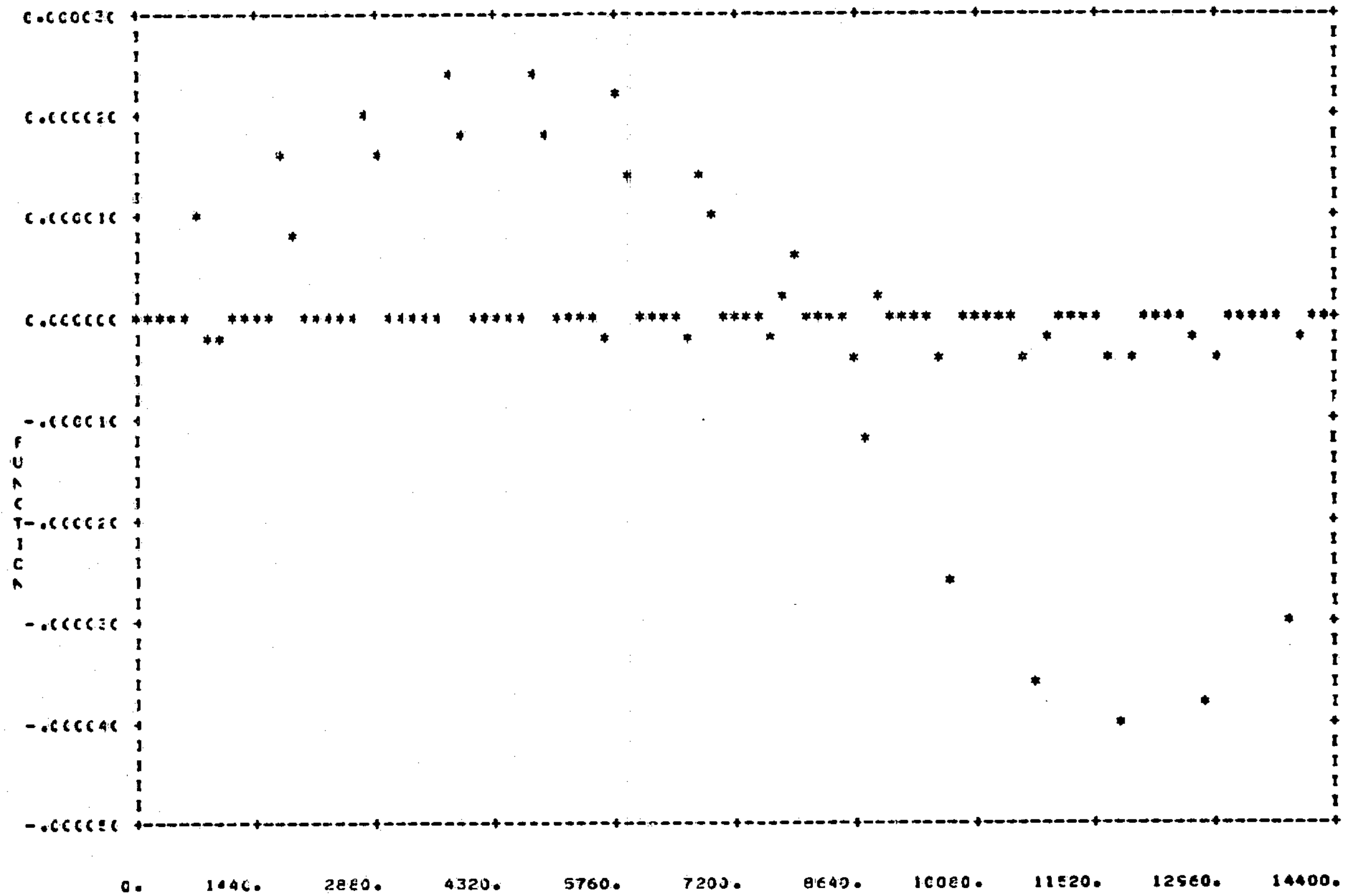

ORDINATES MULTIPLIED BY 10** 4 BEFORE PLOTTING
THE ABSCISSAE ARE MINUTES FROM THE EPOCH

Figure 1b–Plot of Data from Comparison of Orbit 3 Minus Orbit 1 Eccentricity.

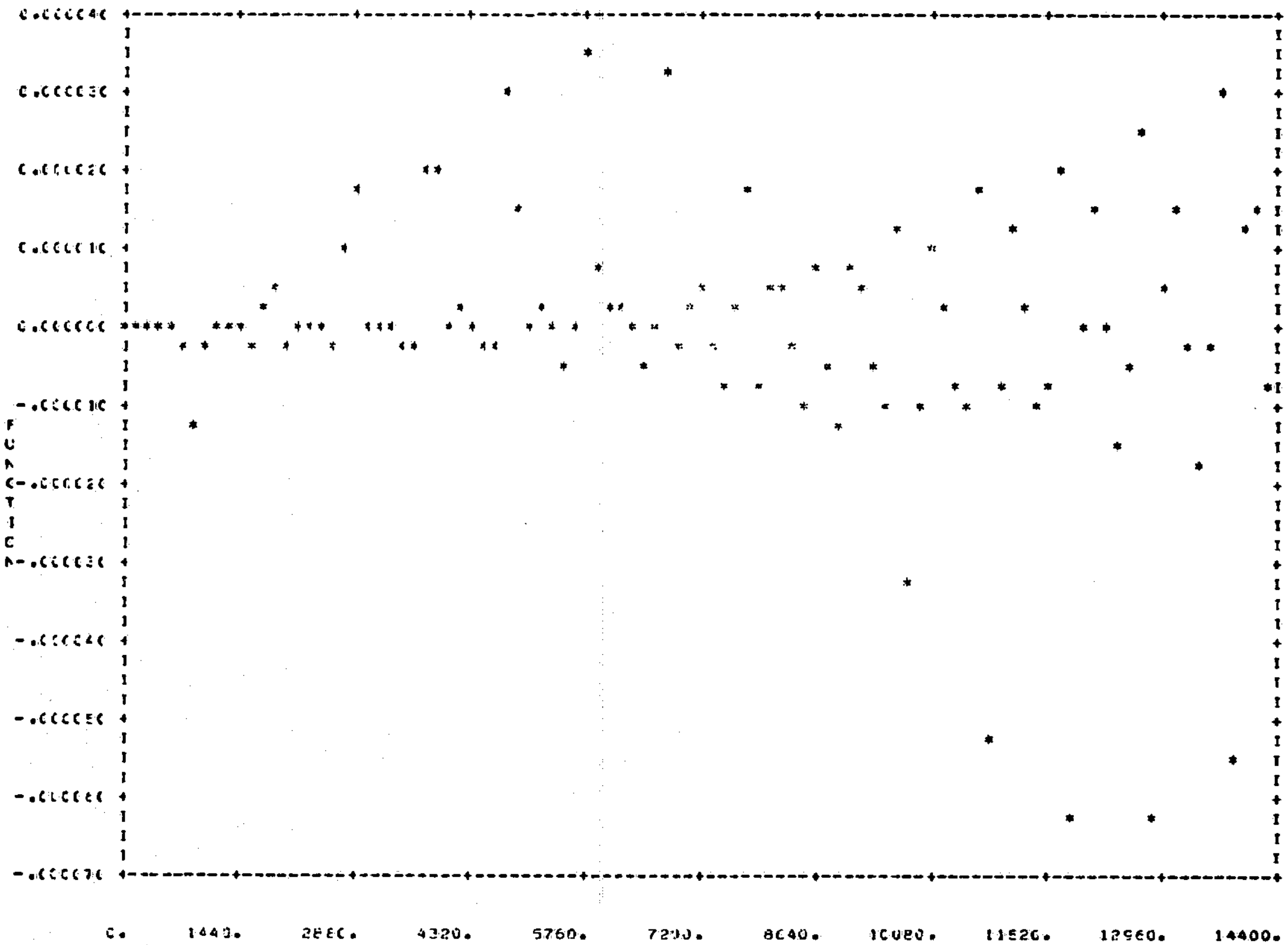

ORDINATES MULTIPLIED BY 10** 5 BEFORE PLOTTING
THE ABSCISSAS ARE MINUTES FROM THE EPOCH

Figure 1c–Plot of Data from Comparison of Orbit 3 Minus Orbit 1 Inclination.

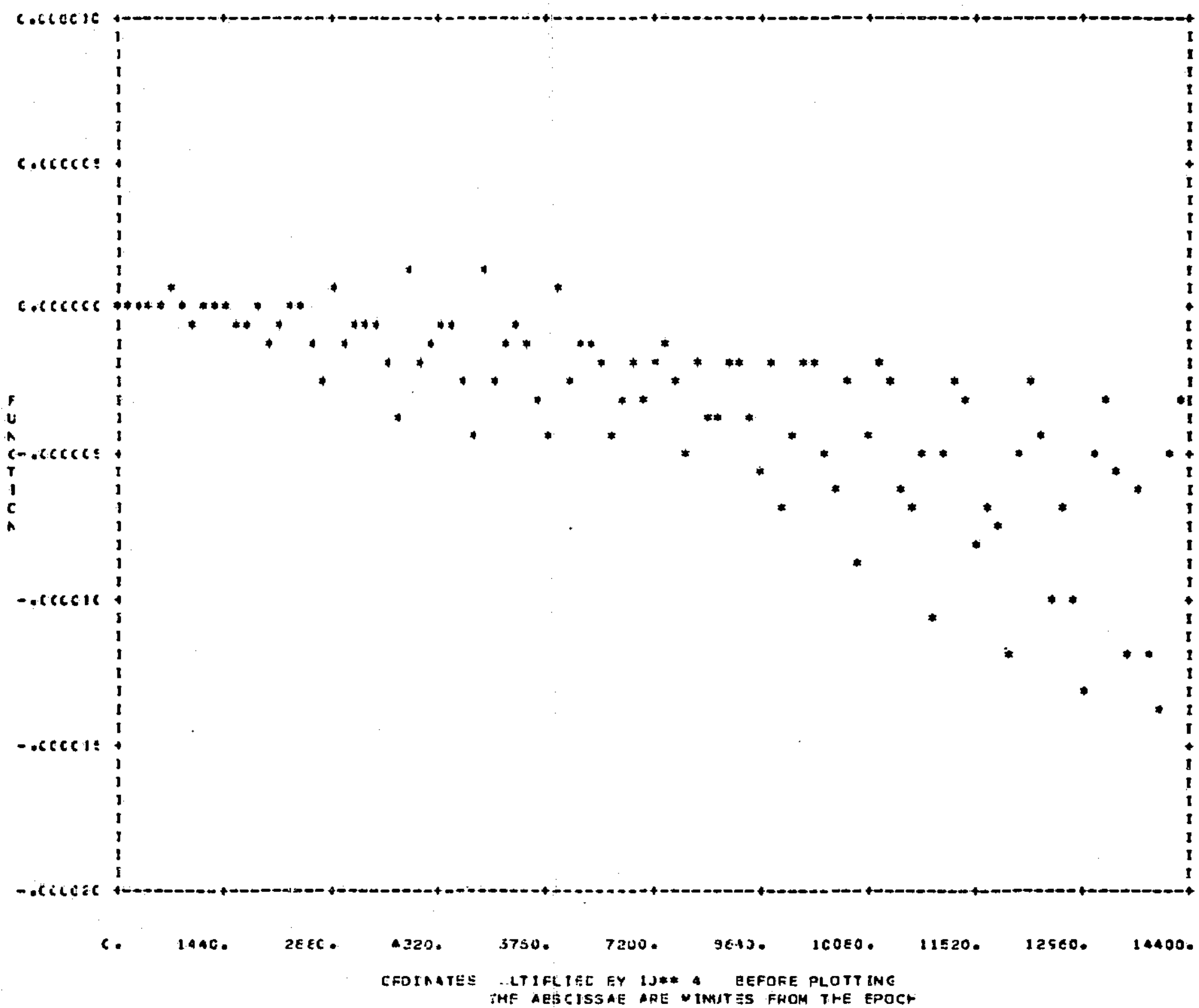

Figure 1d–Plot of Data from Comparison of Orbit 3 Minus Orbit 1 Right Ascension of Ascending Node.

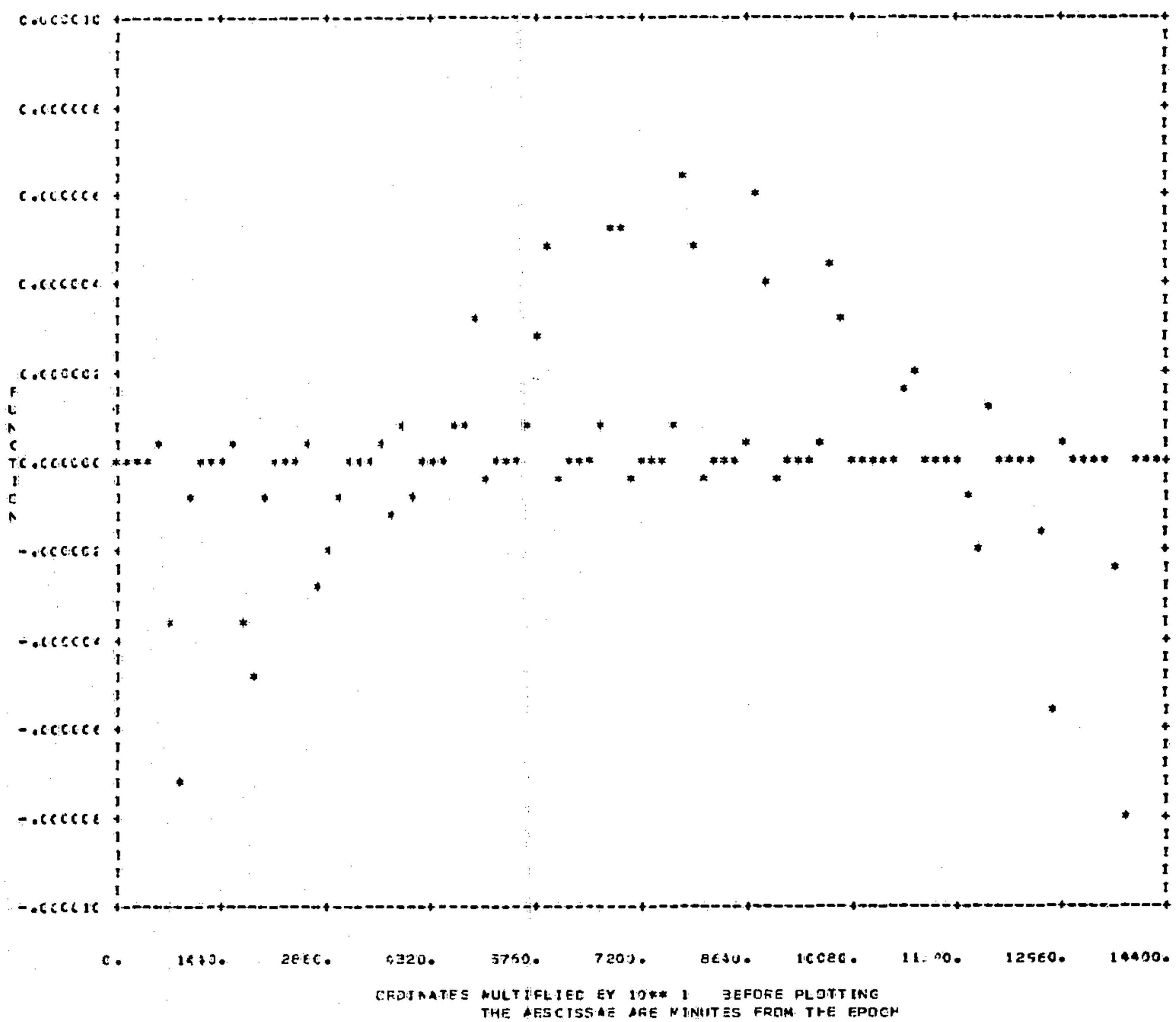

Figure 1e–Plot of Data from Comparison of Orbit 3 Minus Orbit 1 Argument of Perigee.

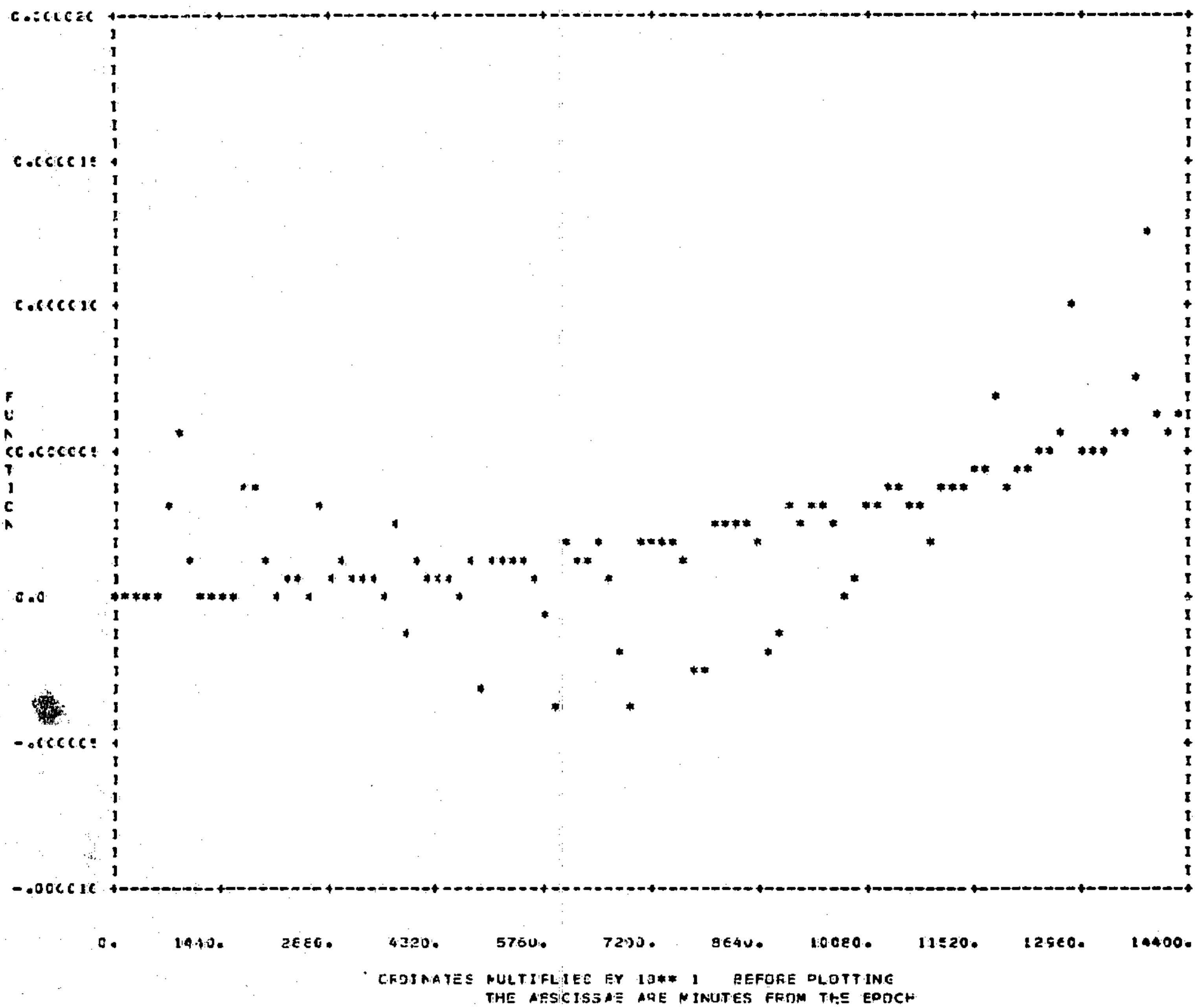

Figure 1f–Plot of Data from Comparison of Orbit 3 Minus Orbit 1 Mean Anomaly.

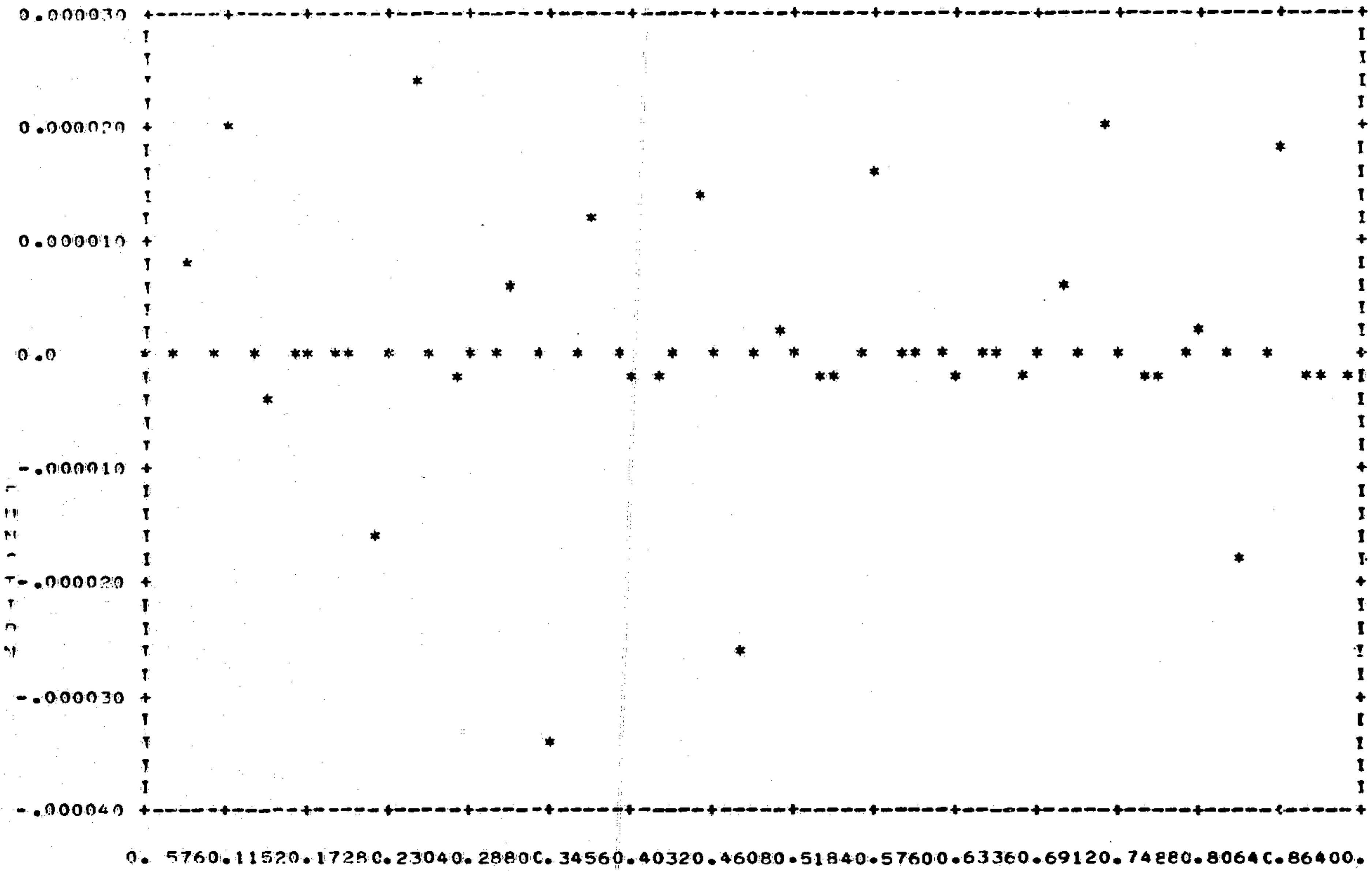

ORDINATES MULTIPLIED BY 10** 3 BEFORE PLOTTING
THE ABSCISSAE ARE MINUTES FROM THE EPOCH

Figure 2a–Plot of Data from Comparison of Orbit 4 Minus Orbit 2 Semi Major Axis.

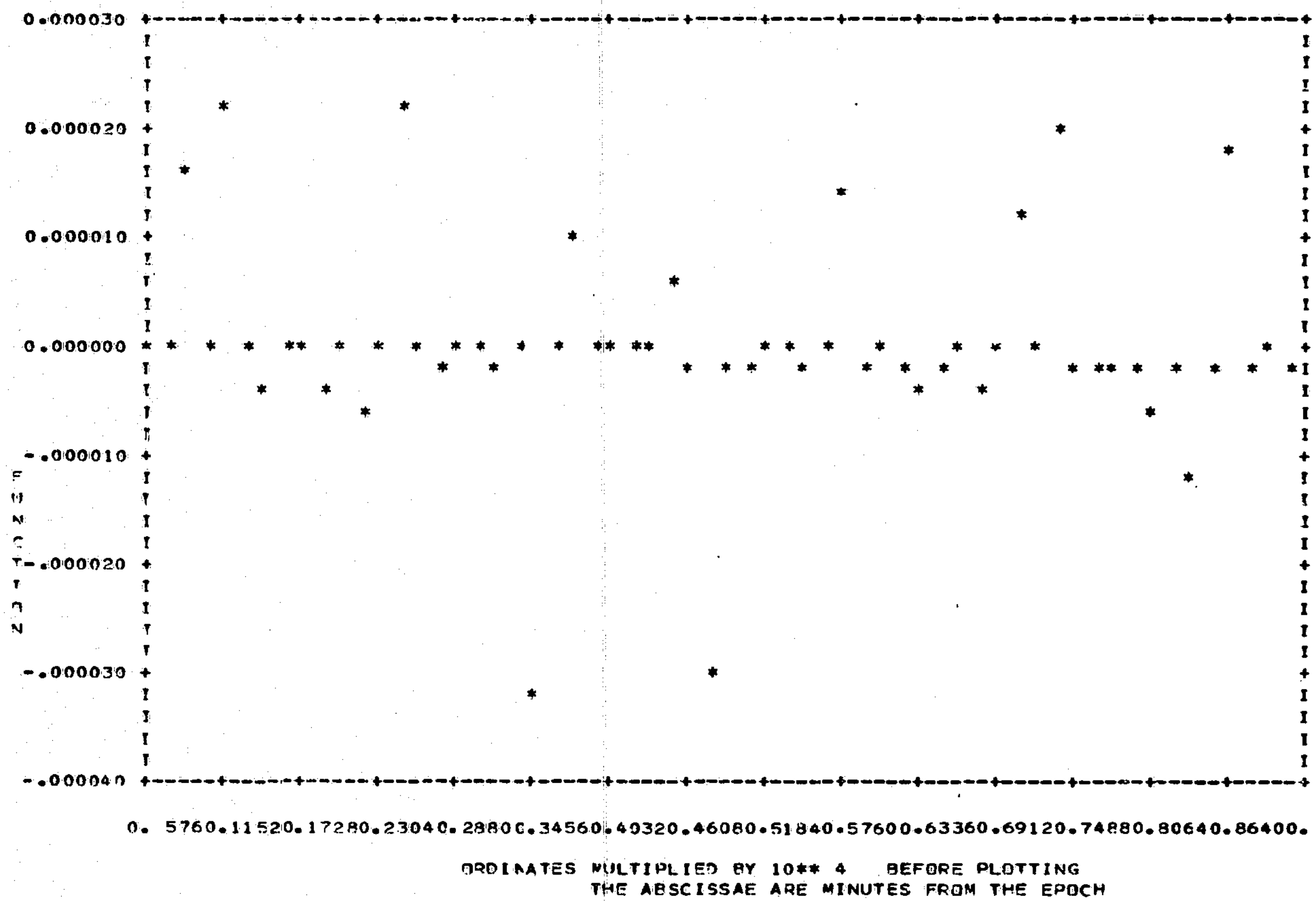

Figure 2b-Plot of Data from Comparison of Orbit 4 Minus Orbit 2 Eccentricity.

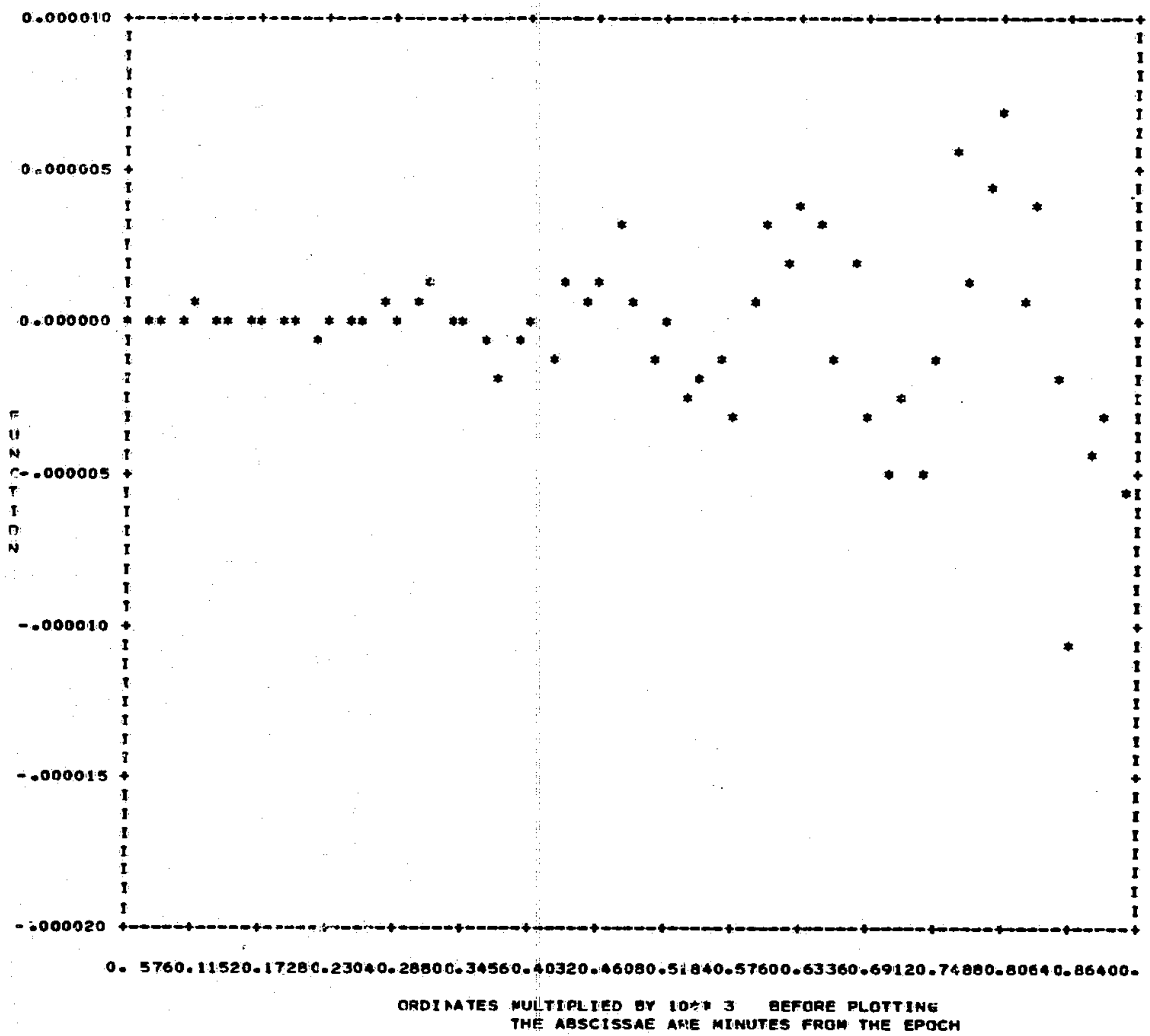

Figure 2c–Plot of Data from Comparison of Orbit 4 Minus Orbit 2 Inclination.

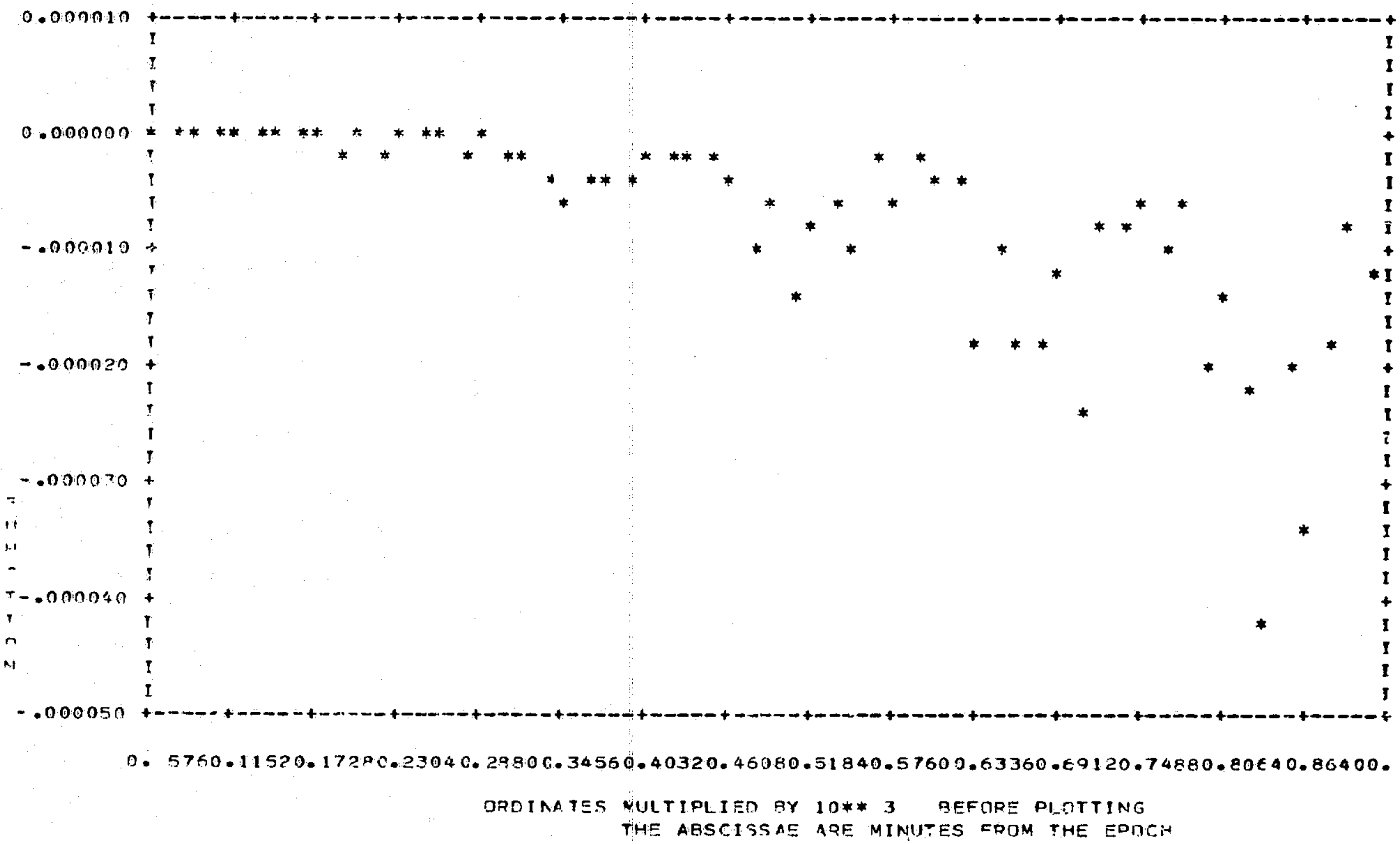

Figure 2d–Plot of Data from Comparison of Orbit 4 Minus Orbit 2 Right Ascension of Ascending Node.

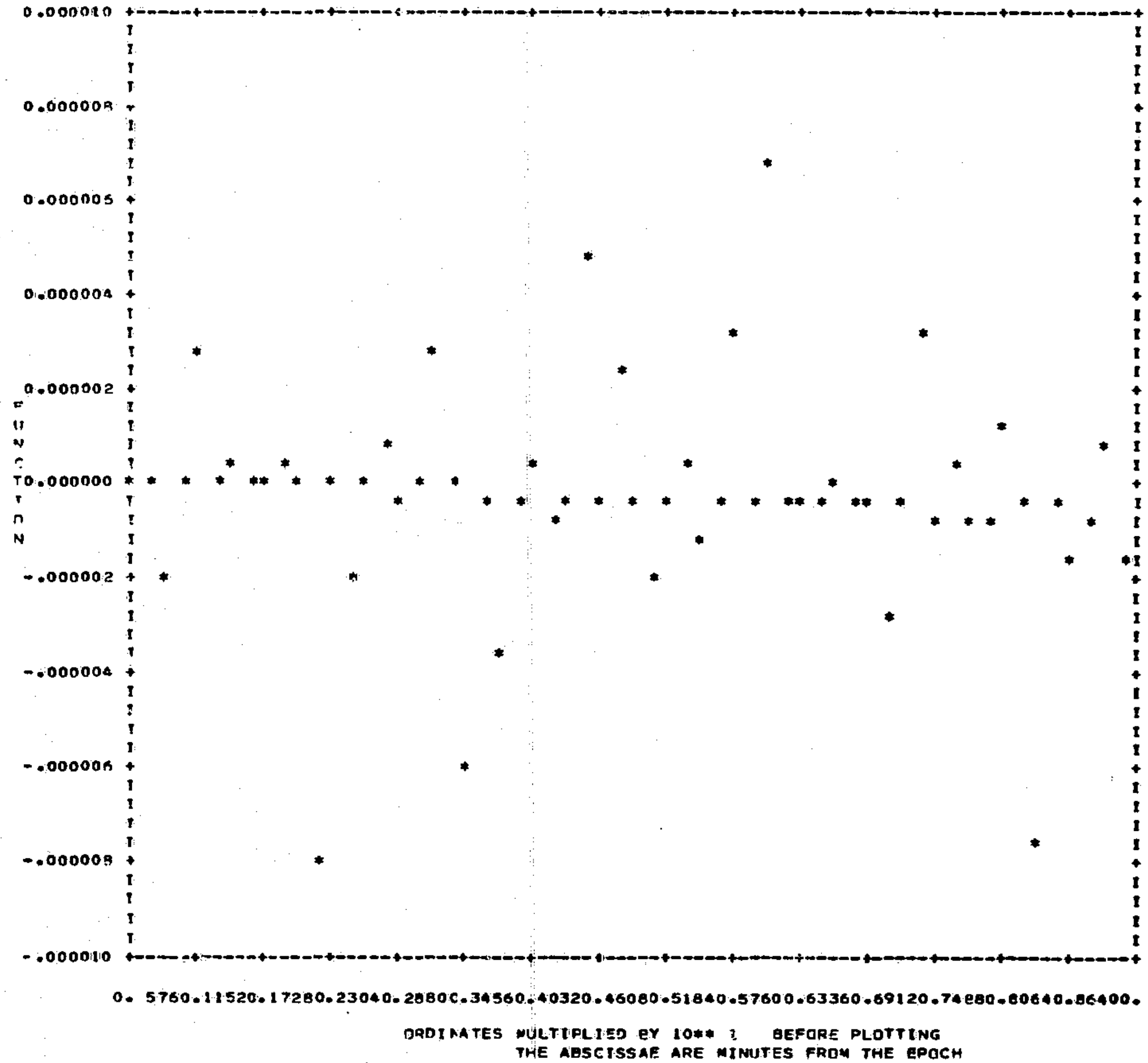

Figure 2e-Plot of Data from Comparison of Orbit 4 Minus Orbit 2 Argument of Perigee.

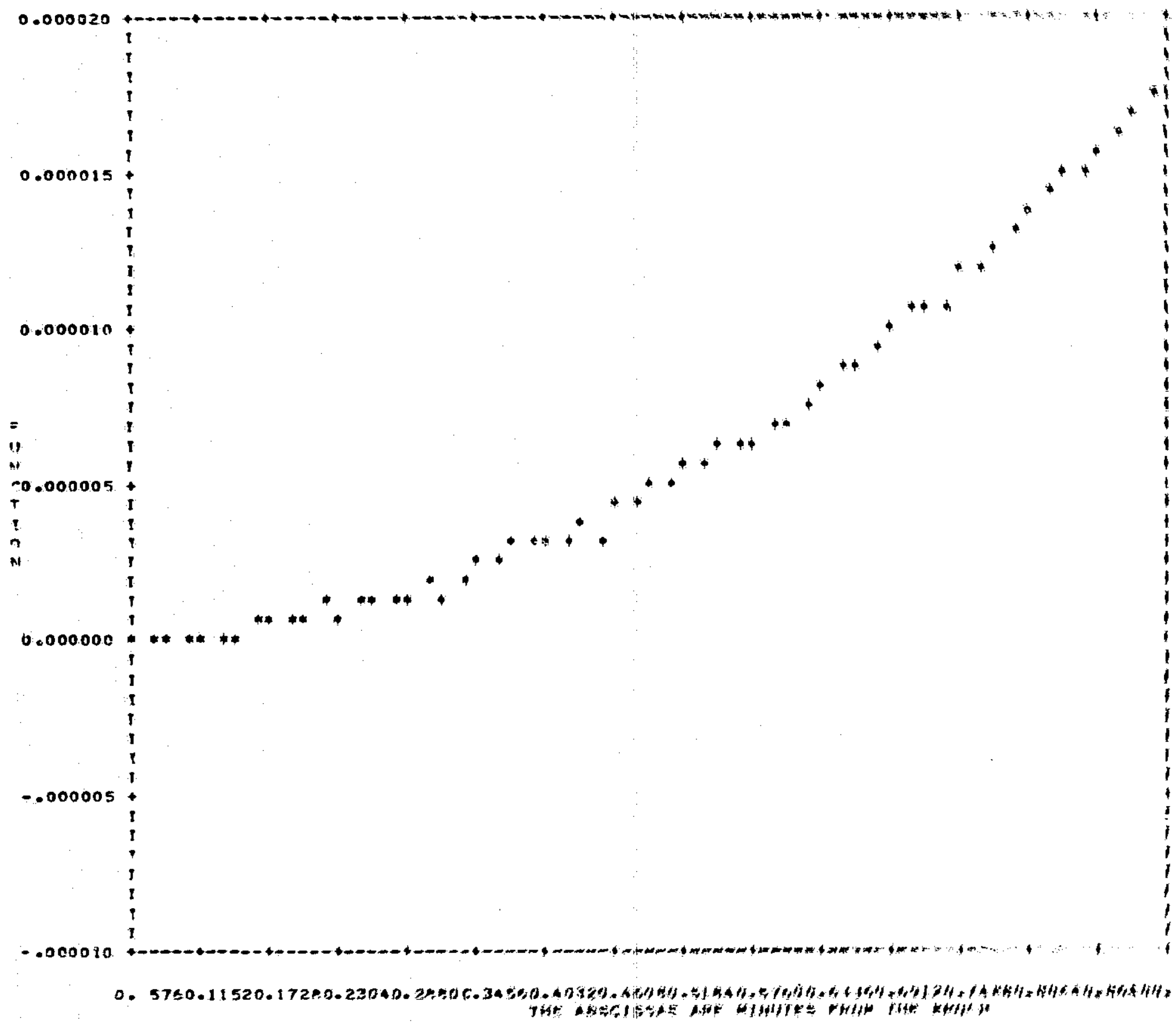

Figure 2f-Plot of Data from Comparison of Orbit 4 Minus Orbit 2 Mean Anomaly

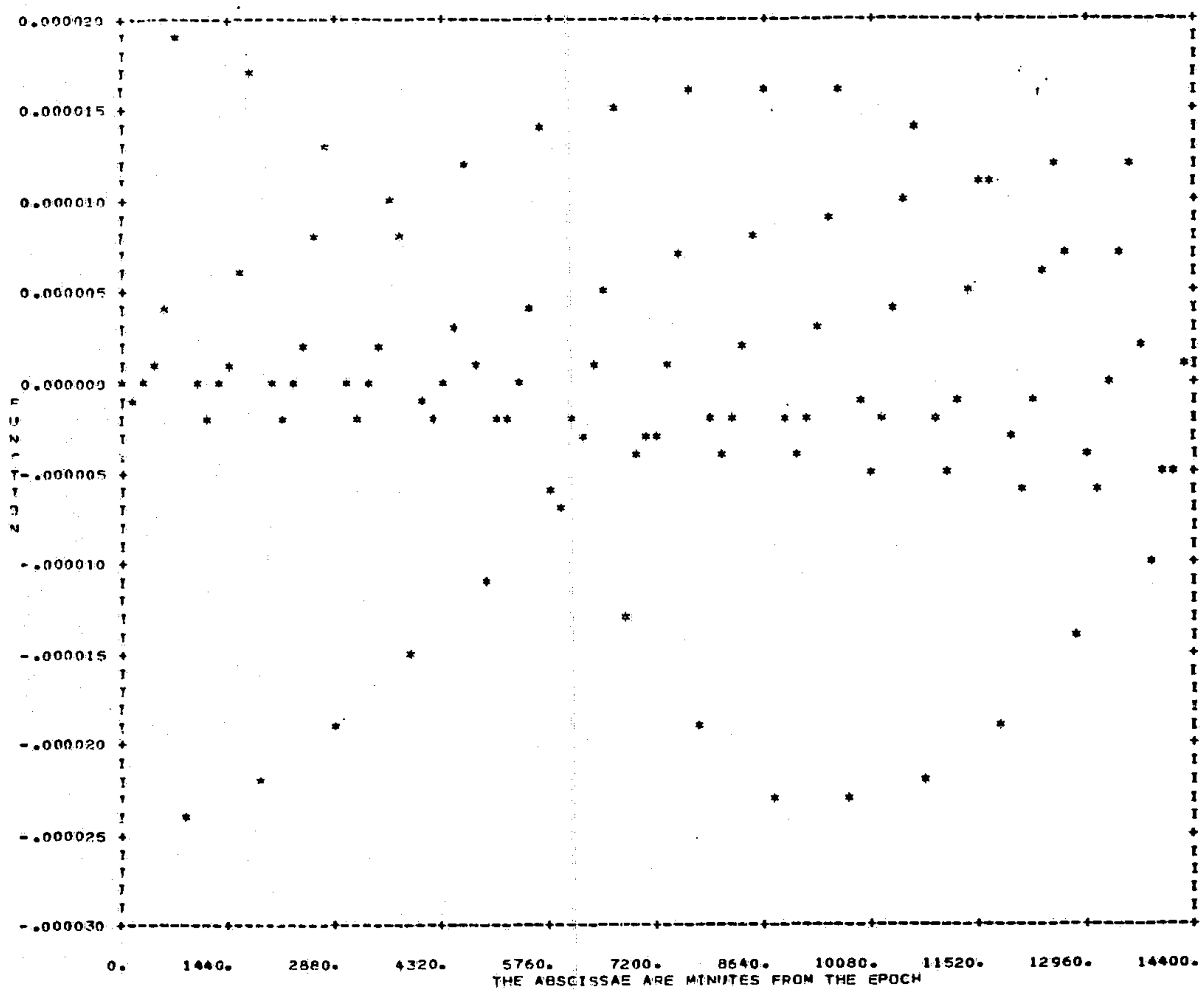

Figure 3a–Plot of Data from Comparison of Orbit 7 Minus Orbit 1 Semi Major Axis.

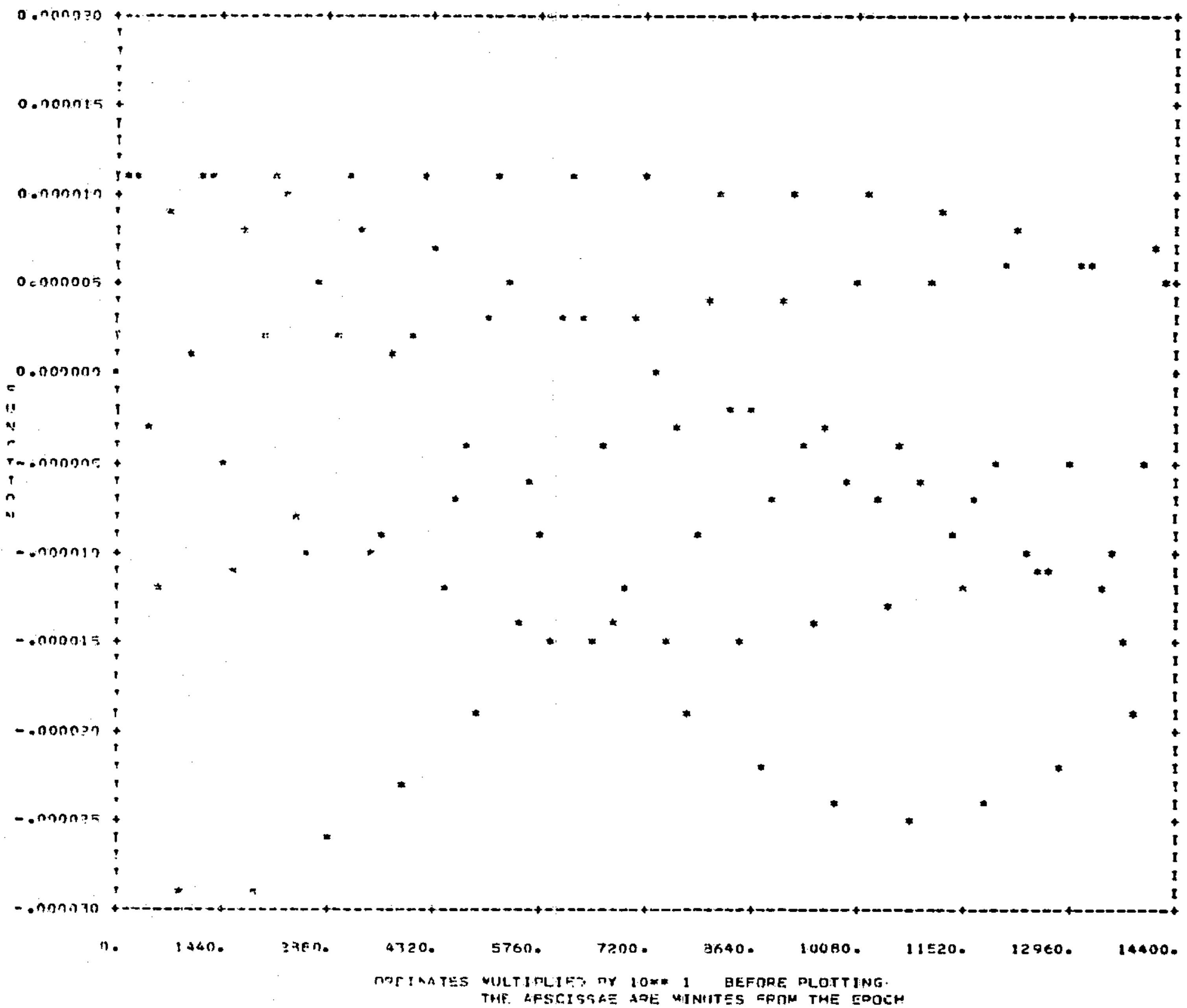

Figure 3b-Plot of Data from Comparison of Orbit 7 Minus Orbit 1 Eccentricity.

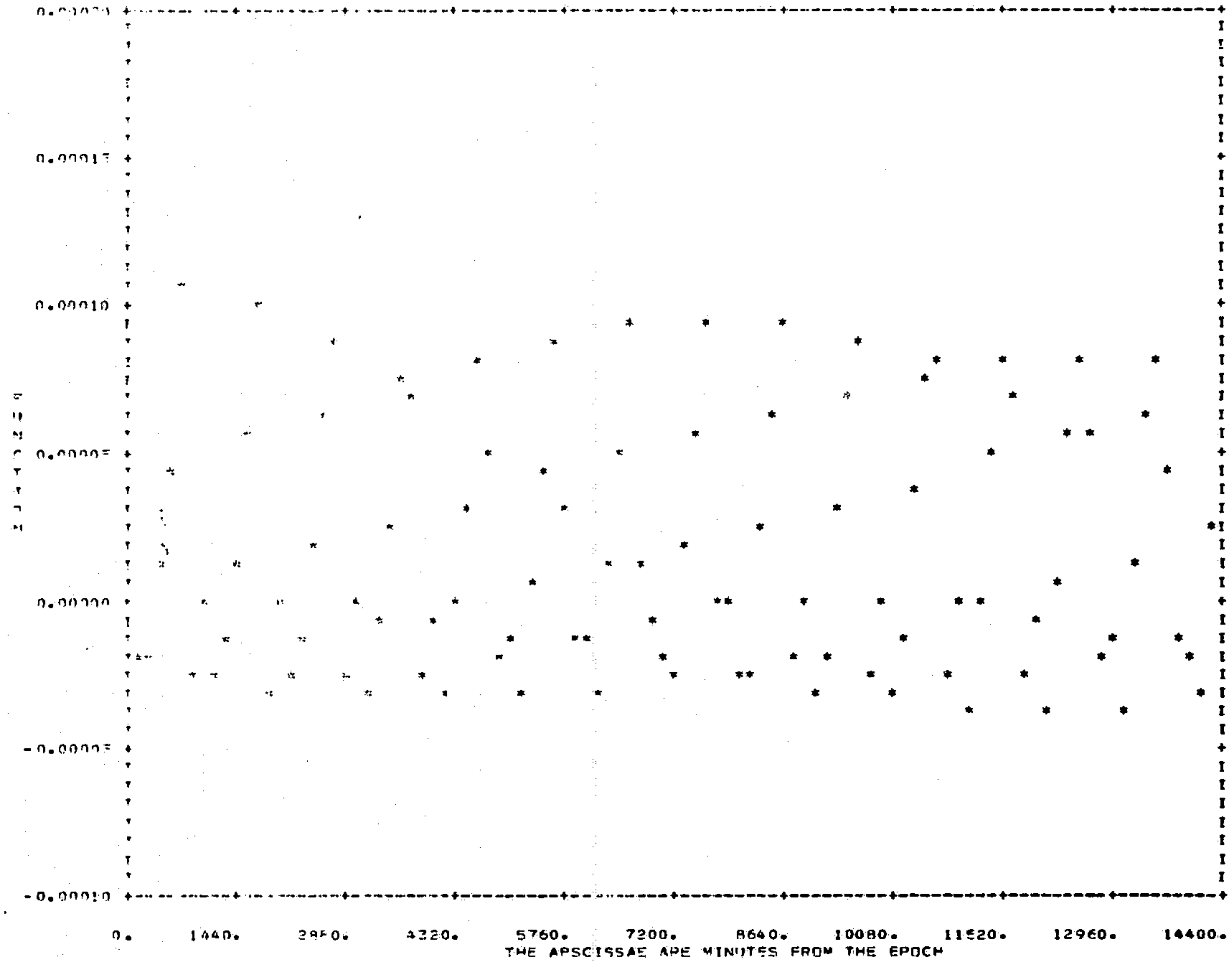

Figure 3c–Plot of Data from Comparison of Orbit 7 Minus Orbit 1 Inclination.

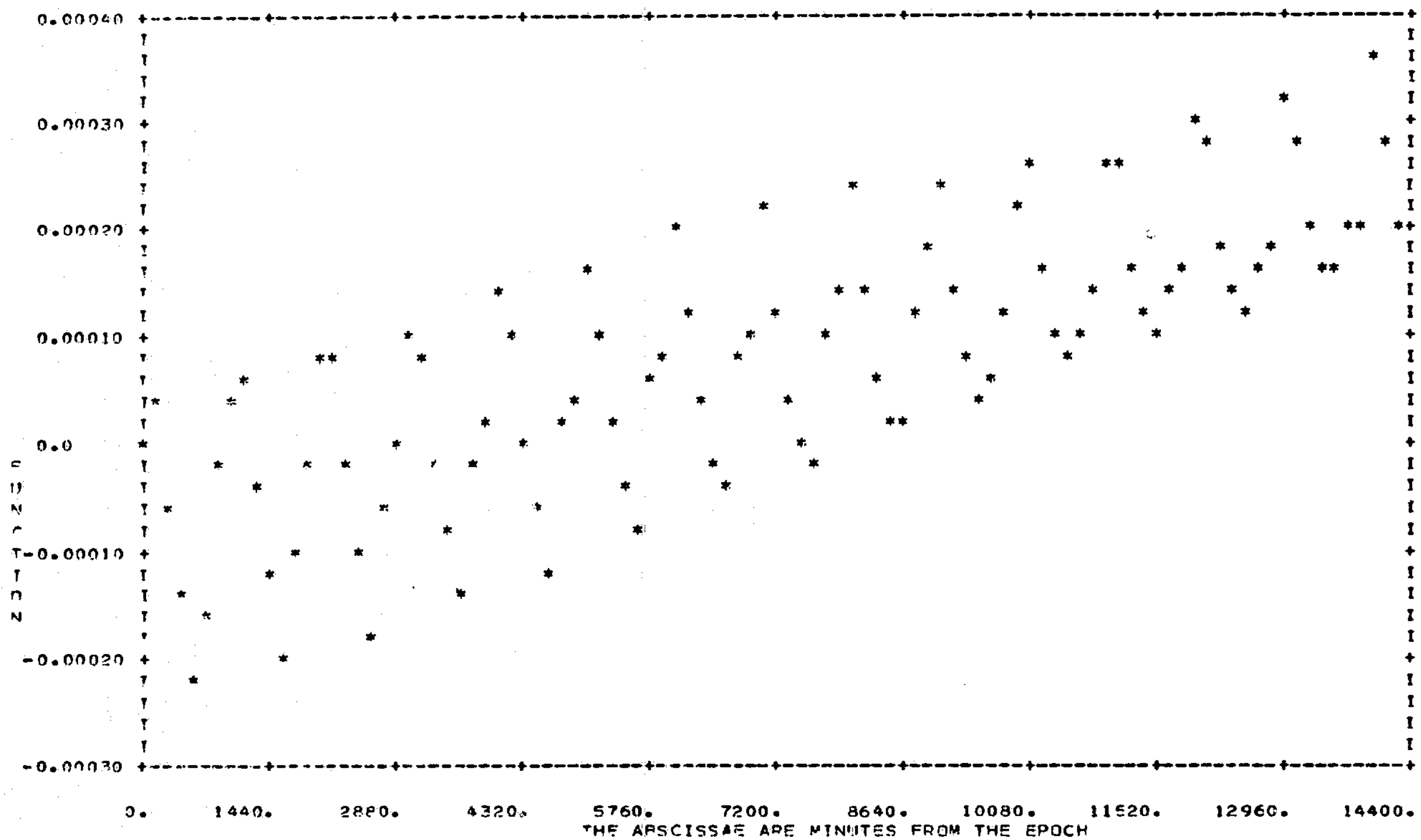

Figure 3d–Plot of Data from Comparison of Orbit 7 Minus Orbit 1 Right Ascension of Ascending Node.

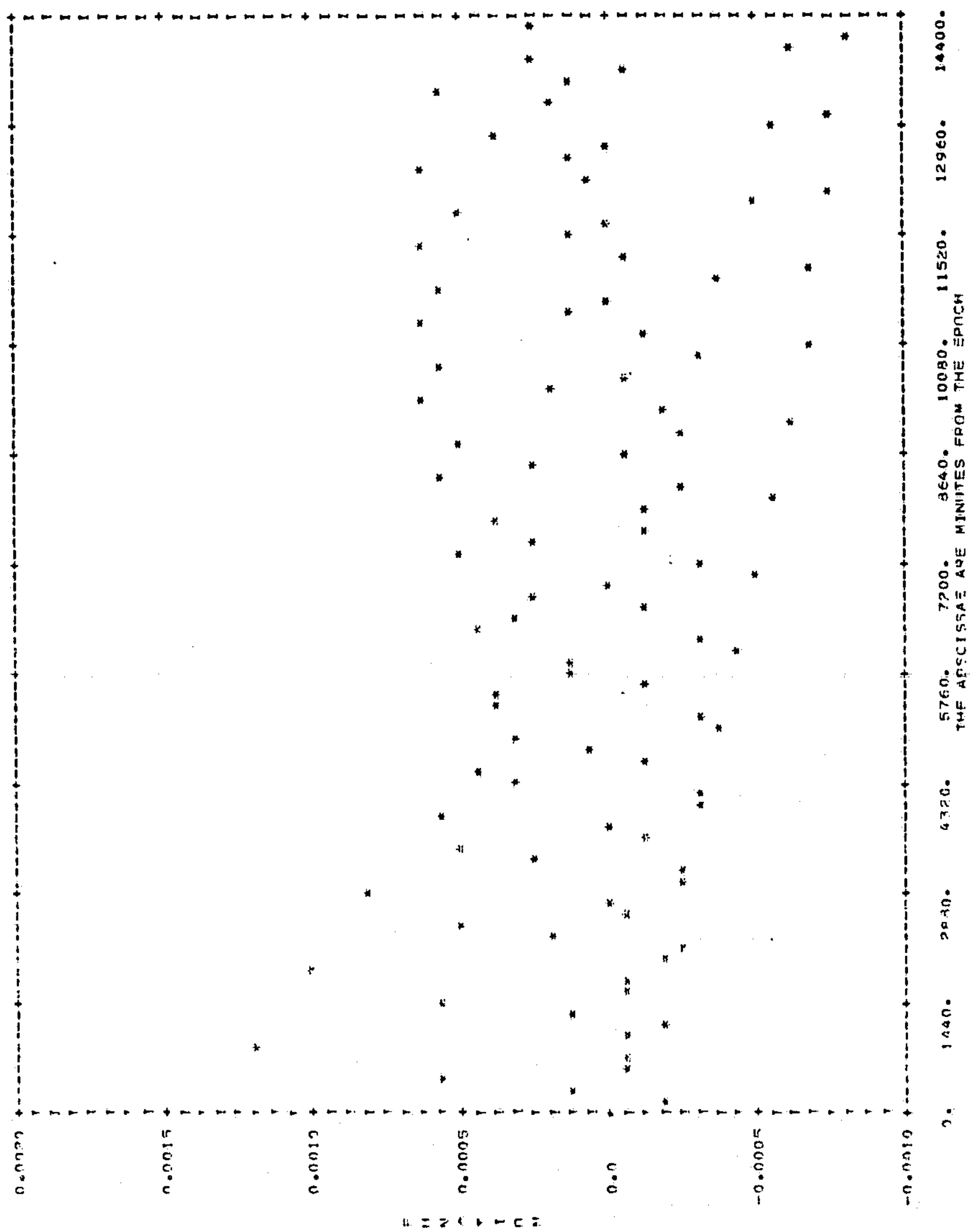

Figure 3e–Plot of Data from Comparison of Orbit 7 Minus Orbit 1 Argument of Perigee.

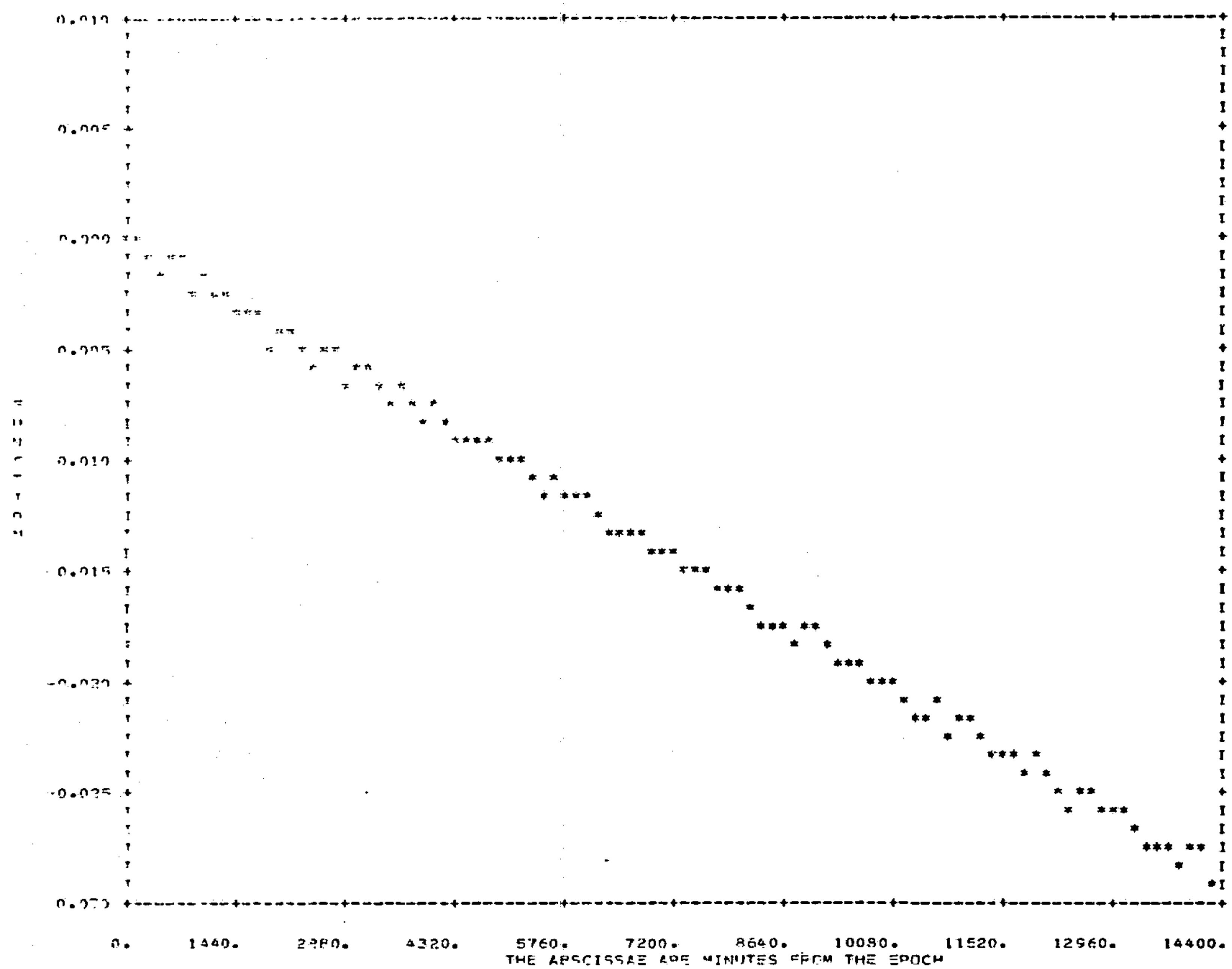

Figure 3f–Plot of Data from Comparison of Orbit 7 Minus Orbit 1 Mean Anomaly.

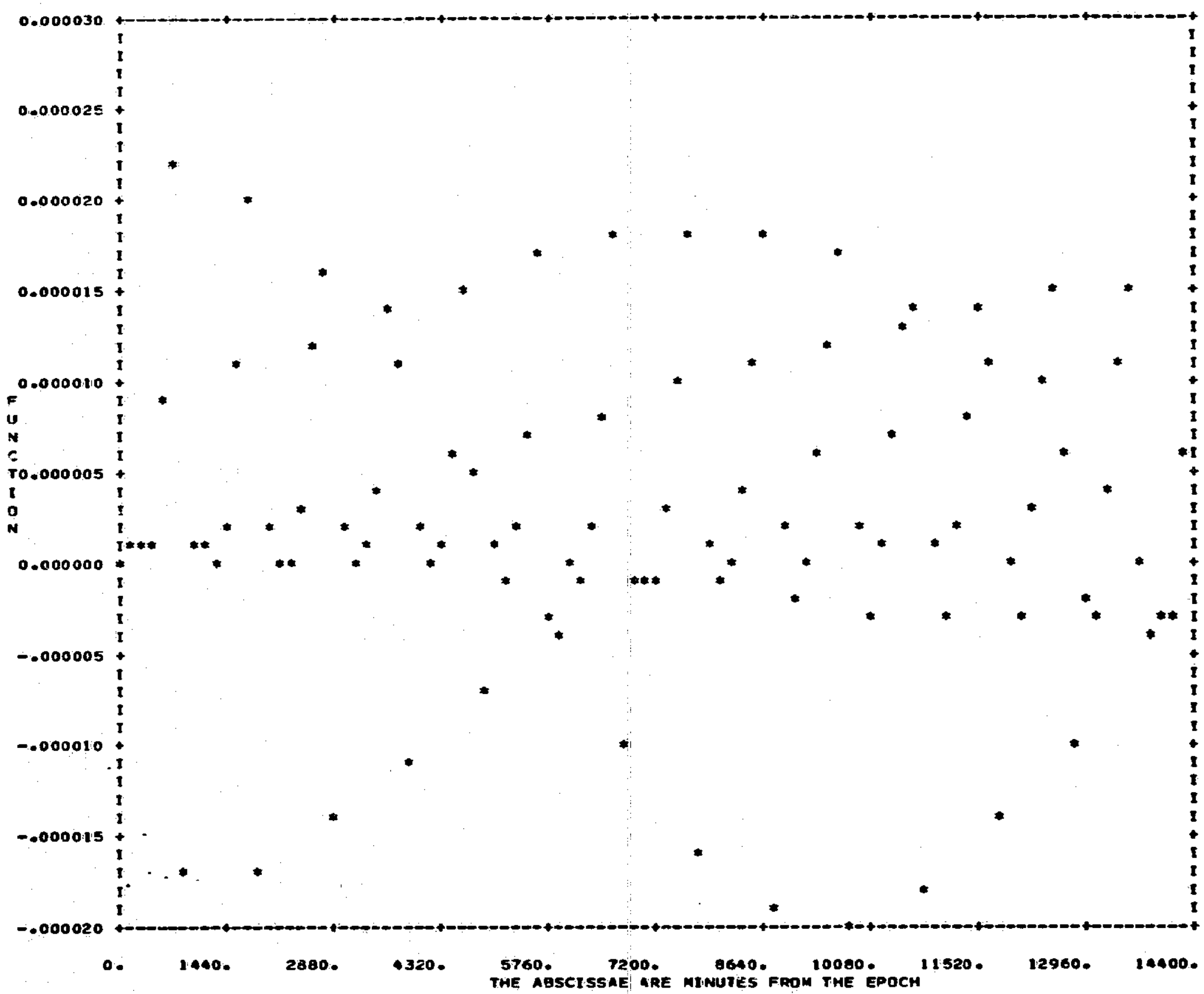

Figure 4a-Plot of Data from Comparison of Orbit 9 Minus Orbit 1 Semi Major Axis.

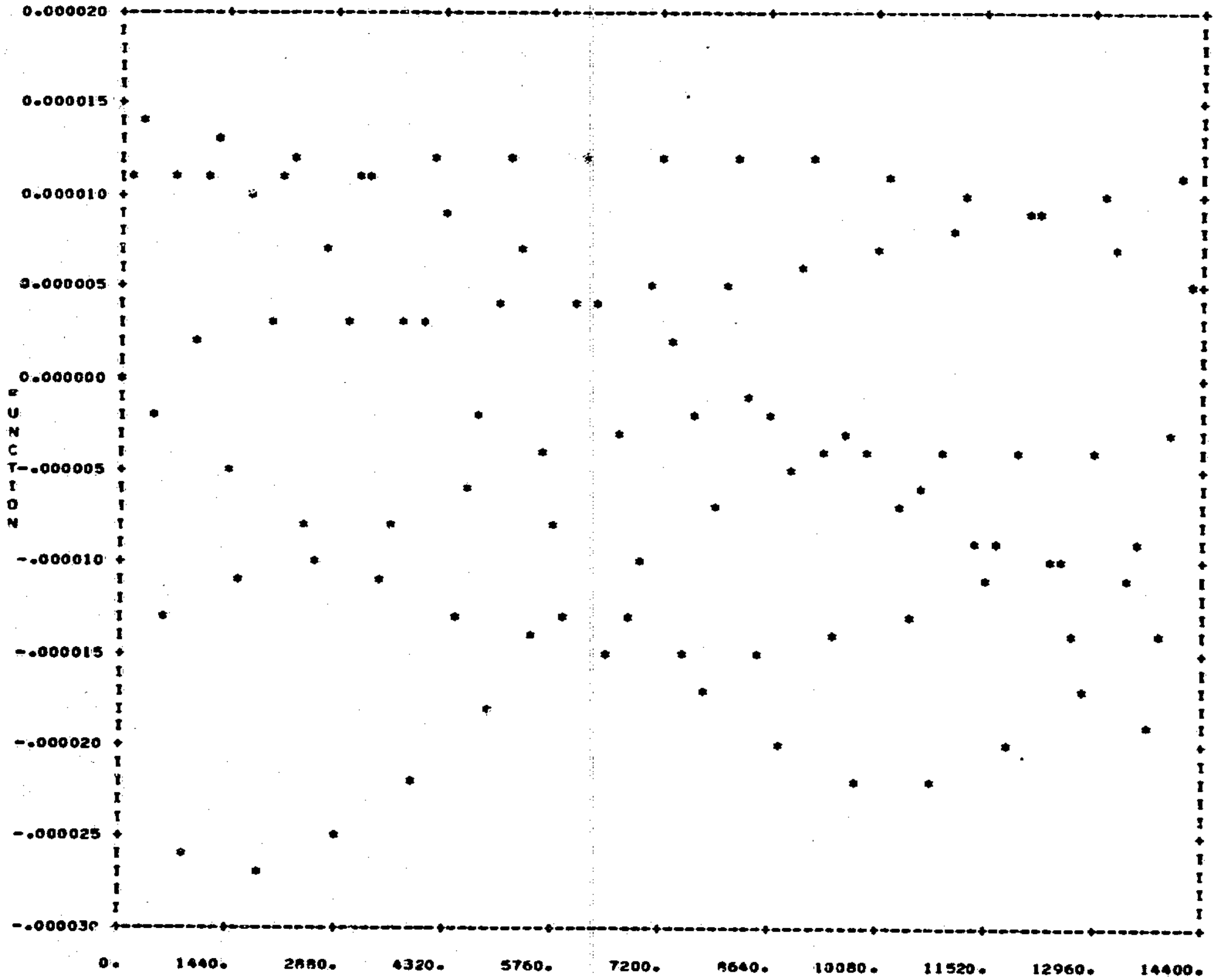

ORDINATES MULTIPLIED BY 10** 1 BEFORE PLOTTING
THE ABSCISSAE ARE MINUTES FROM THE EPOCH

Figure 4b-Plot of Data from Comparison of Orbit 9 Minus Orbit 1 Eccentricity.

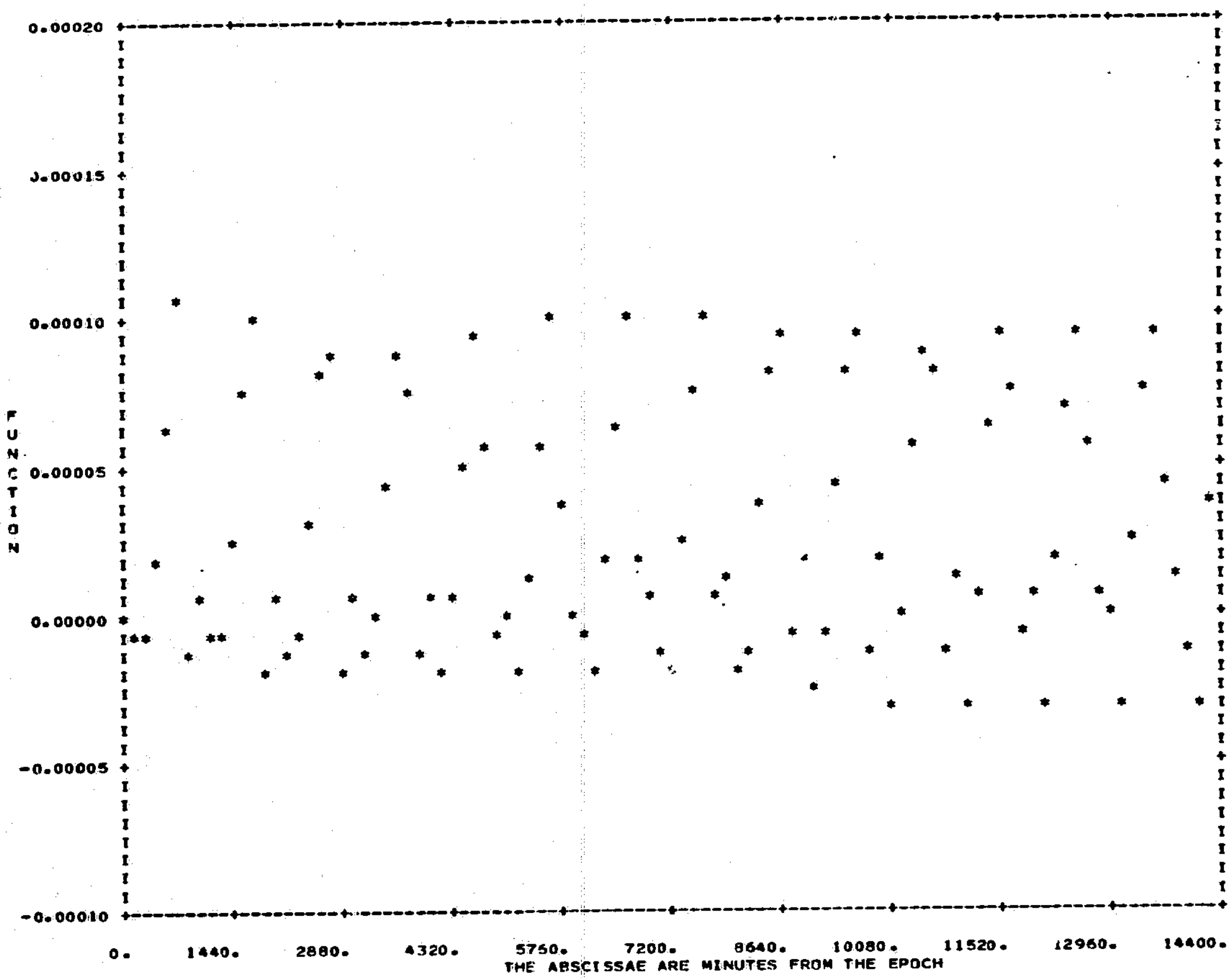

Figure 4c–Plot of Data from Comparison of Orbit 9 Minus Orbit 1 Inclination.

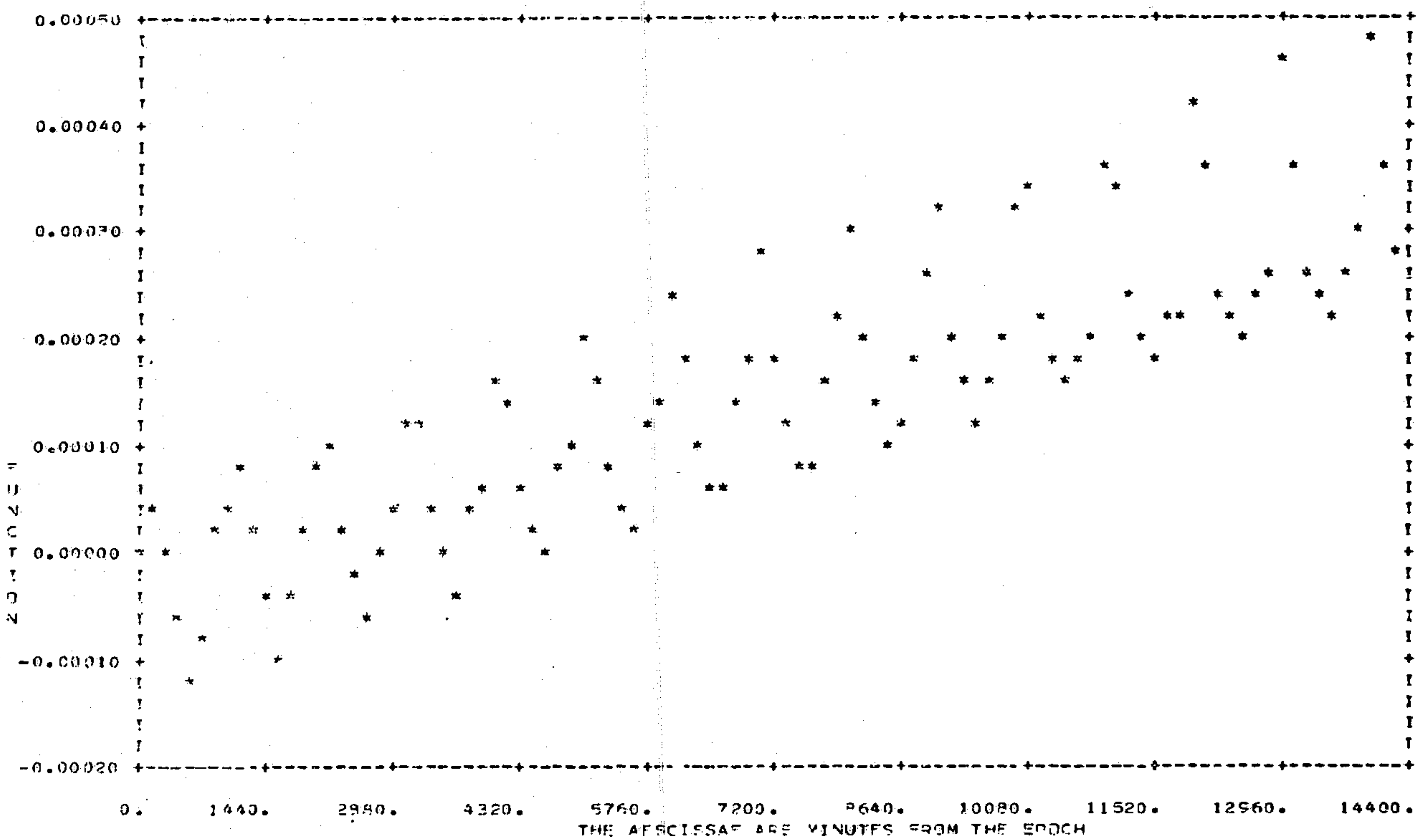

Figure 4d–Plot of Data from Comparison of Orbit 9 Minus Orbit 1 Right Ascension of Ascending Node.

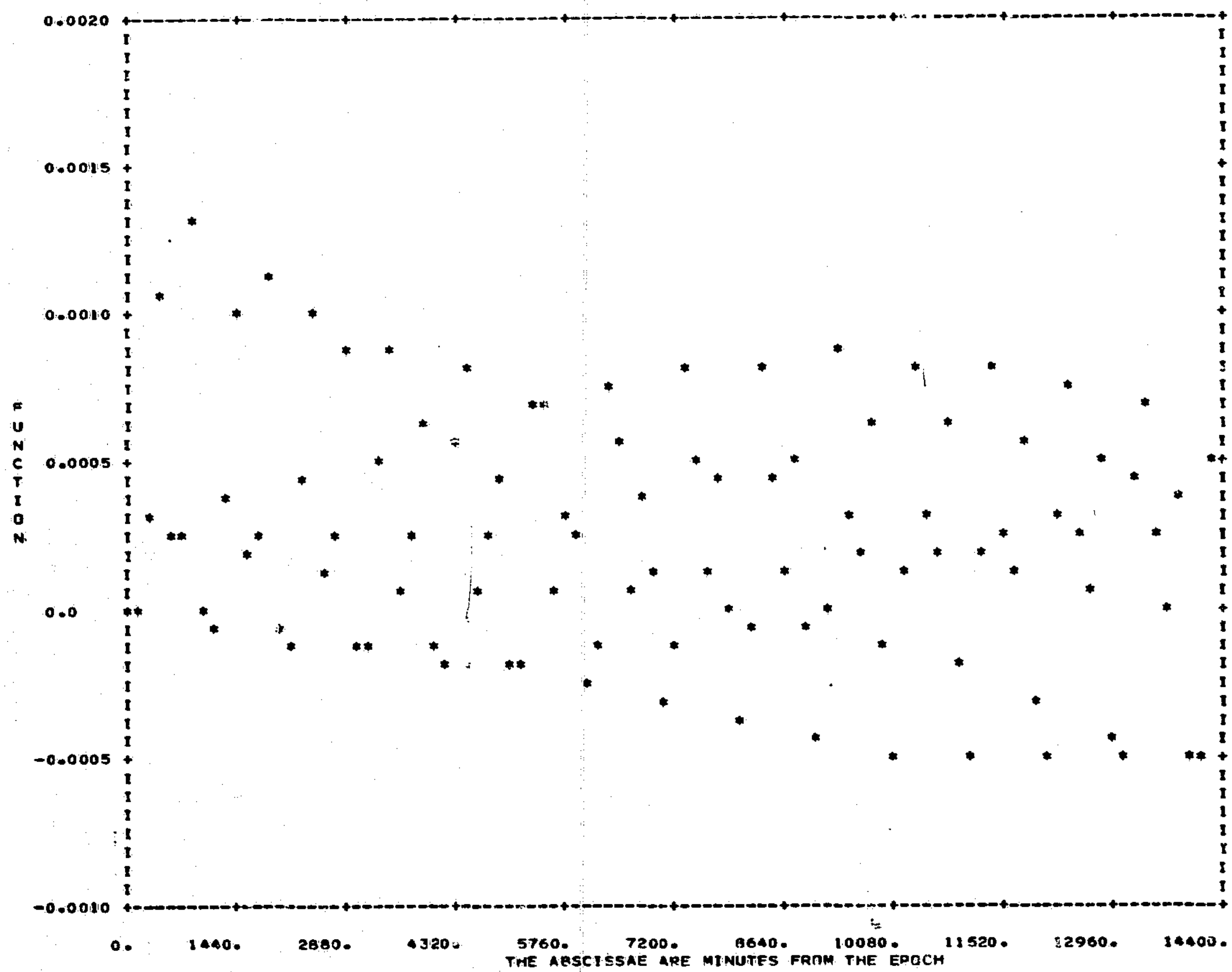

Figure 4e–Plot of Data from Comparison of Orbit 9 Minus Orbit 1 Argument of Perigee.

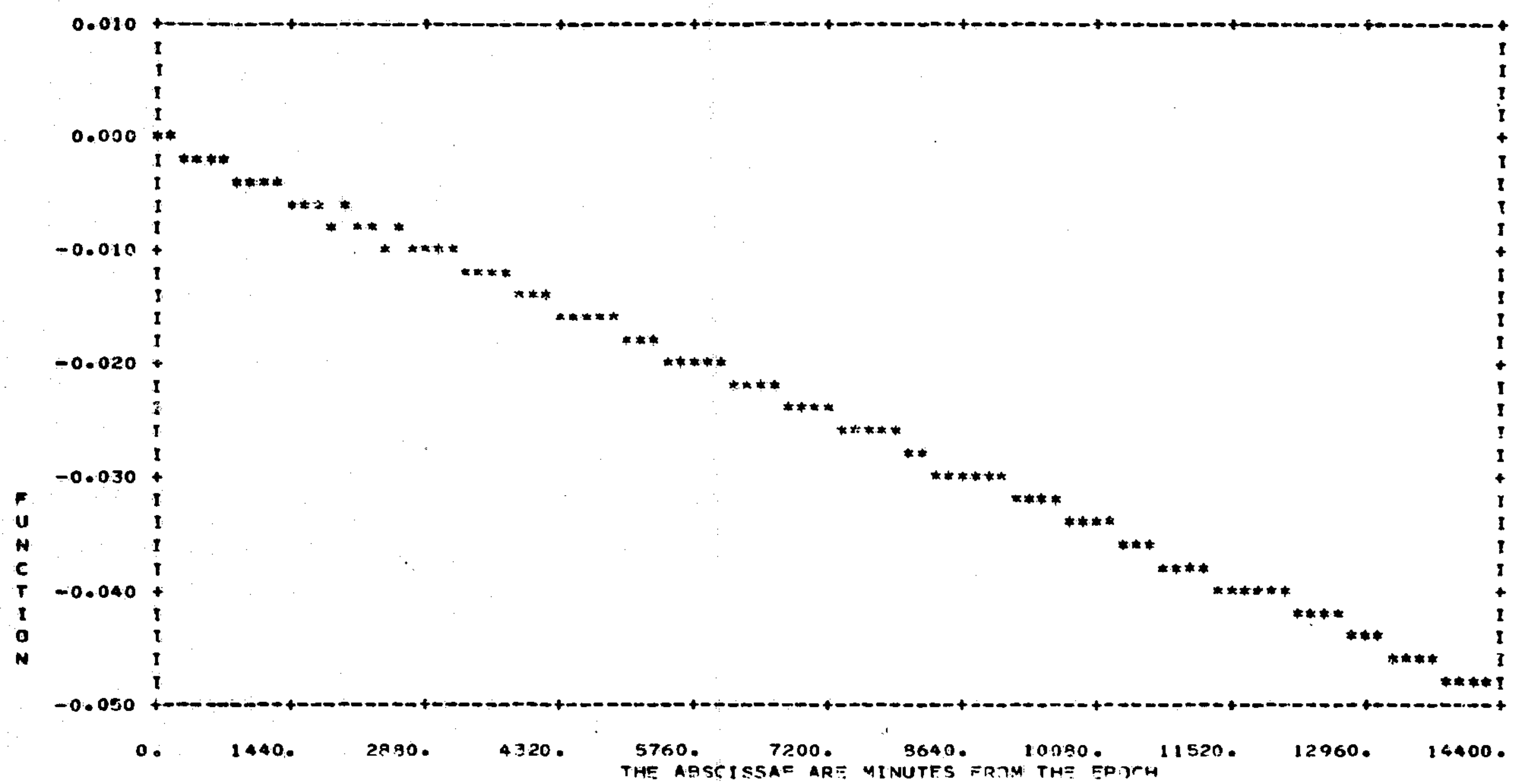

Figure 4f–Plot of Data from Comparison of Orbit 9 Minus Orbit 1 Mean Anomaly.

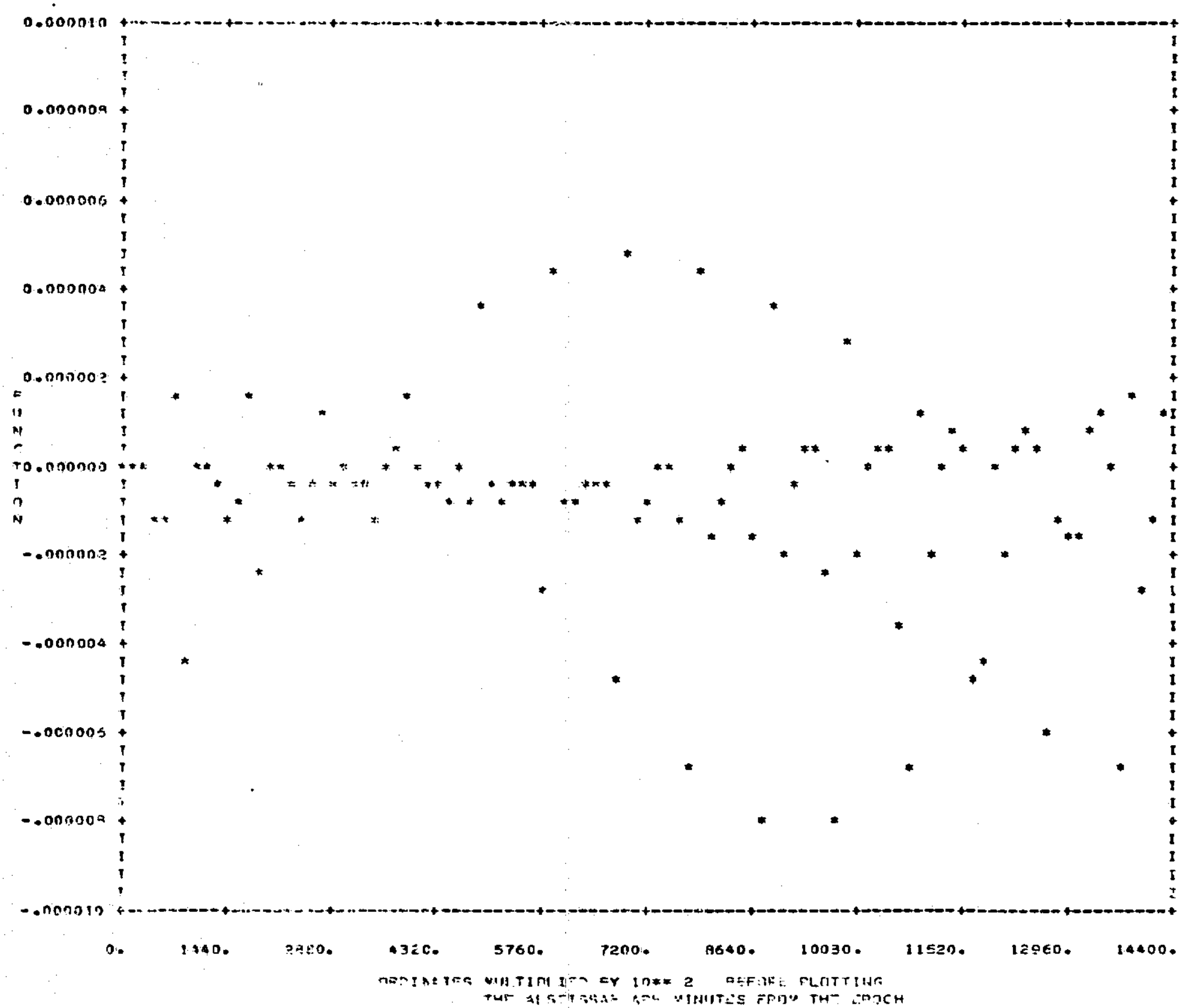

Figure 5a–Plot of Data from Comparison of Orbit 11 Minus Orbit 1 Semi Major Axis.

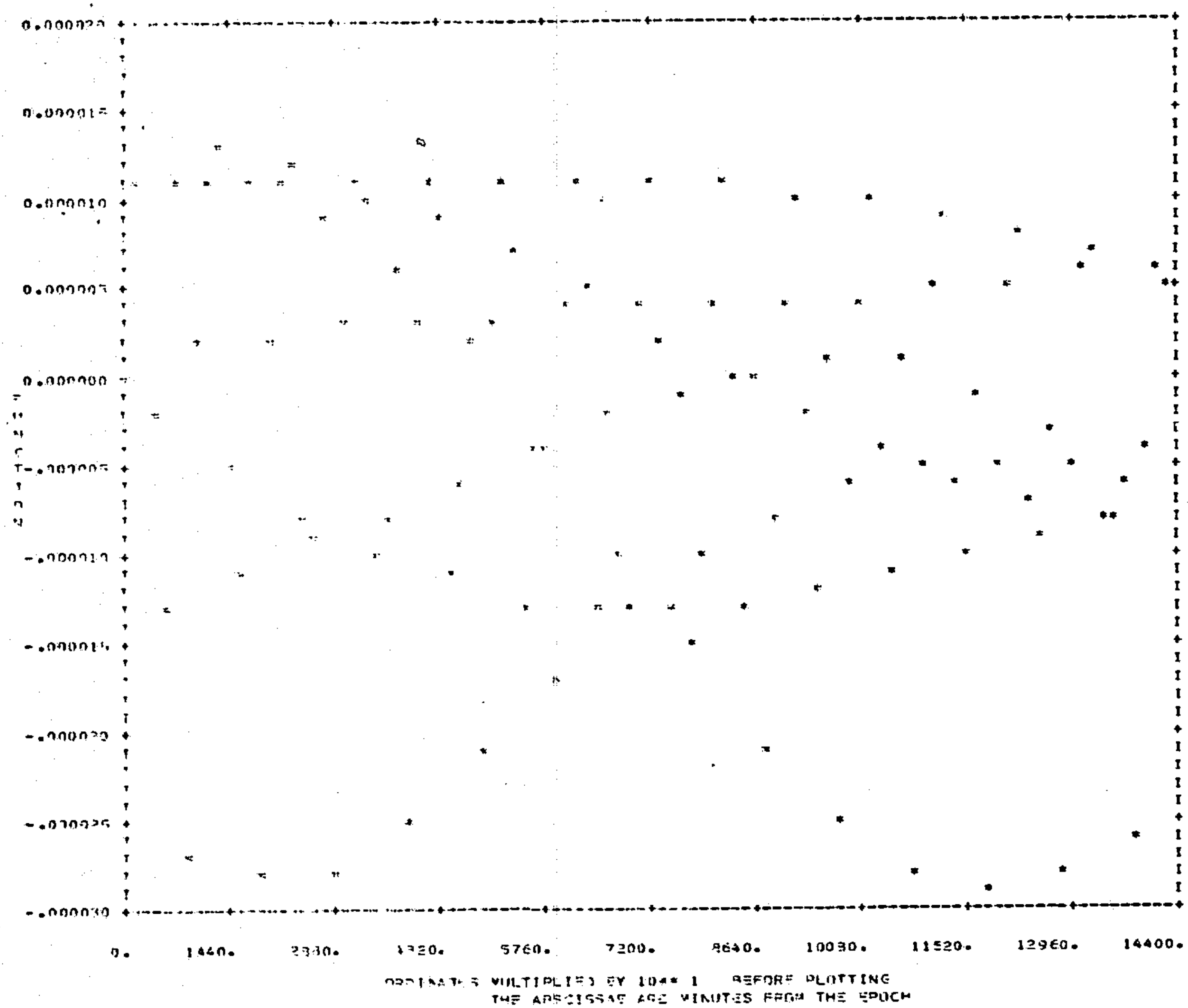

Figure 5b–Plot of Data from Comparison of Orbit 11 Minus Orbit 1 Eccentricity.

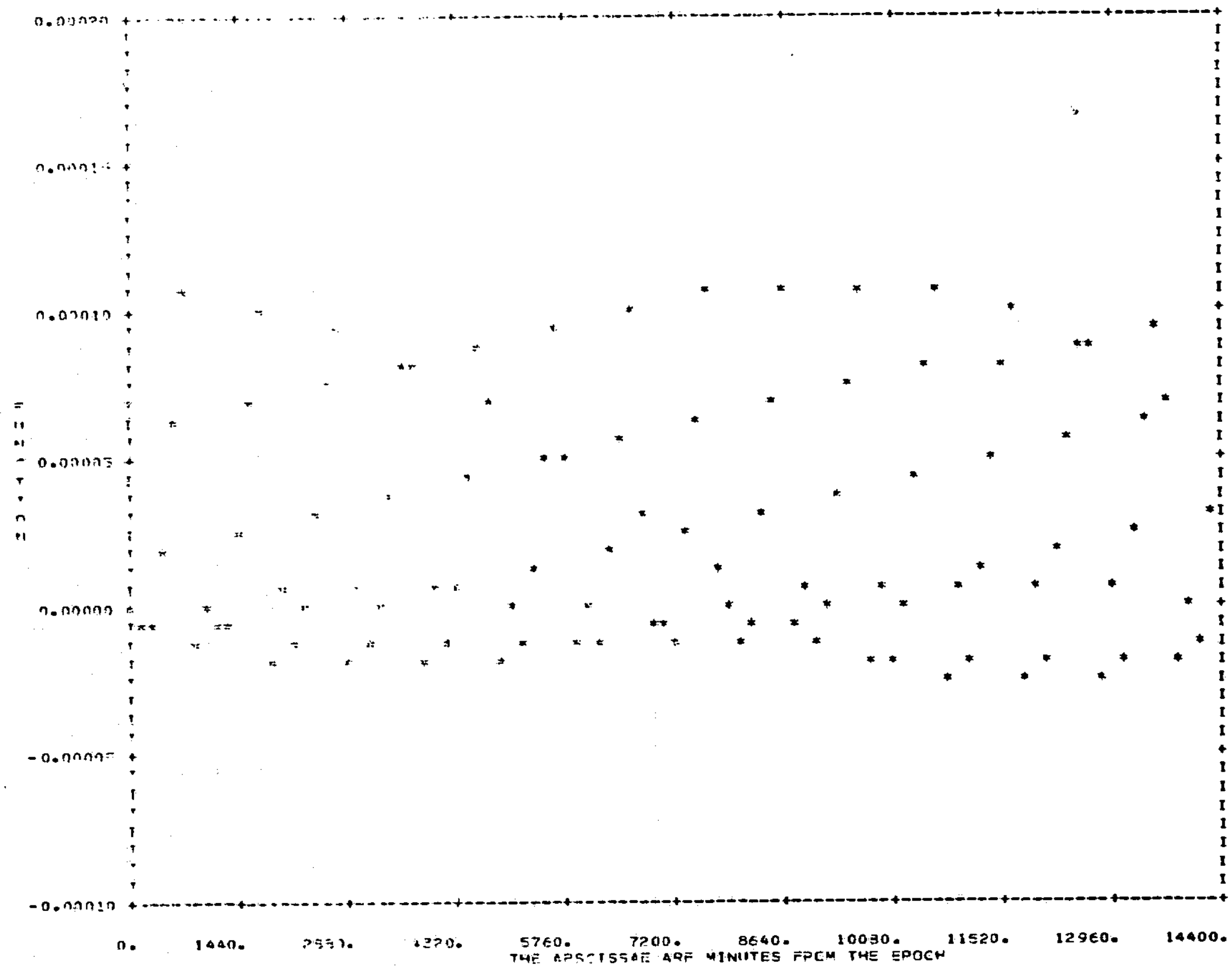

Figure 5c–Plot of Data from Comparison of Orbit 11 Minus Orbit 1 Inclination.

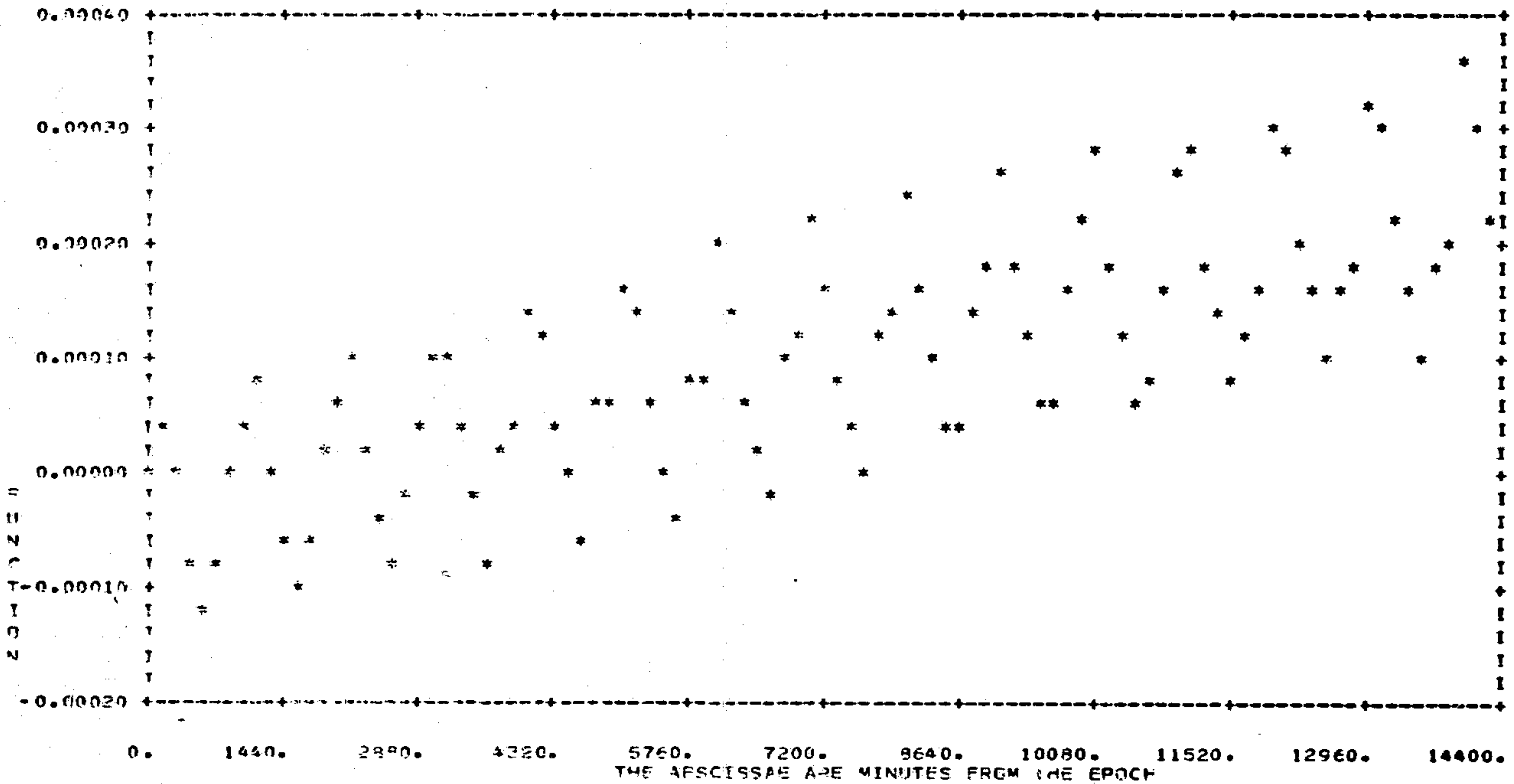

Figure 5d-Plot of Data from Comparison of Orbit 11 Minus Orbit 1 Right Ascension of Ascending Node.

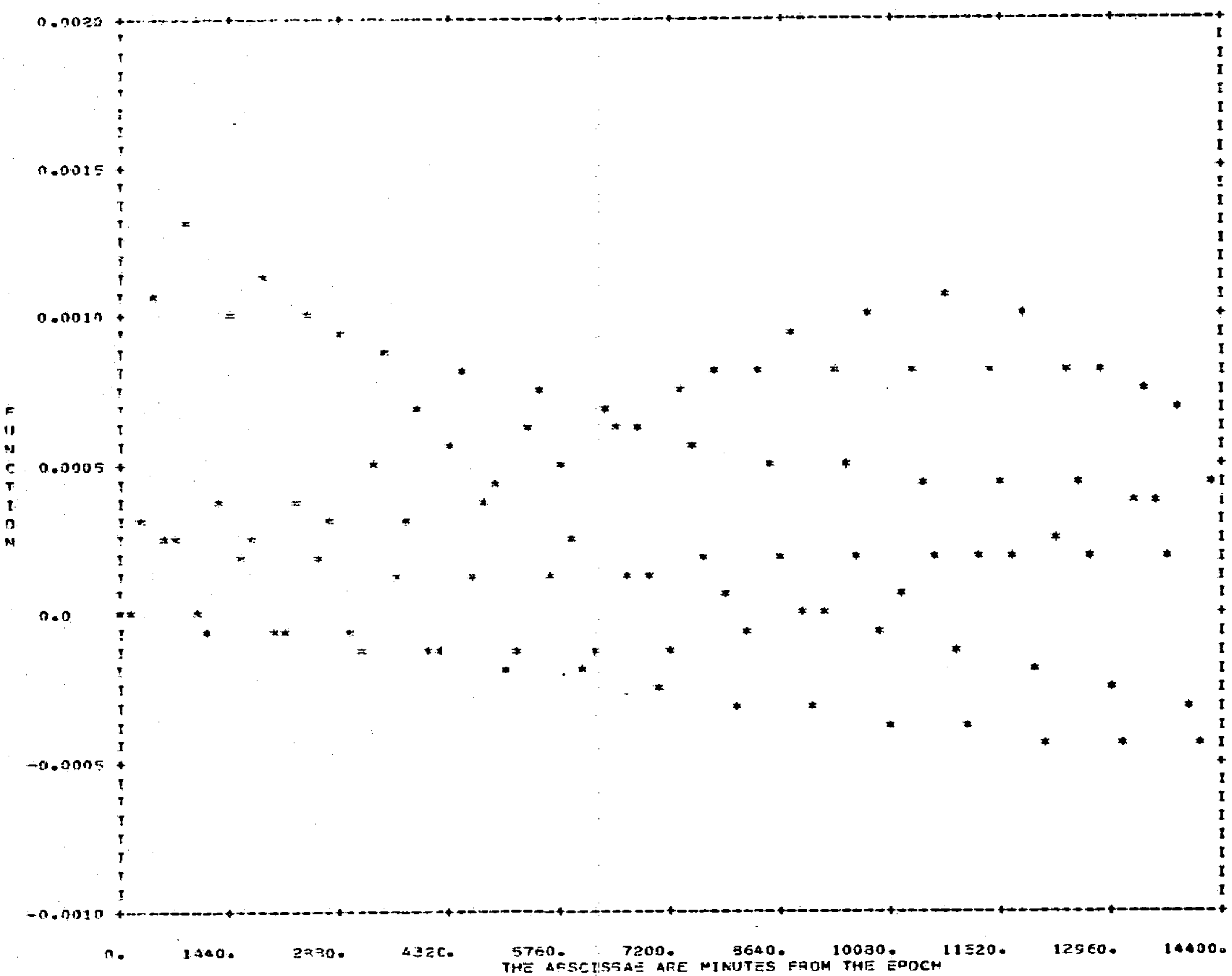

Figure 5e–Plot of Data from Comparison of Orbit 11 Minus Orbit 1 Argument of Perigee.

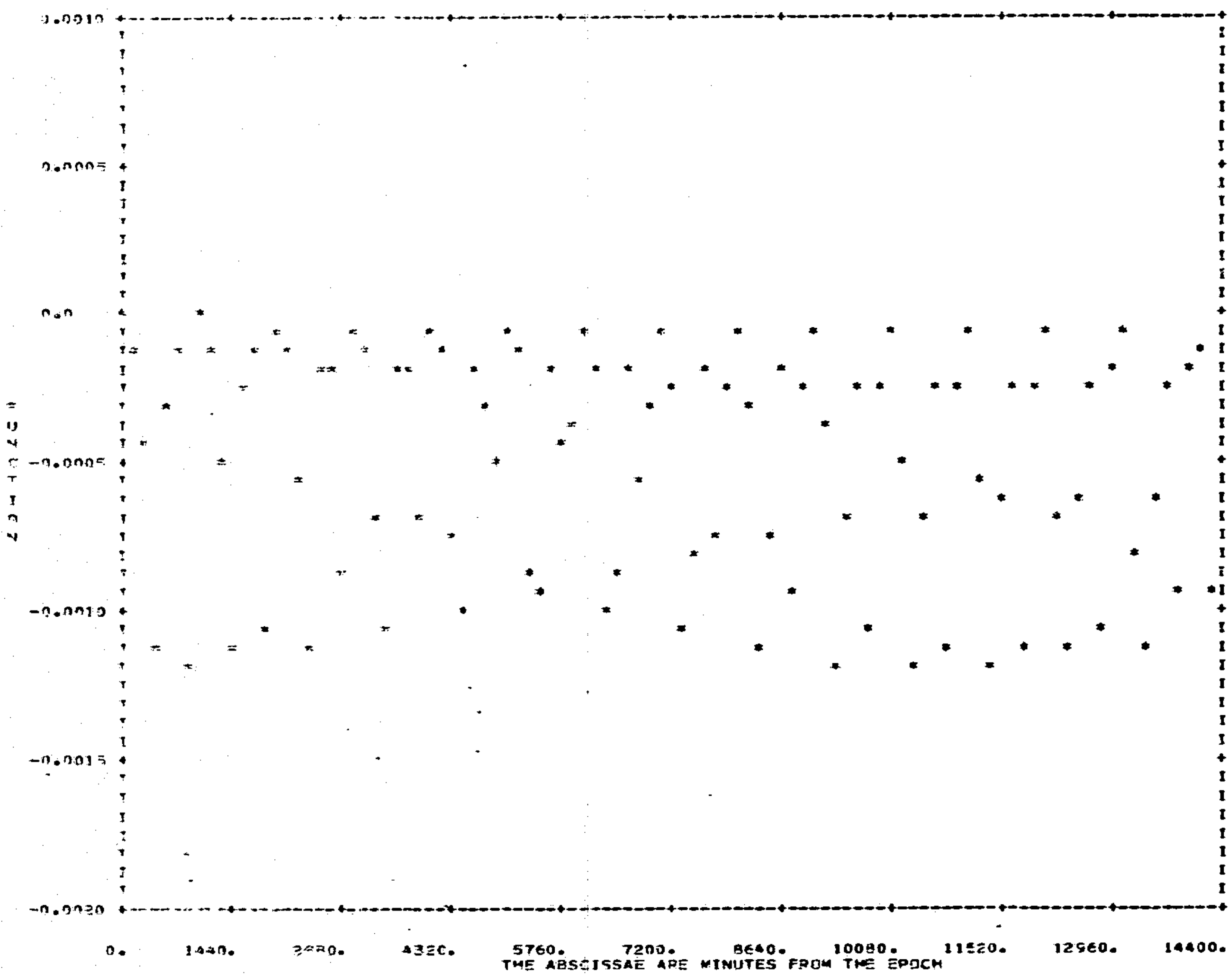

Figure 5f–Plot of Data from Comparison of Orbit 11 Minus Orbit 1 Mean Anomaly.

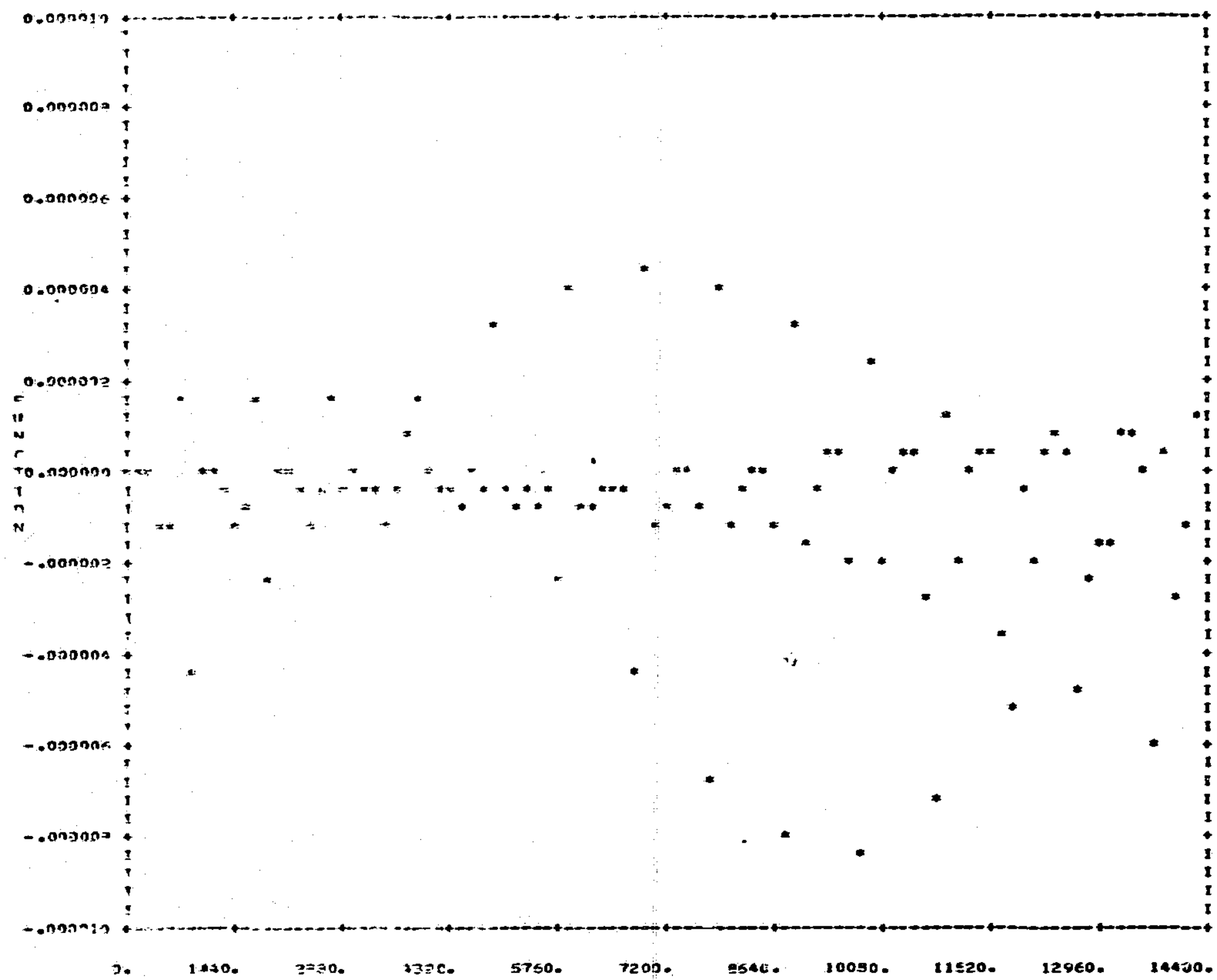

Figure 6a–Plot of Data from Comparison of Orbit 13 Minus Orbit 1 Semi Major Axis.

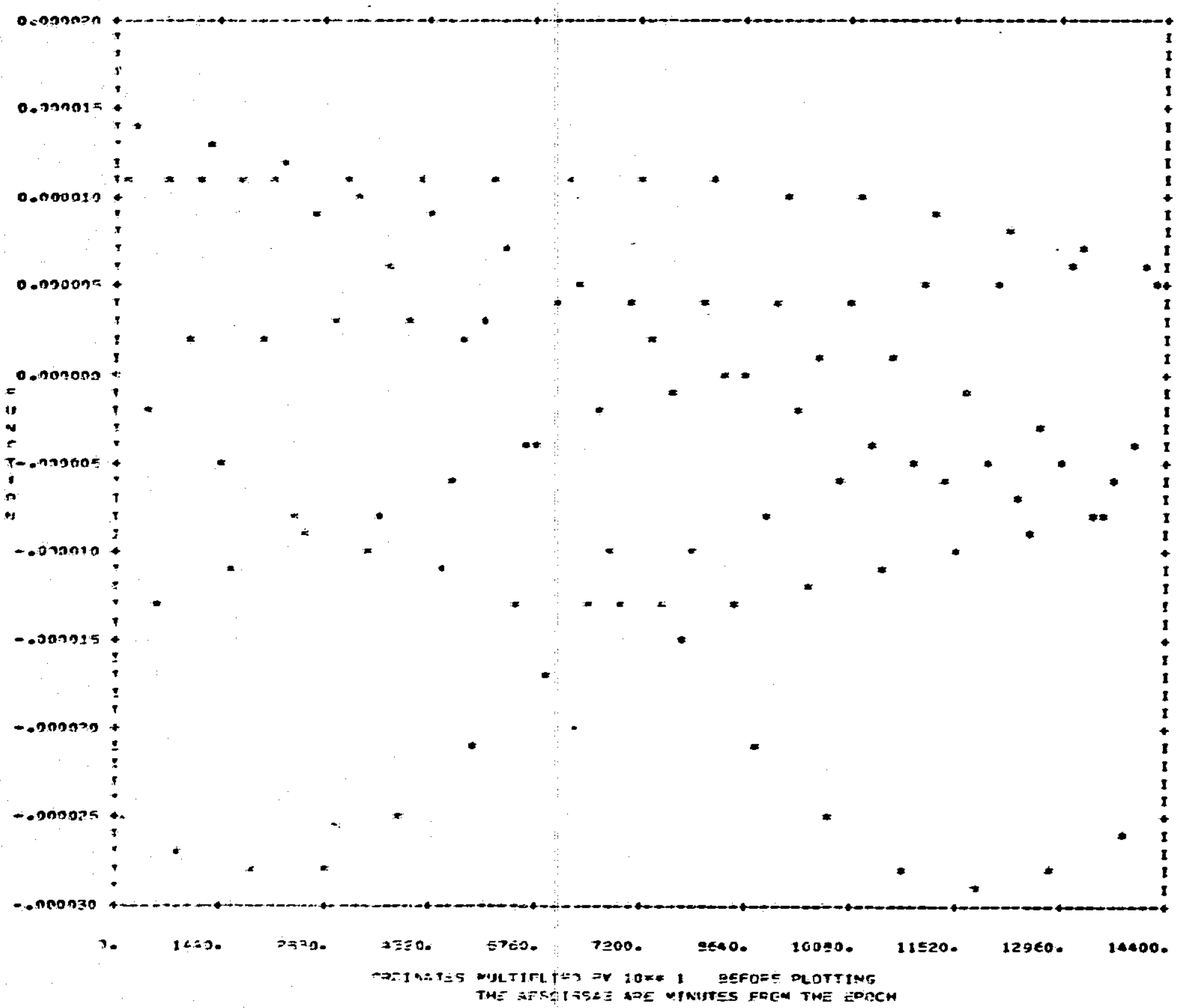

Figure 6b–Plot of Data from Comparison of Orbit 13 Minus Orbit 1 Eccentricity.

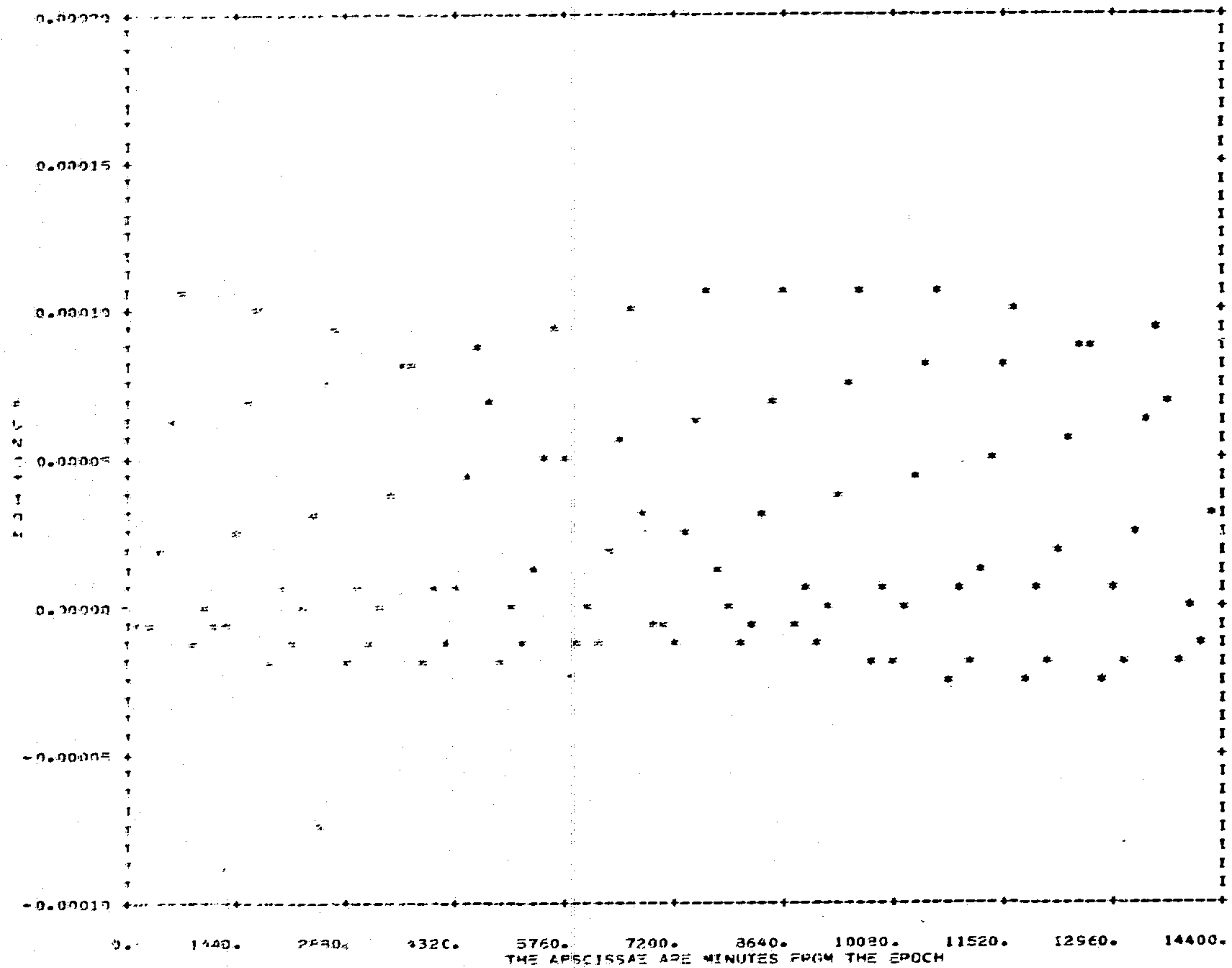

Figure 6c–Plot of Data from Comparison of Orbit 13 Minus Orbit 1 Inclination.

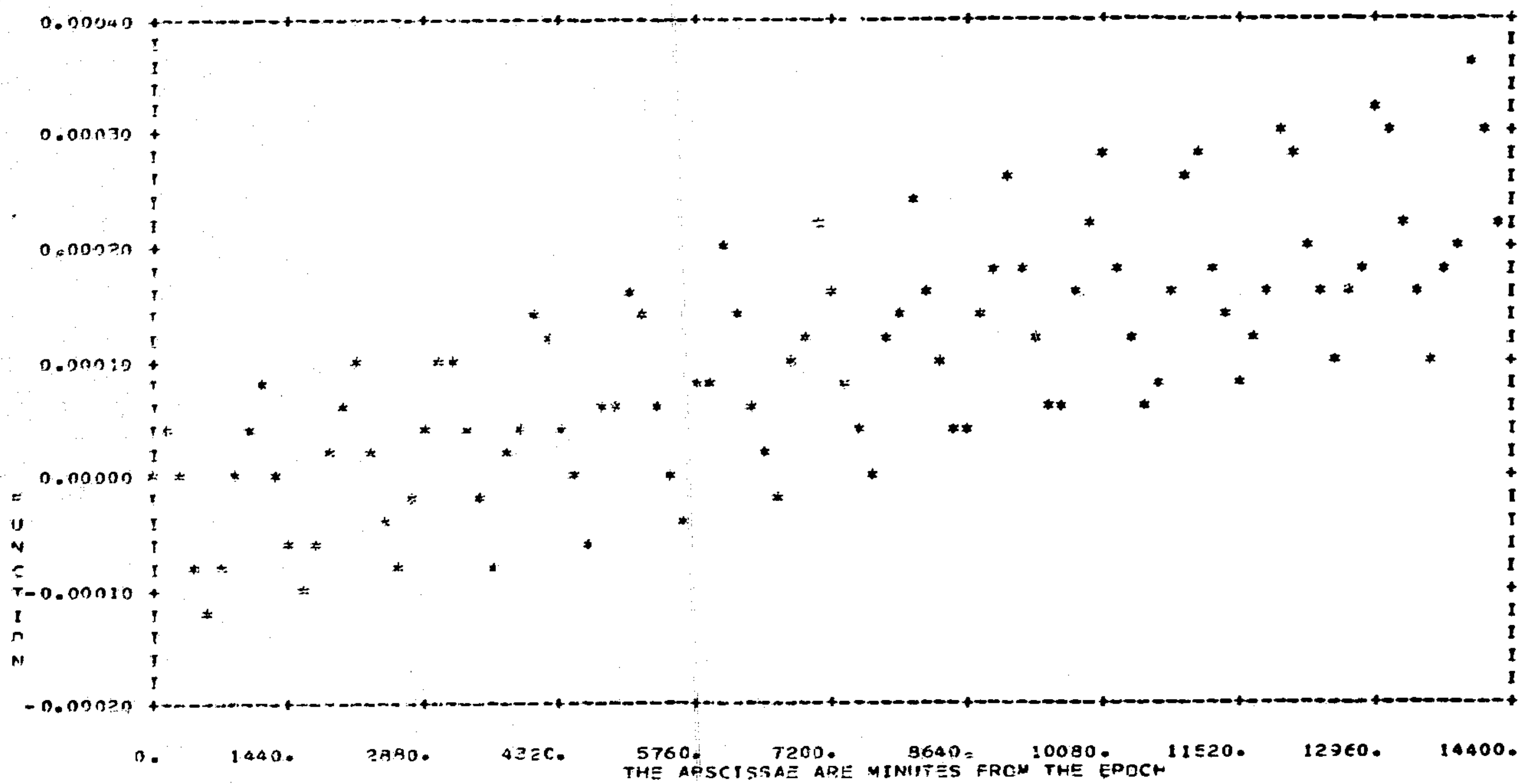

Figure 6d–Plot of Data from Comparison of Orbit 13 Minus Orbit 1 Right Ascension of Ascending Node.

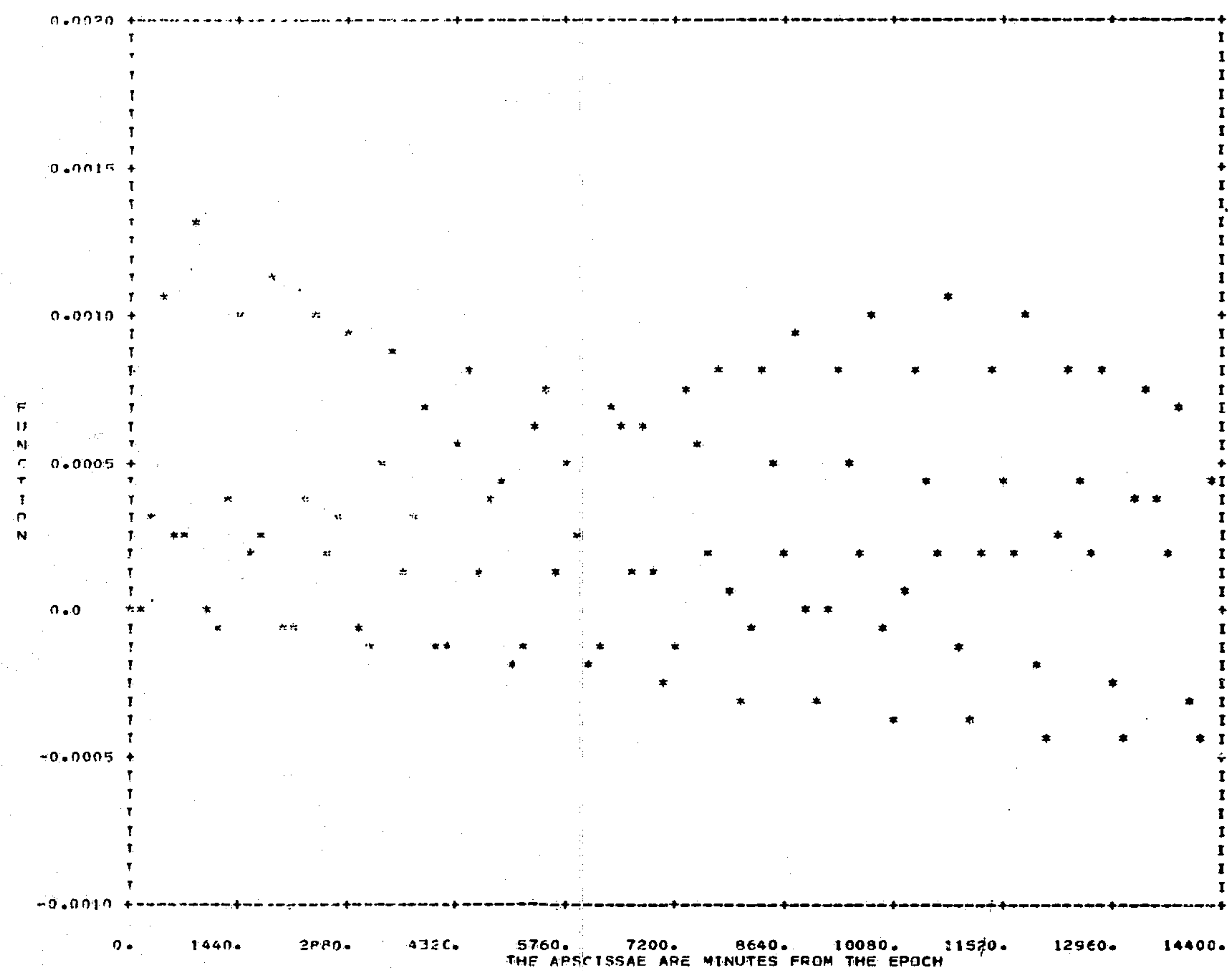

Figure 6e–Plot of Data from Comparison of Orbit 13 Minus Orbit 1 Argument of Perigee.

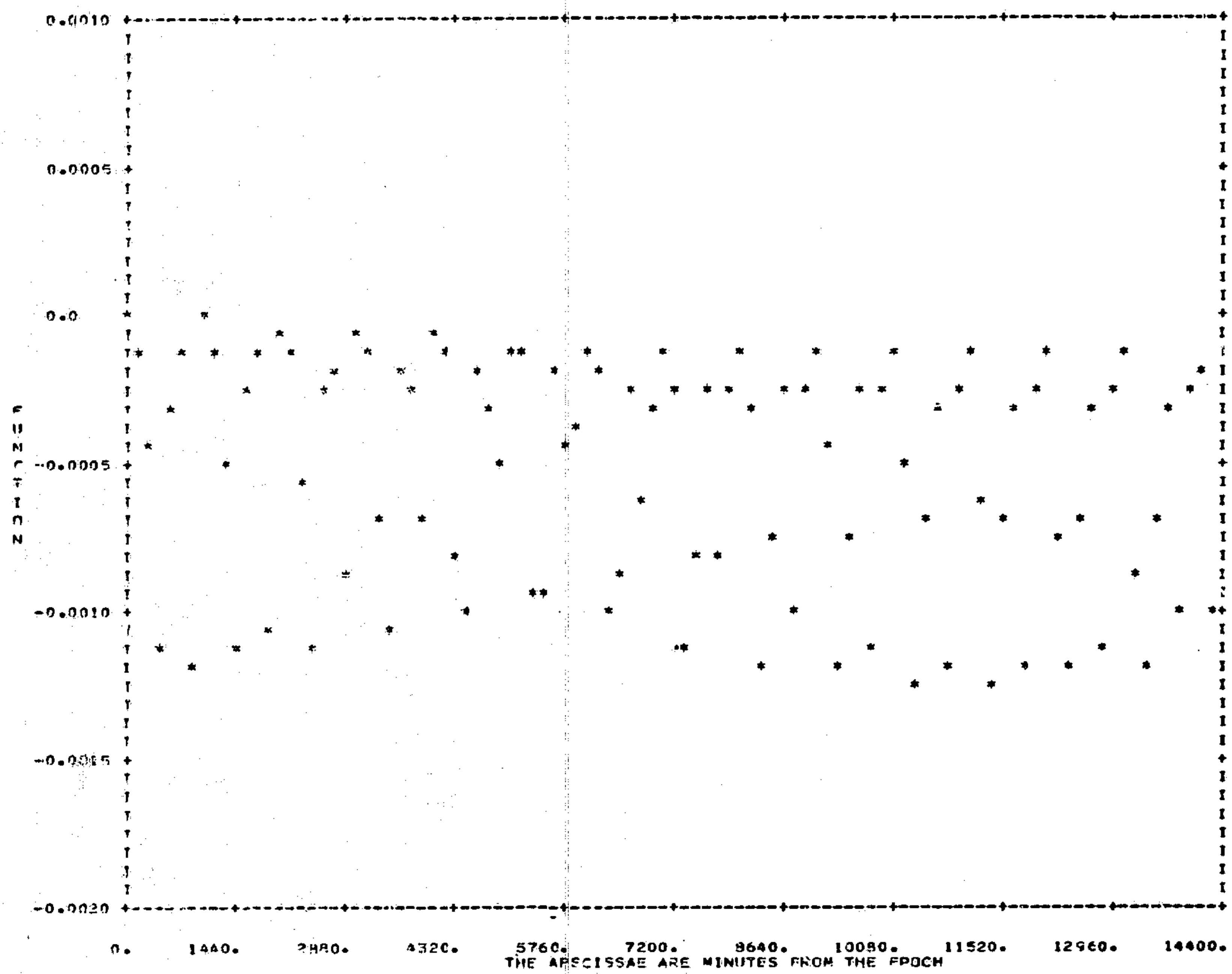

Figure 6f–Plot of Data from Comparison of Orbit 13 Minus Orbit 1 Mean Anomaly.

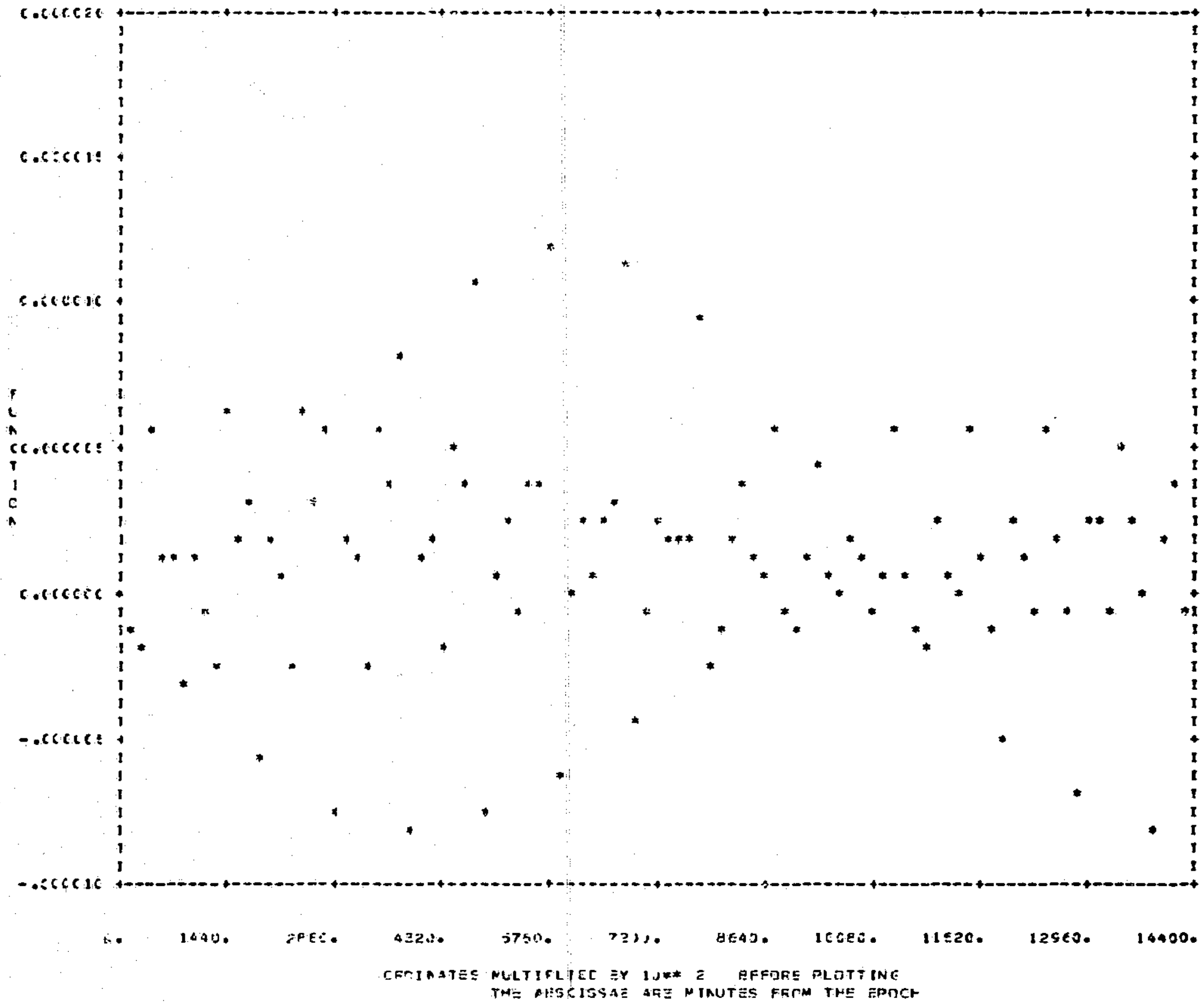

Figure 7a–Plot of Data from Comparison of Orbit 15 Minus Orbit 1 Semi Major Axis.

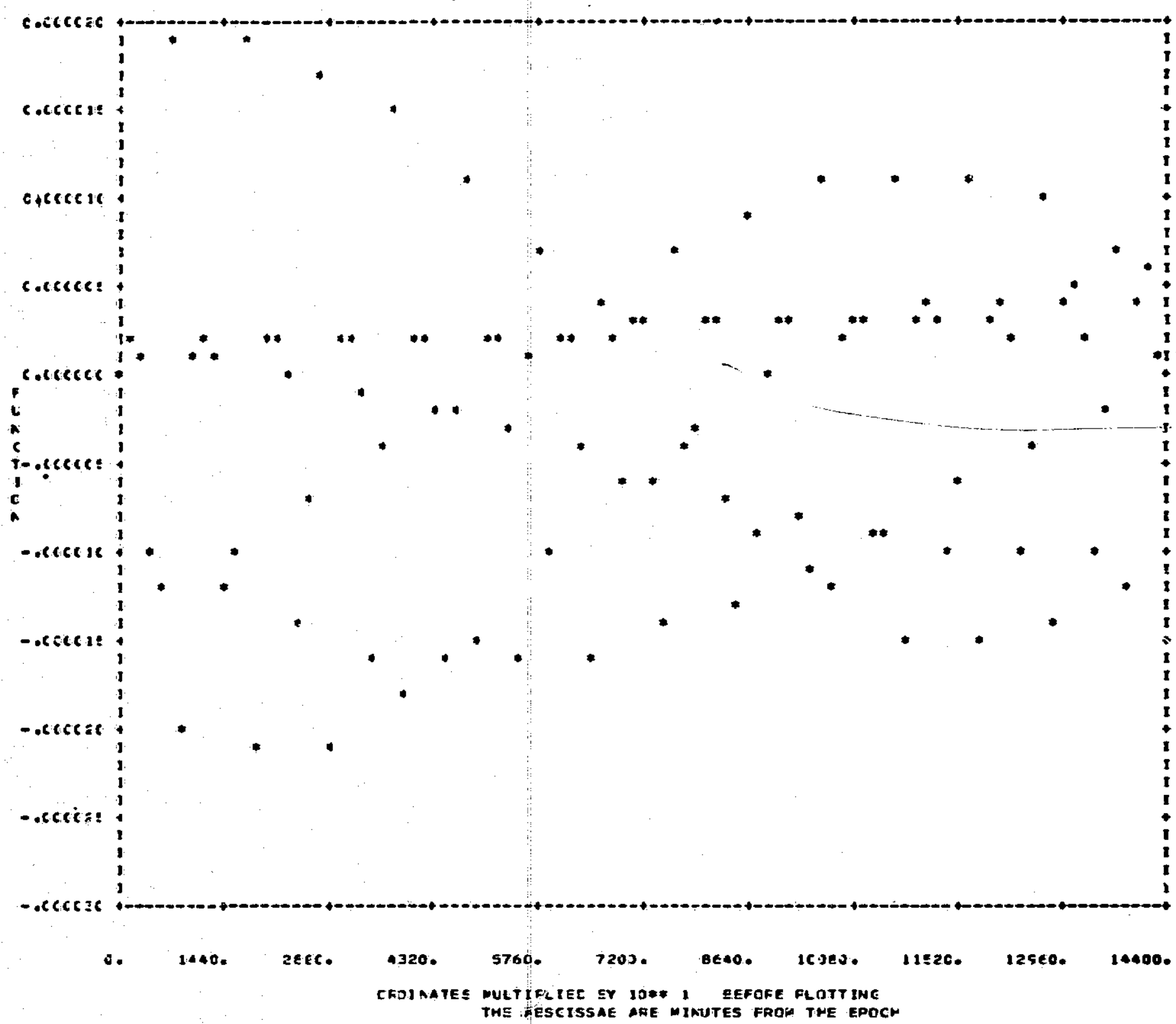

Figure 7b–Plot of Data from Comparison of Orbit 15 Minus Orbit 1 Eccentricity.

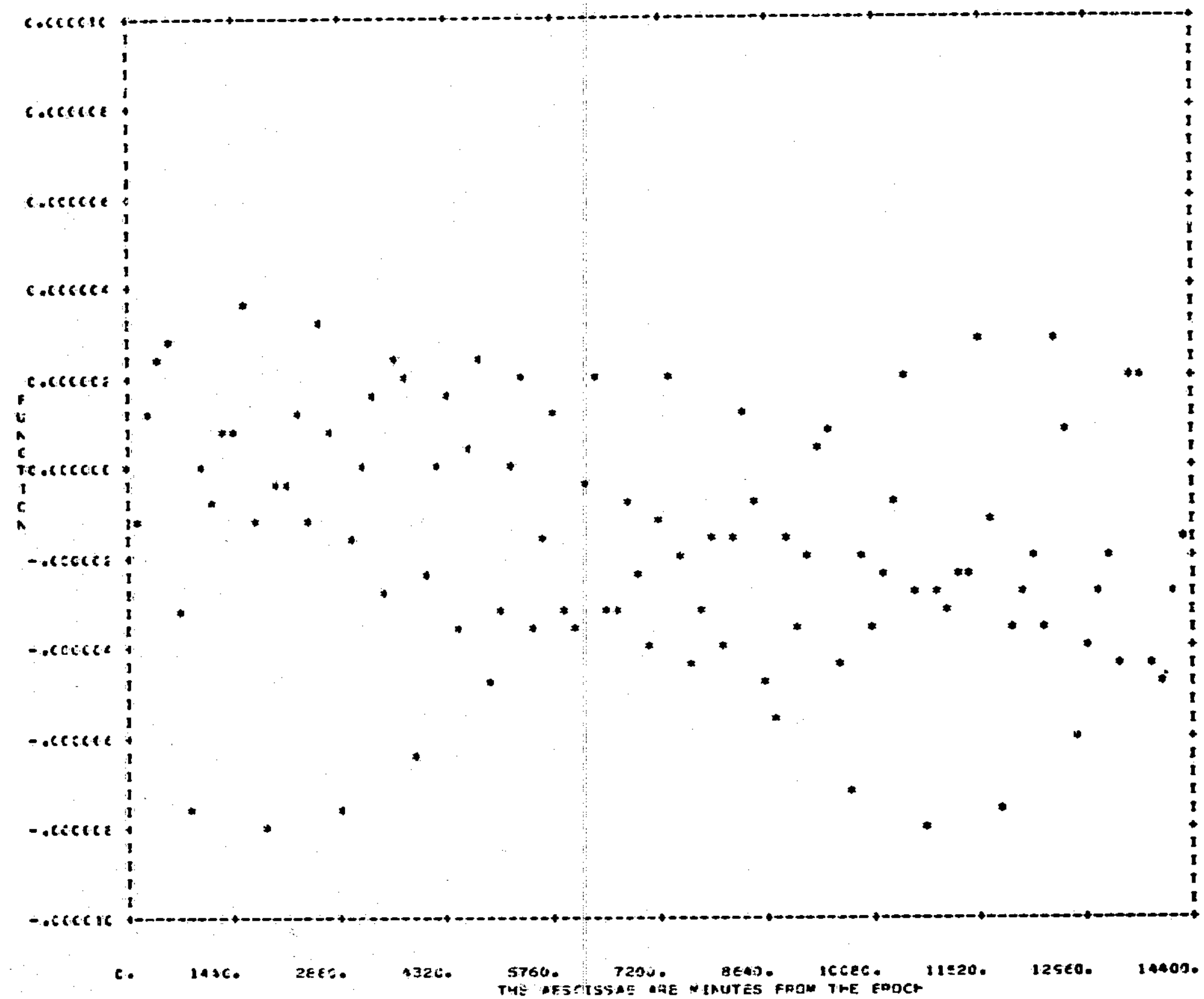

Figure 7c–Plot of Data from Comparison of Orbit 15 Minus Orbit 1 Inclination.

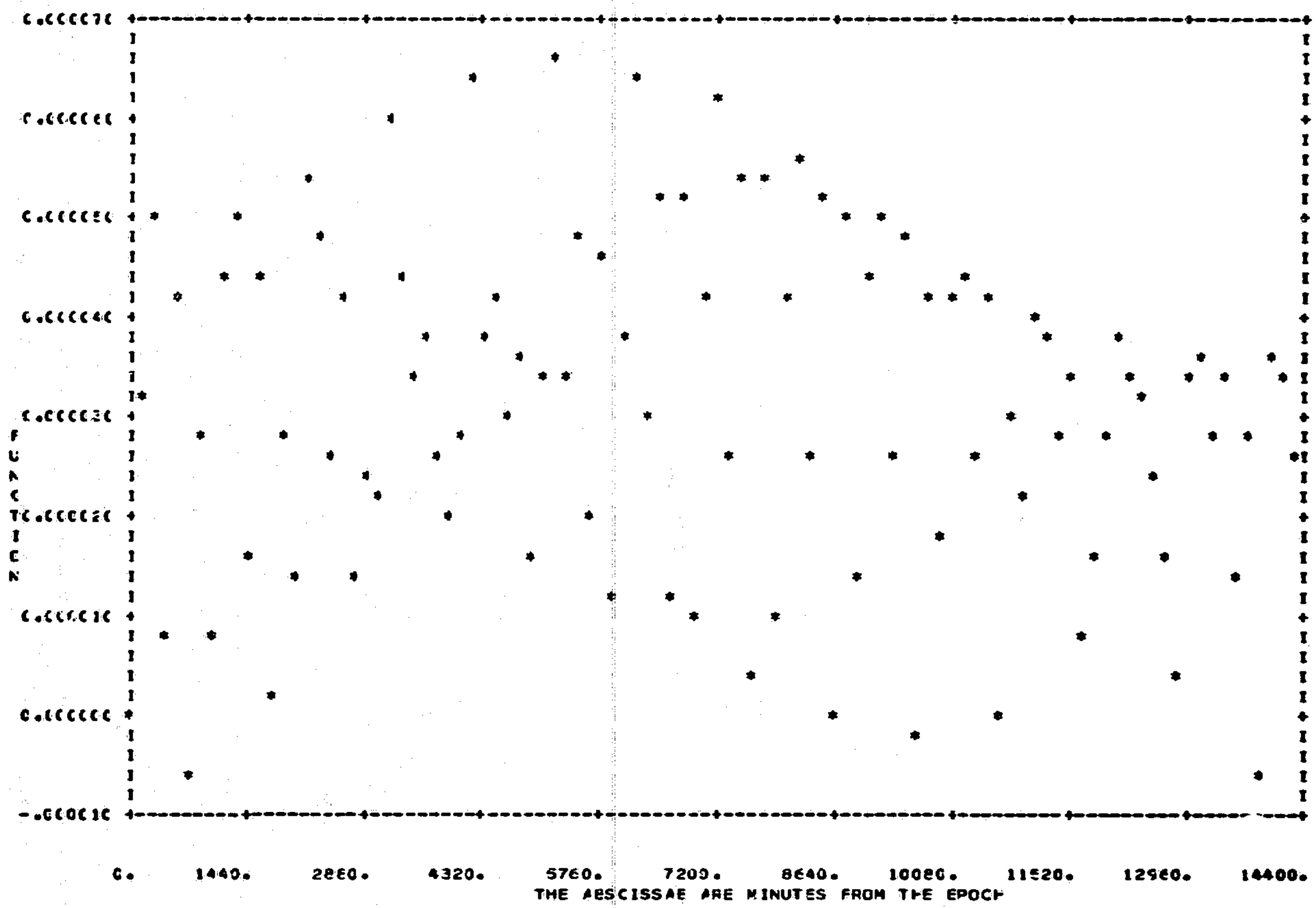

Figure 7d–Plot of Data from Comparison of Orbit 15 Minus Orbit 1 Right Ascension of Ascending Node.

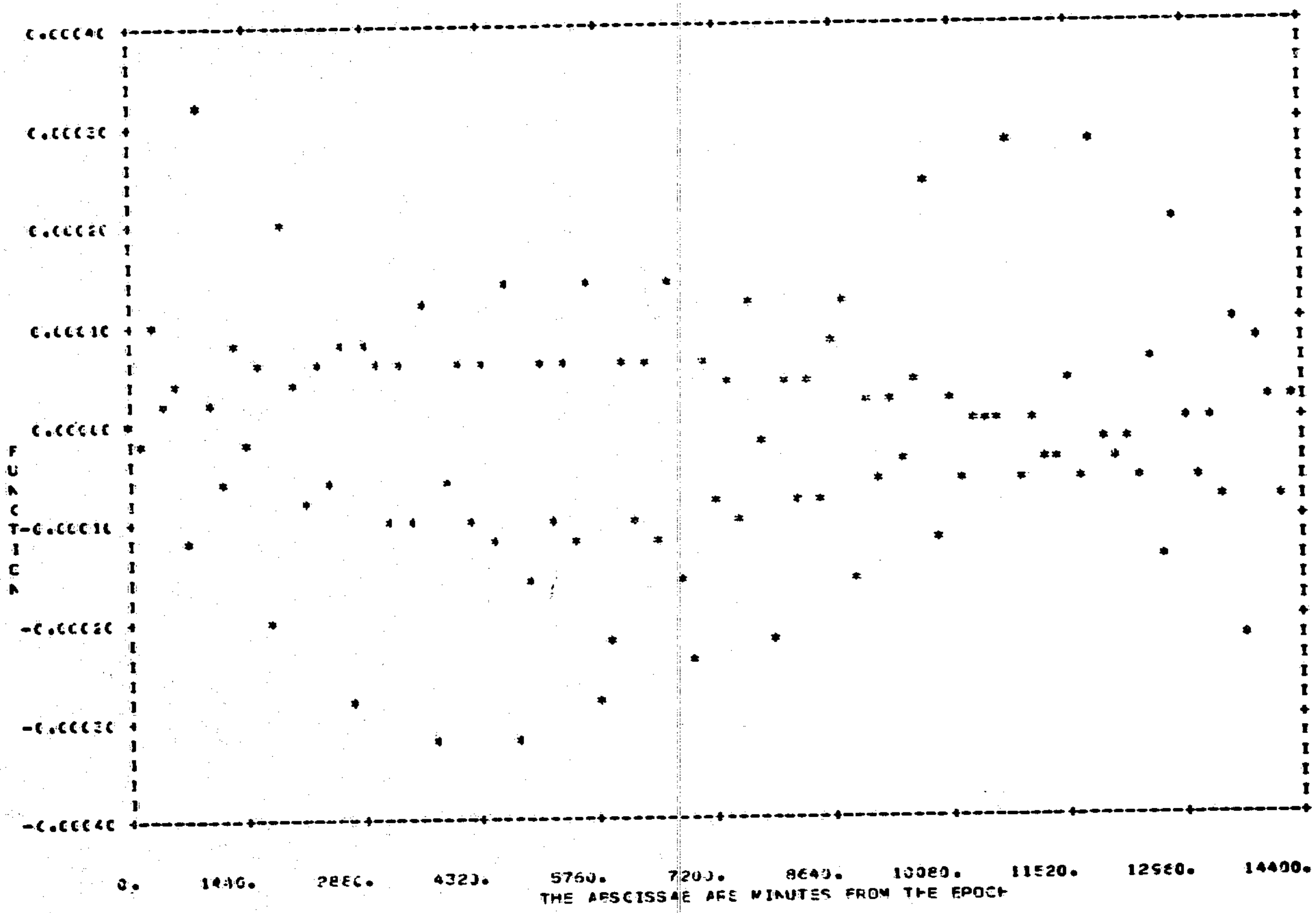

Figure 7e–Plot of Data from Comparison of Orbit 15 Minus Orbit 1 Argument of Perigee.

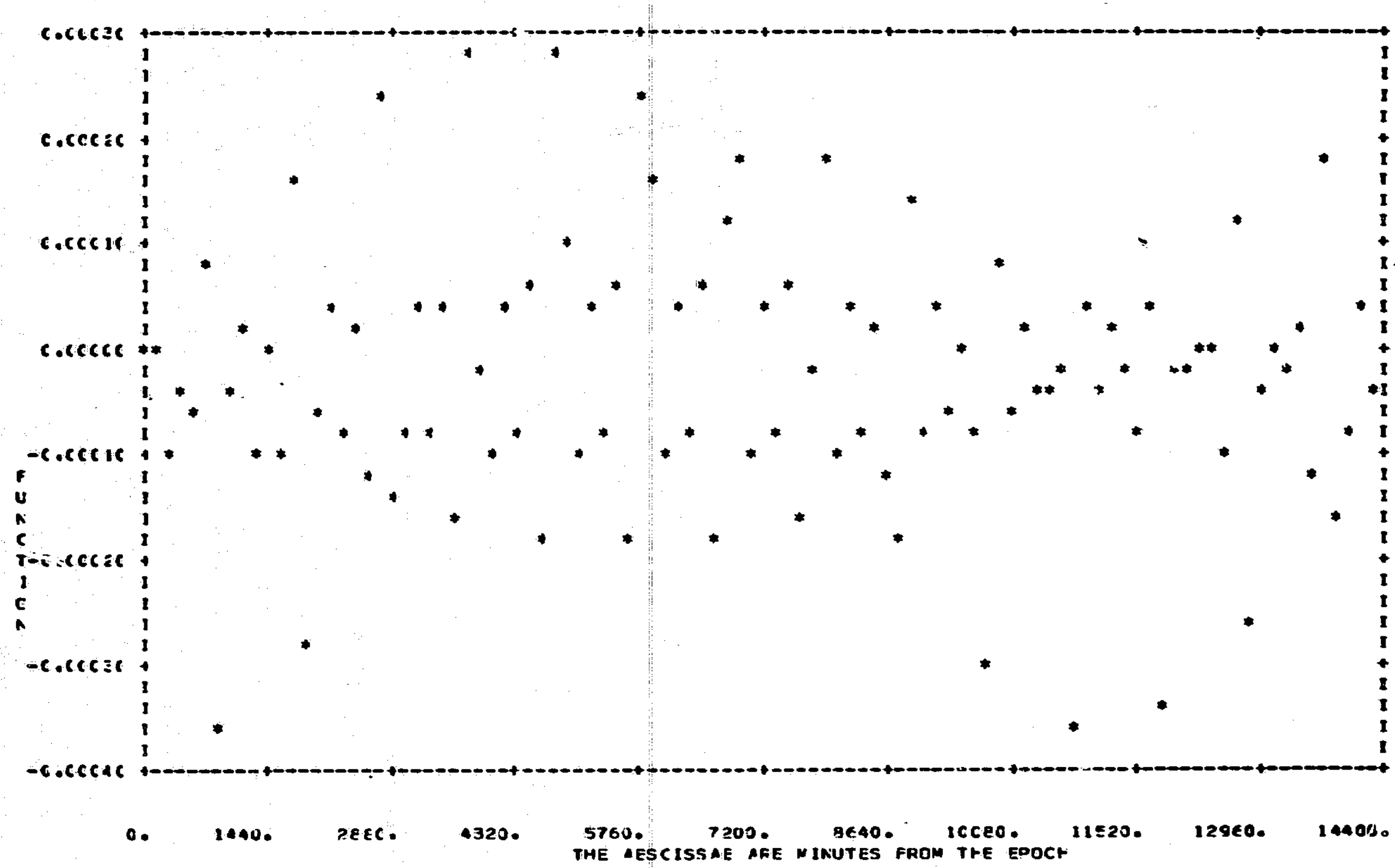

Figure 7f--Plot of Data from Comparison of Orbit 15 Minus Orbit 1 Mean Anomaly.

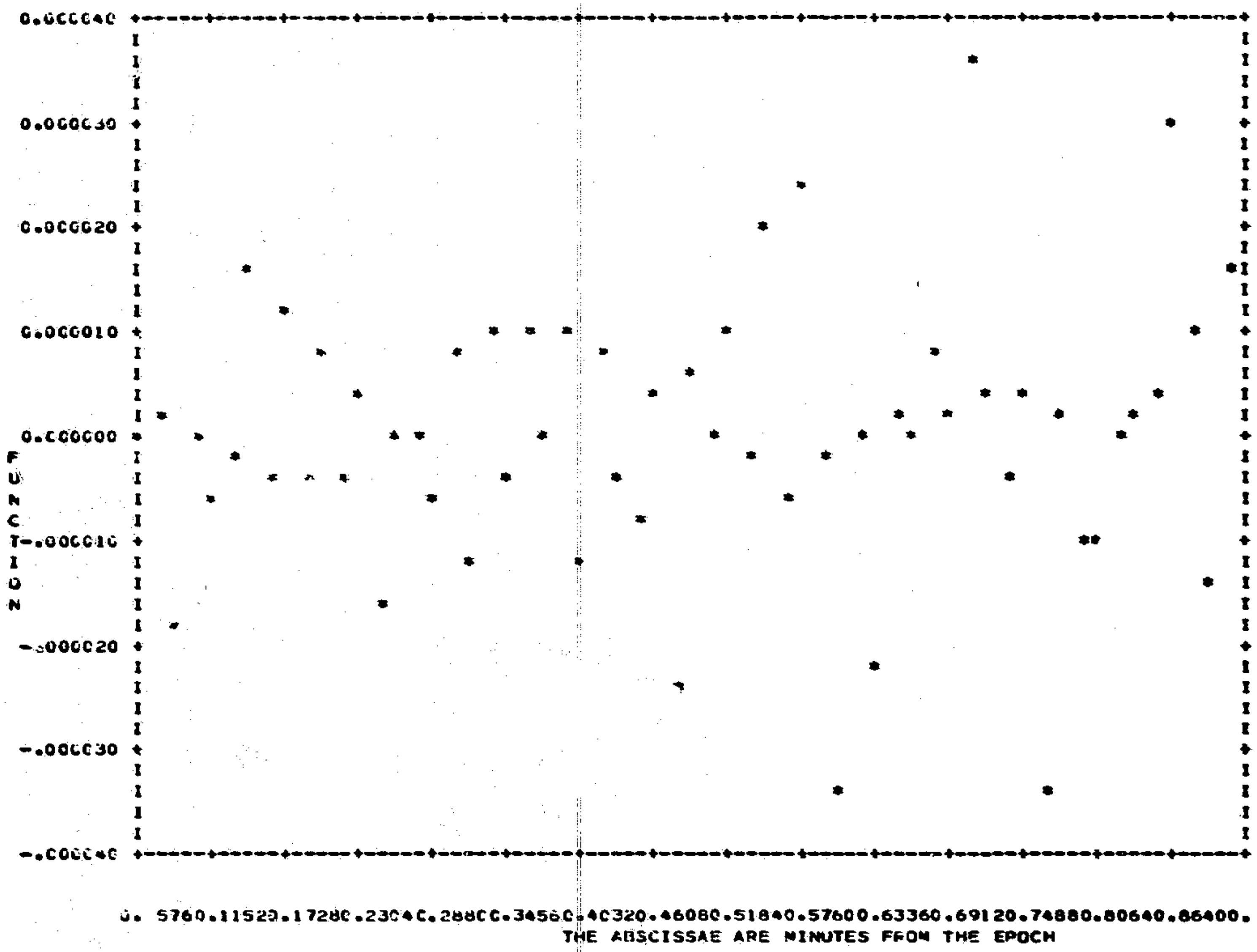

Figure 8a–Plot of Data from Comparison of Orbit 8 Minus Orbit 2 Semi Major Axis.

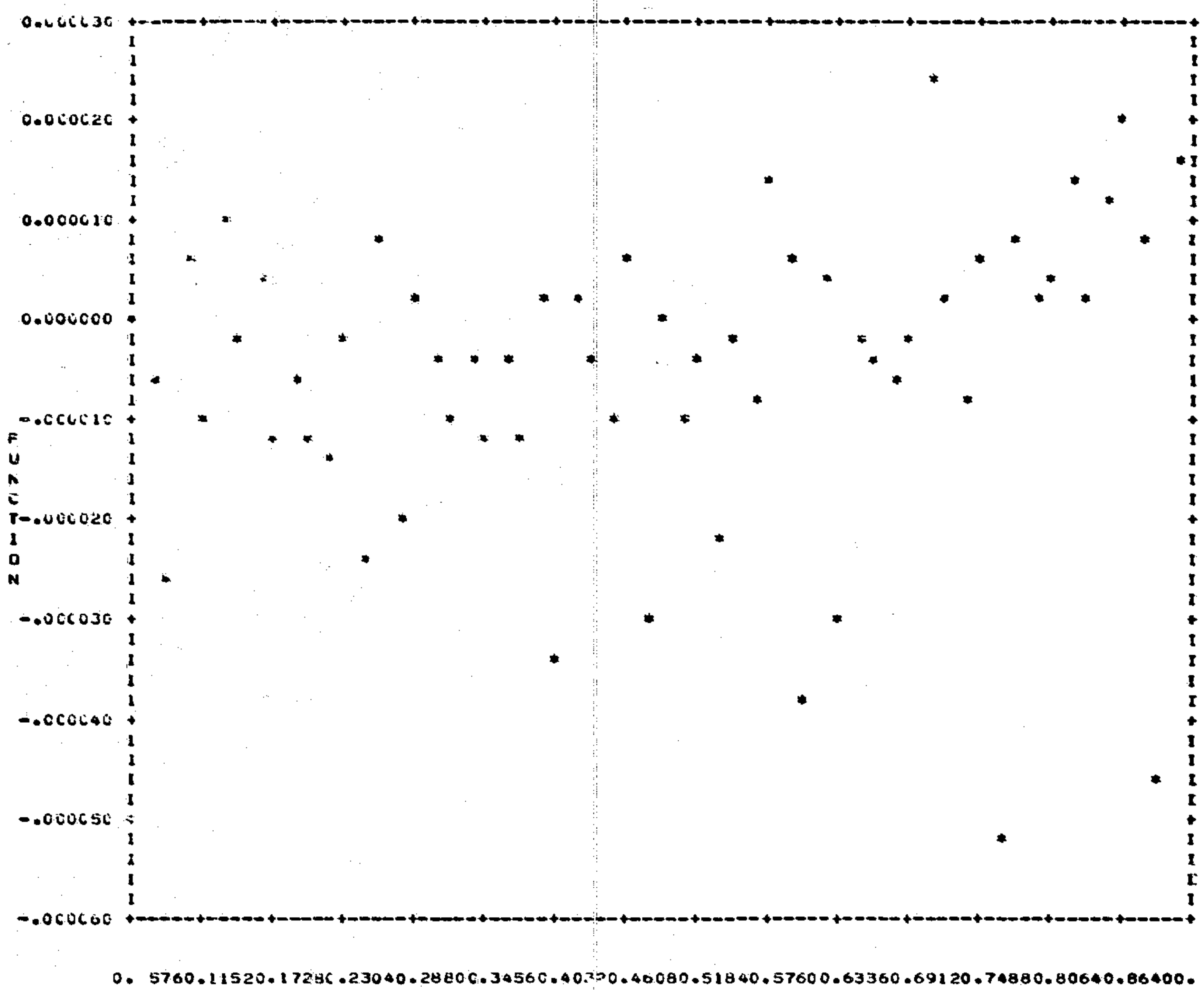

ORDINATES MULTIPLIED BY 10** 1 BEFORE PLOTTING
THE ABSCISSAE ARE MINUTES FROM THE EPOCH

Figure 8b–Plot of Data from Comparison of Orbit 8 Minus Orbit 2 Eccentricity.

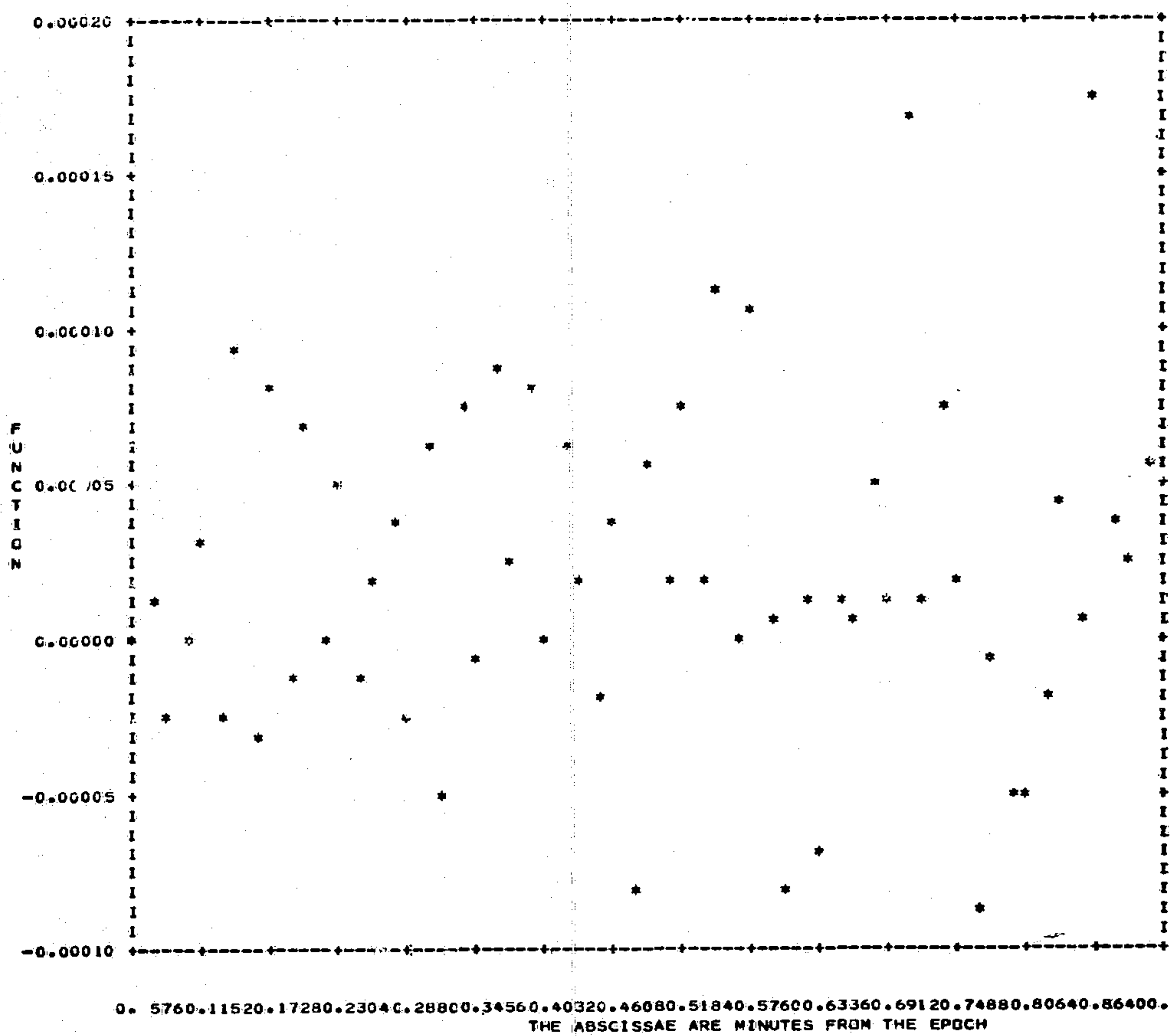

Figure 8c–Plot of Data from Comparison of Orbit 8 Minus Orbit 2 Inclination.

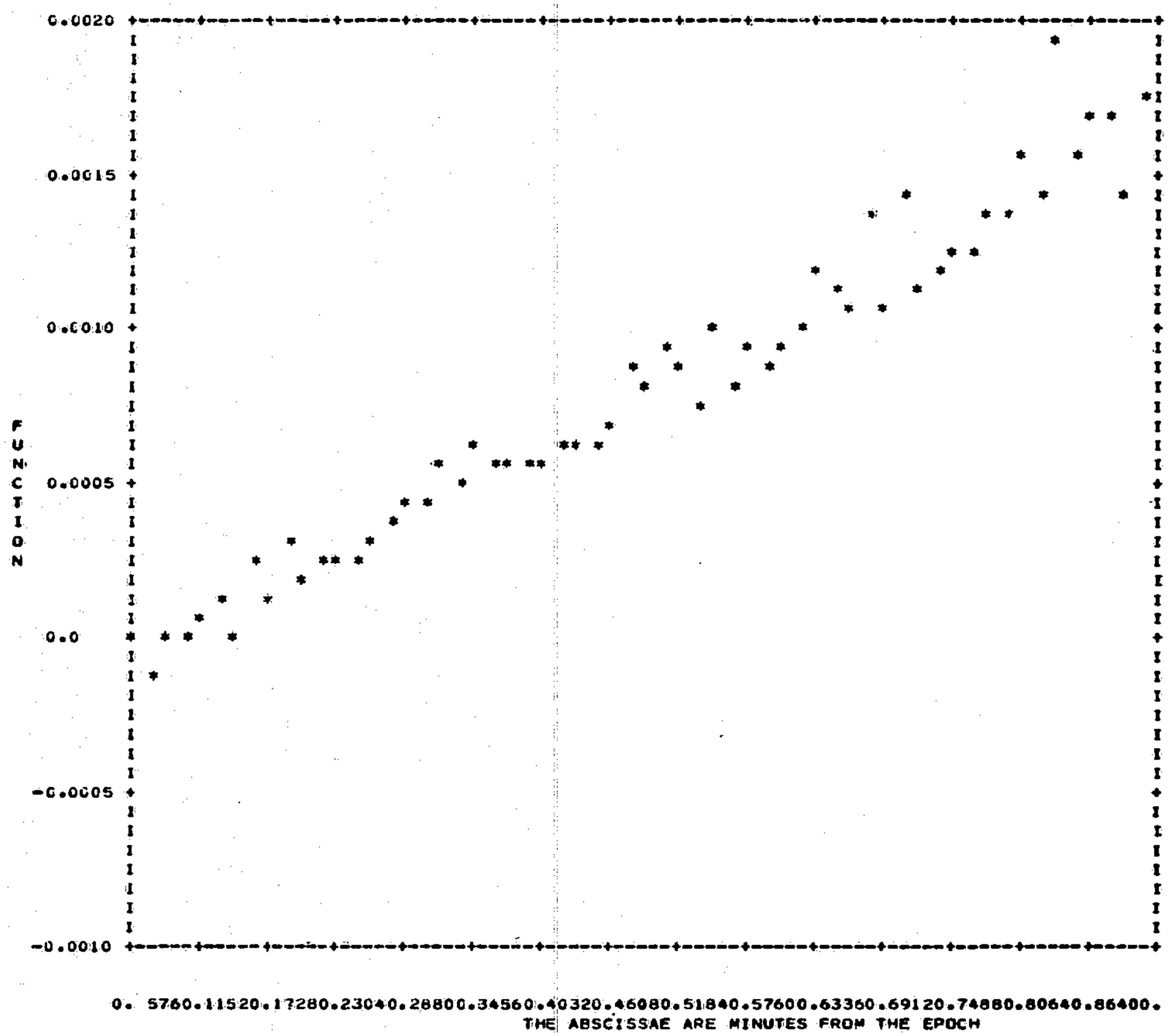

Figure 8d–Plot of Data from Comparison of Orbit 8 Minus Orbit 2 Right Ascension of Ascending Node.

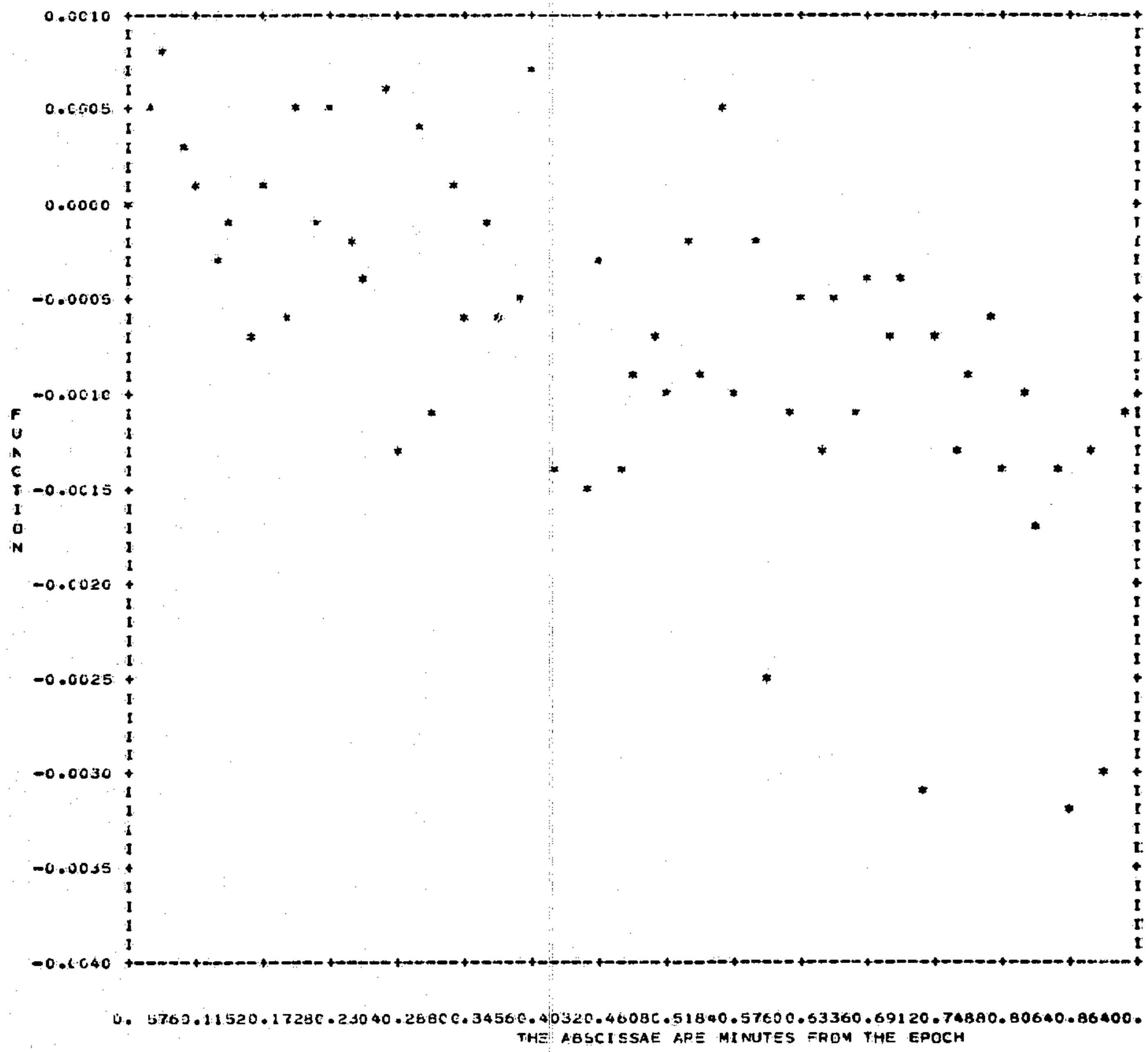

Figure 8e–Plot of Data from Comparison of Orbit 8 Minus Orbit 2 Argument of Perigee.

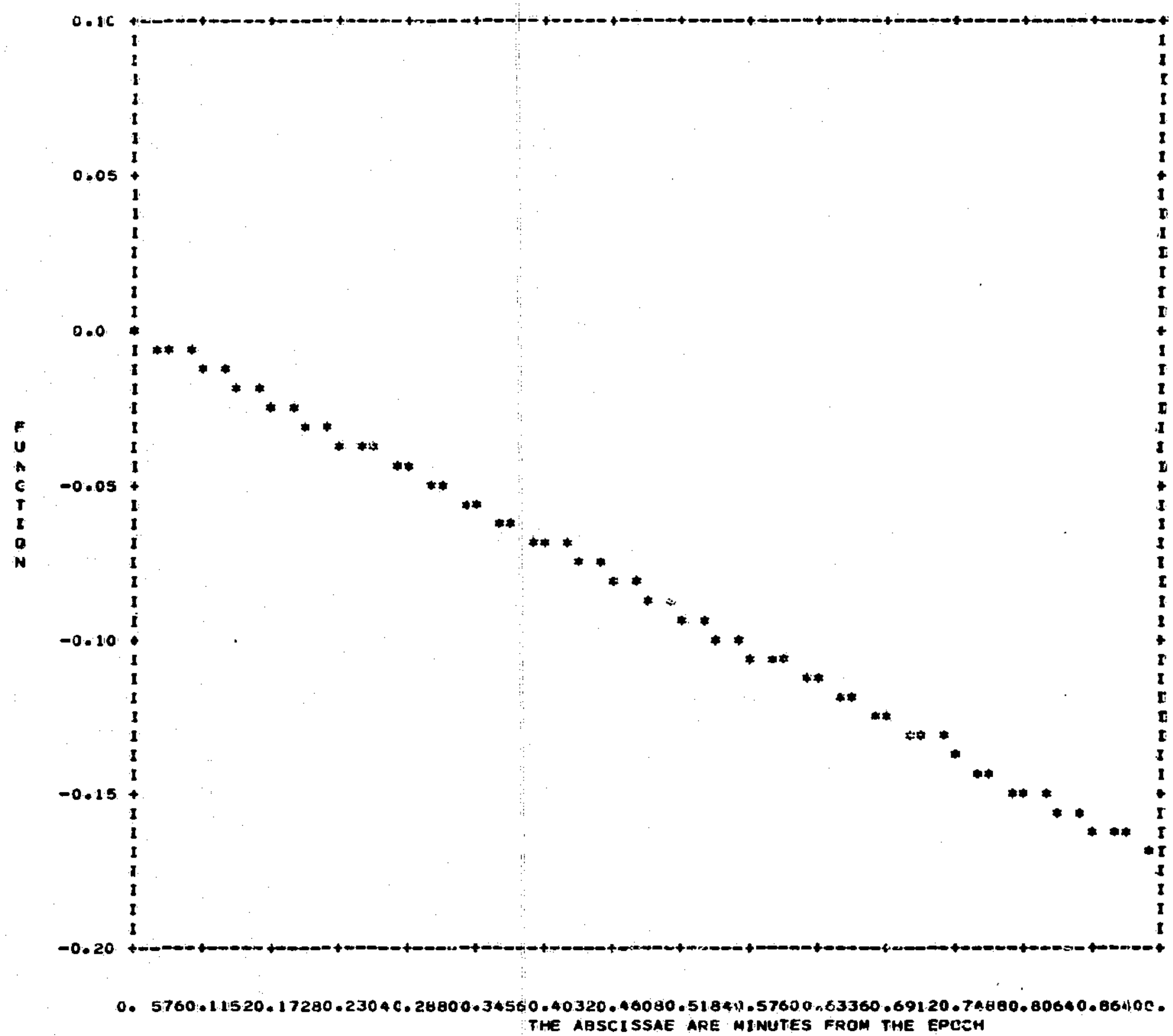

Figure 8f–Plot of Data from Comparison of Orbit 8 Minus Orbit 2 Mean Anomaly.

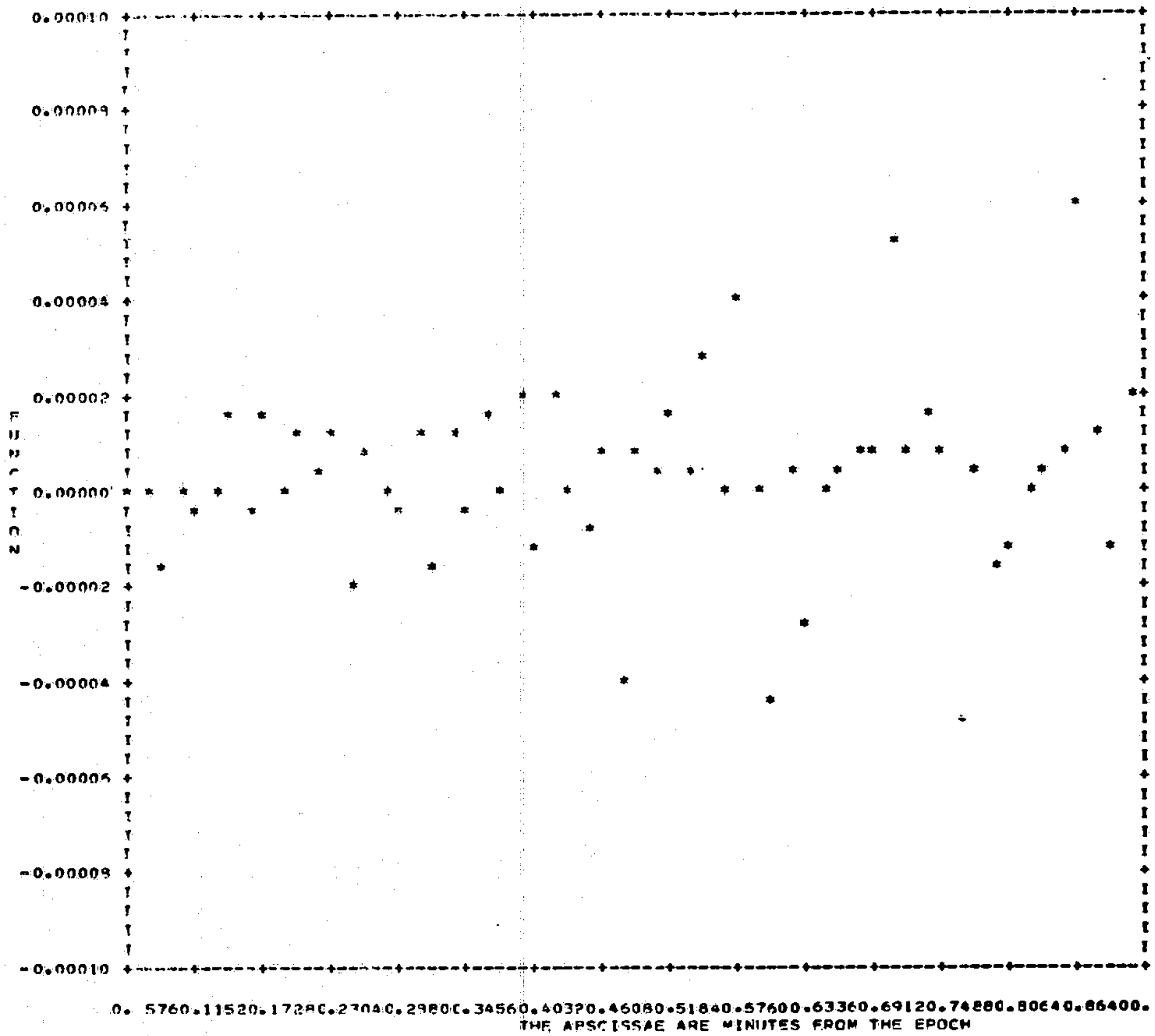

Figure 9a–Plot of Data from Comparison of Orbit 10 Minus Orbit 2 Semi Major Axis.

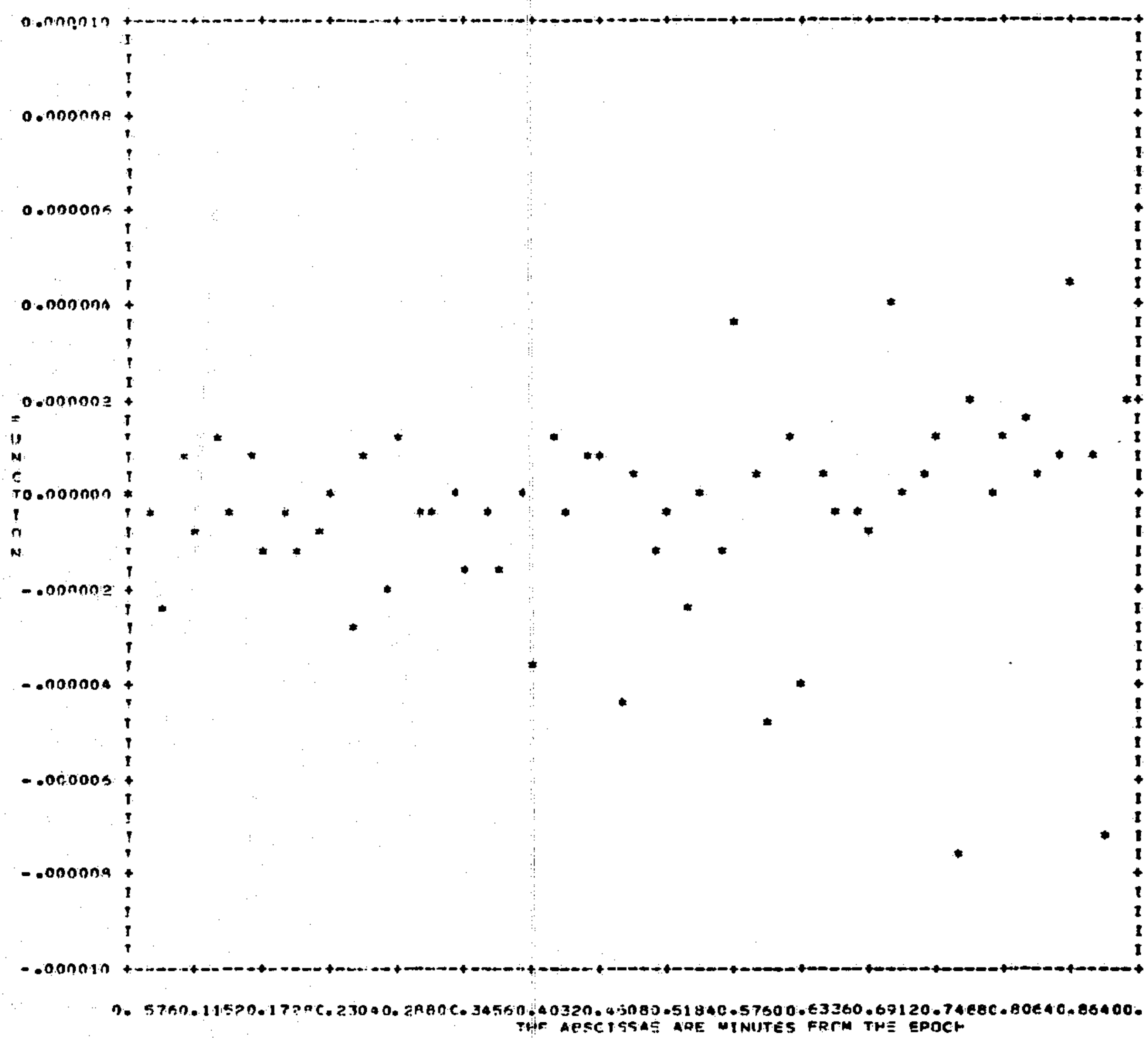

Figure 9b–Plot of Data from Comparison of Orbit 10 Minus Orbit 2 Eccentricity.

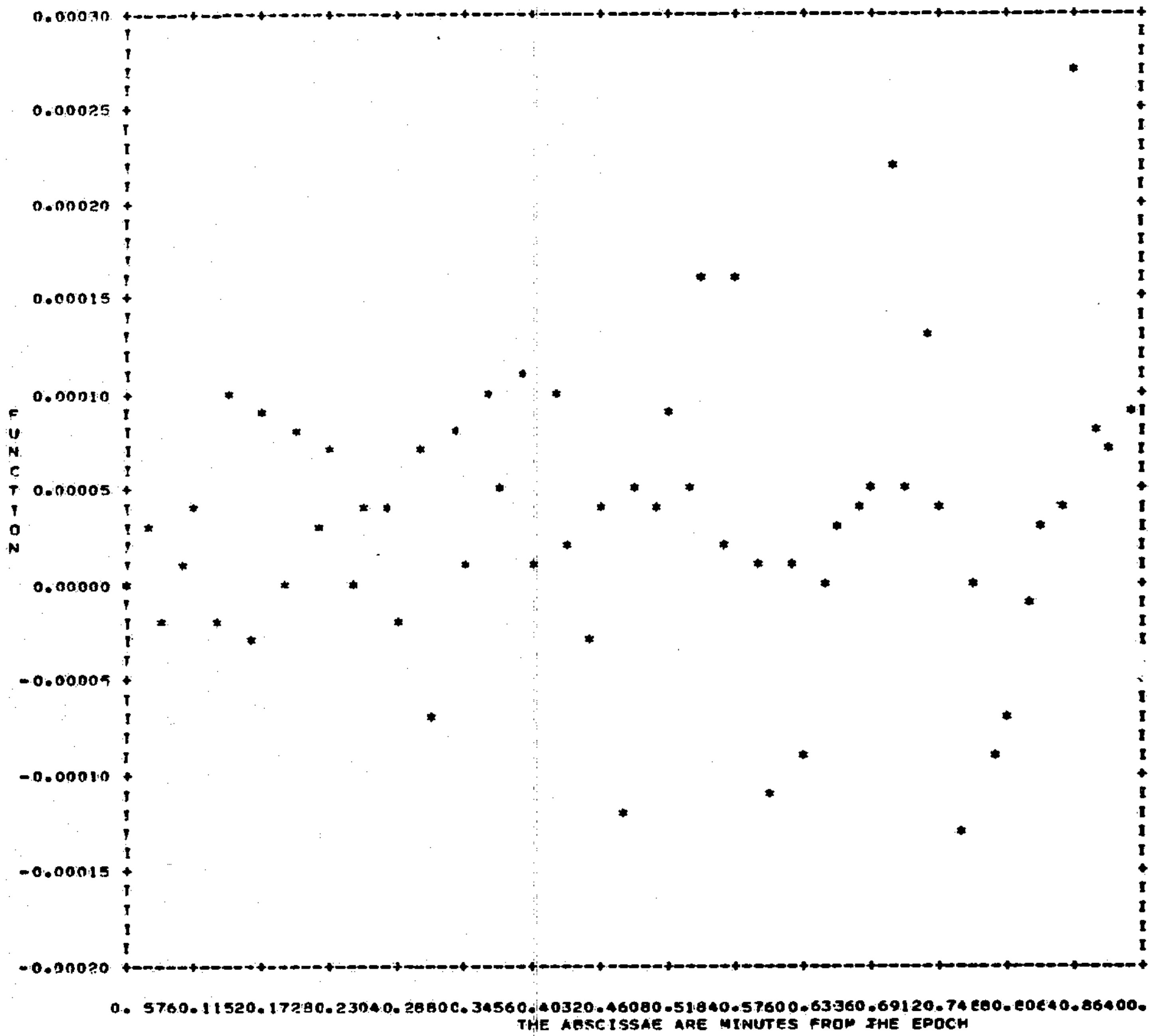

Figure 9c–Plot of Data from Comparison of Orbit 10 Minus Orbit 2 Inclination.

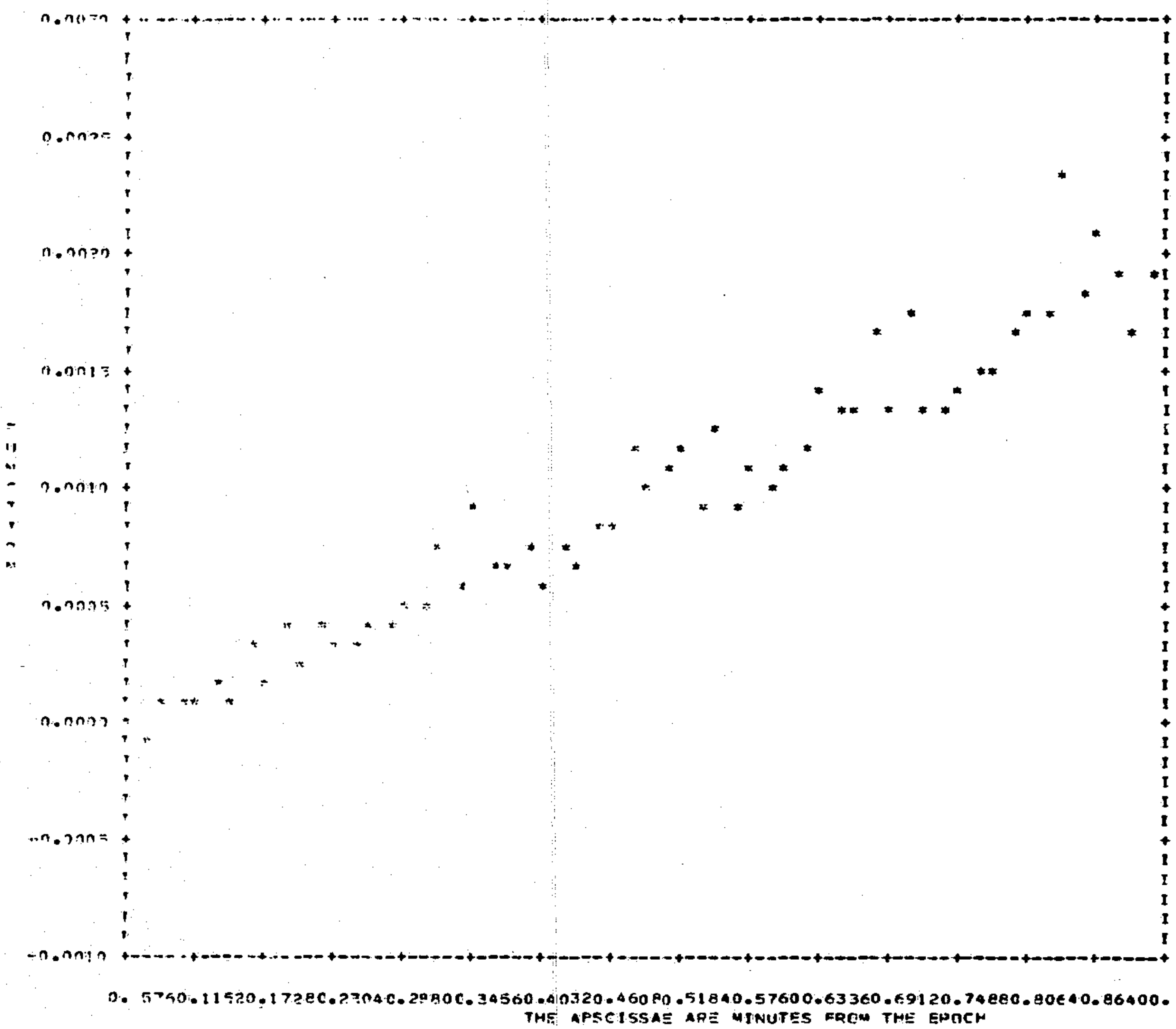

Figure 9d–Plot of Data from Comparison of Orbit 10 Minus Orbit 2 Right Ascension of Ascending Node.

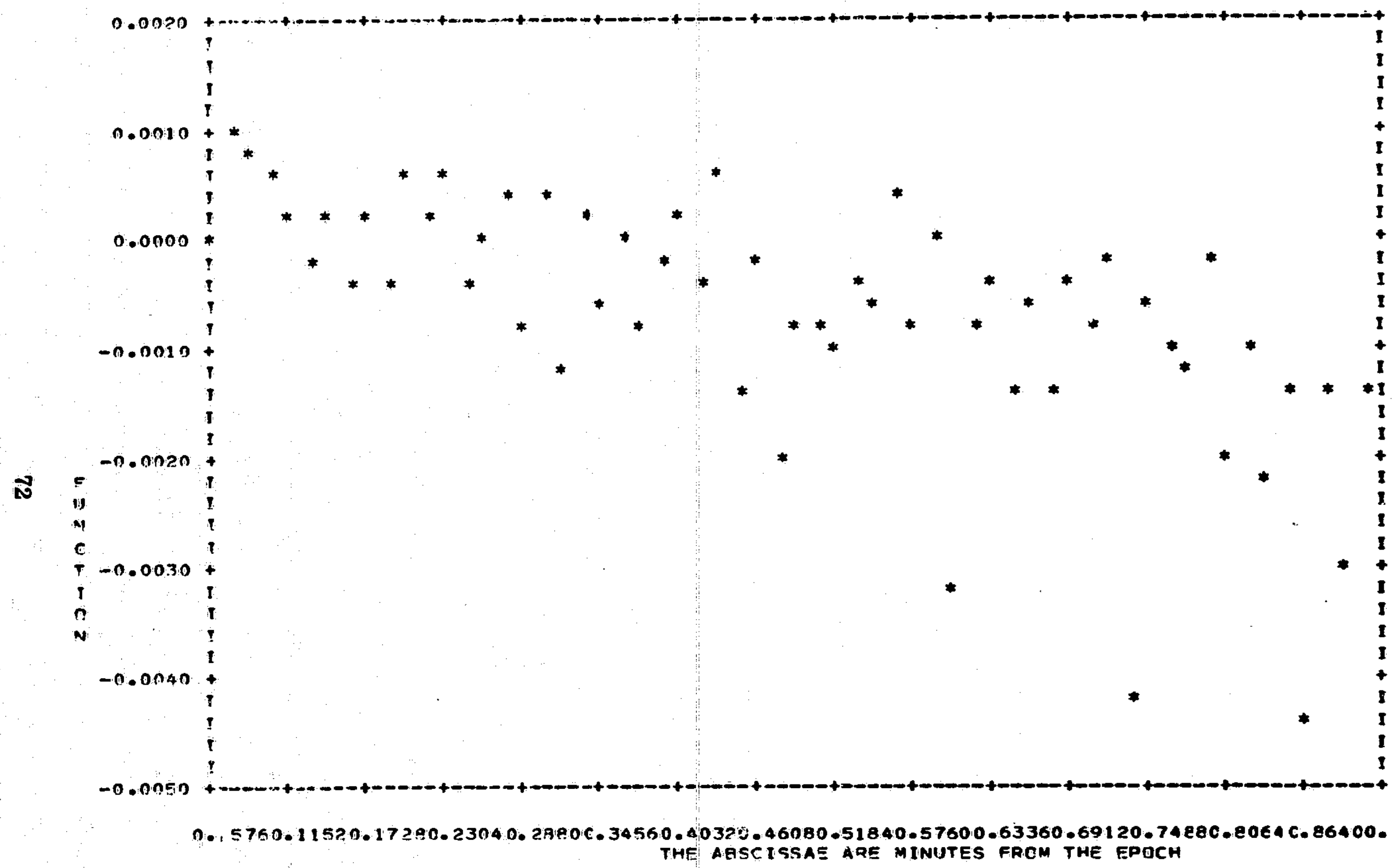

Figure 9e–Plot of Data from Comparison of Orbit 10 Minus Orbit 2 Argument of Perigee.

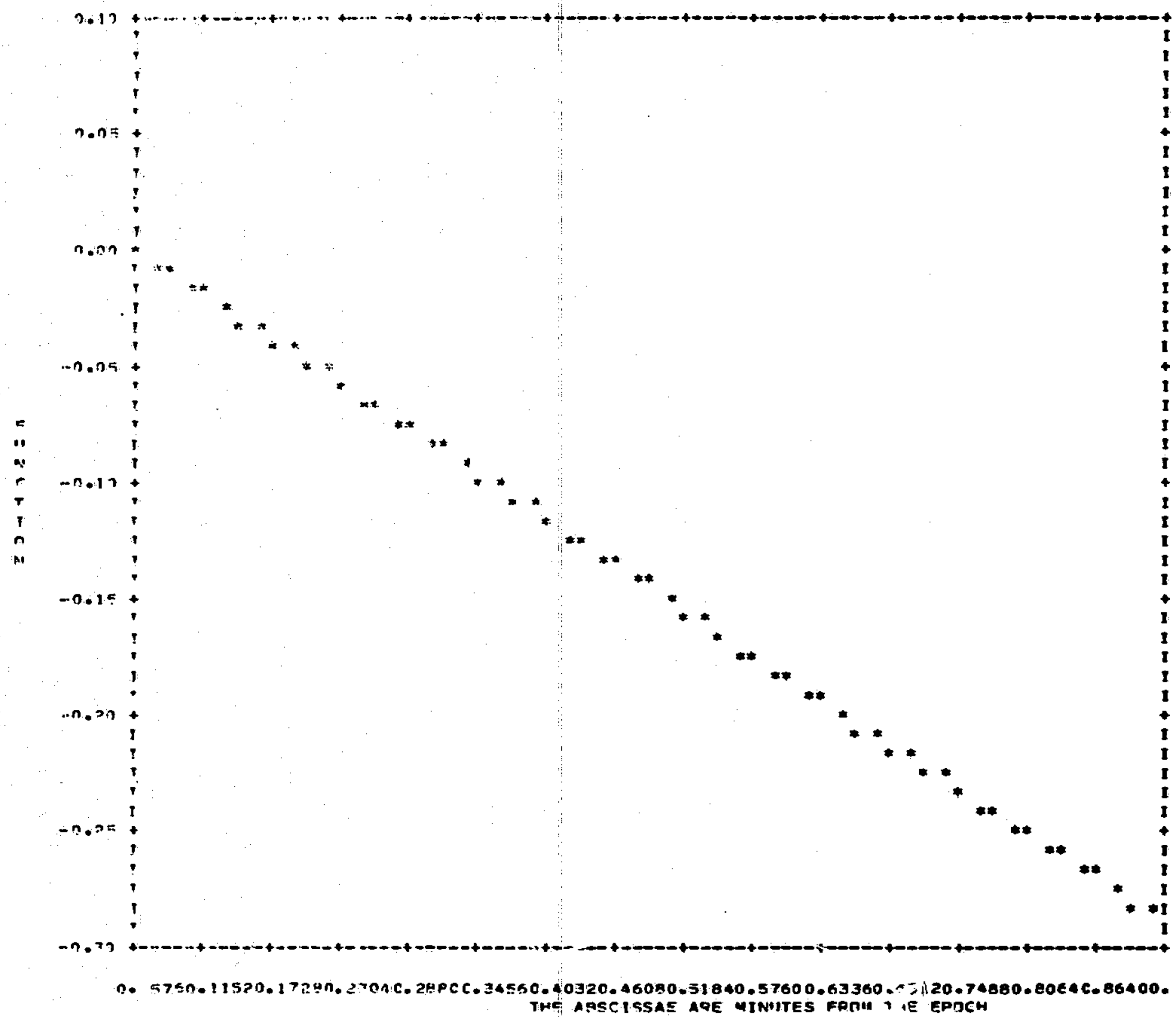

Figure 9f–Plot of Data from Comparison of Orbit 10 Minus Orbit 2 Mean Anomaly.

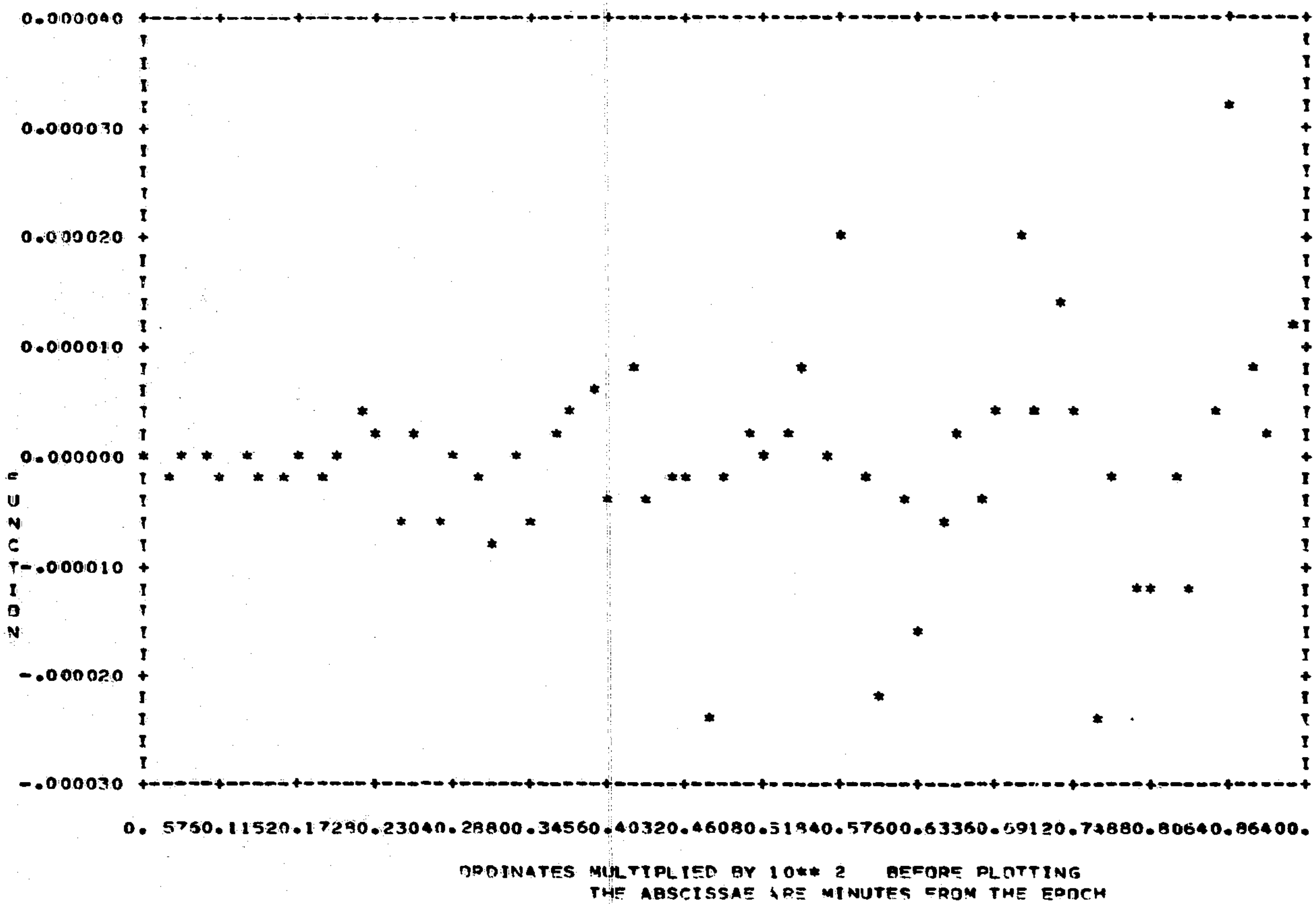

Figure 10a–Plot of Data from Comparison of Orbit 12 Minus Orbit 2 Semi Major Axis.

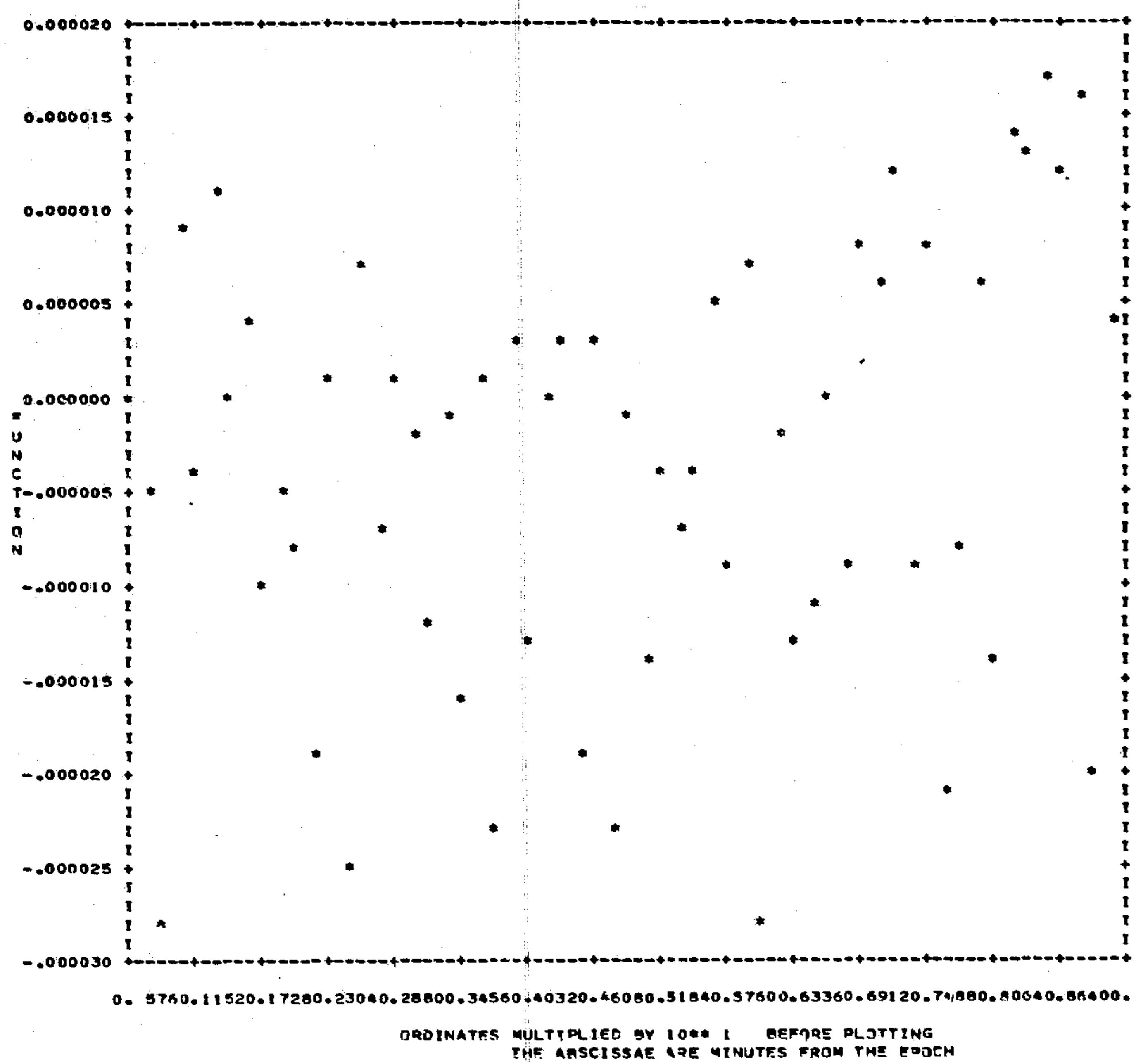

Figure 10b-Plot of Data from Comparison of Orbit 12 Minus Orbit 2 Eccentricity.

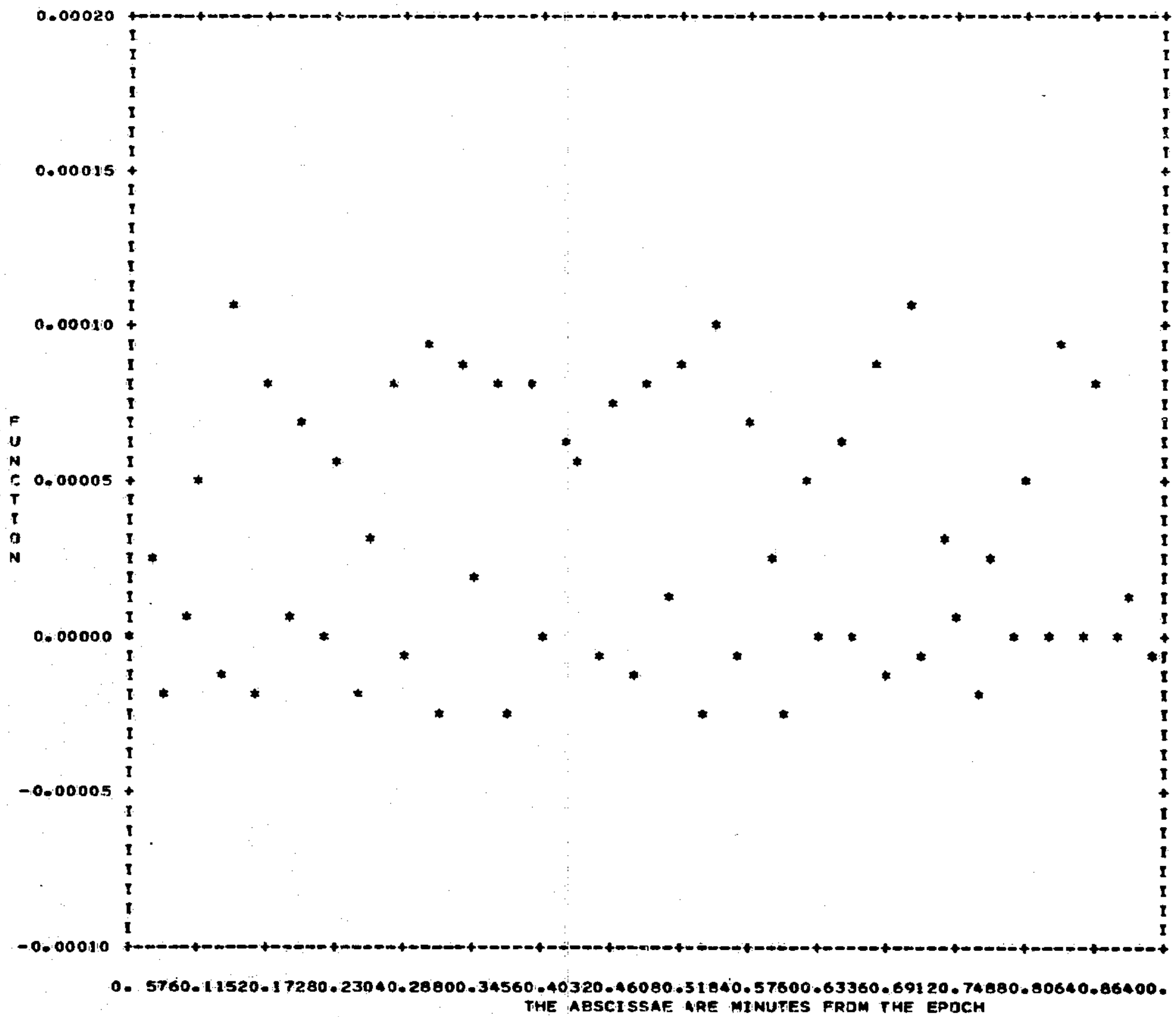

Figure 10c–Plot of Data from Comparison of Orbit 12 Minus Orbit 2 Inclination.

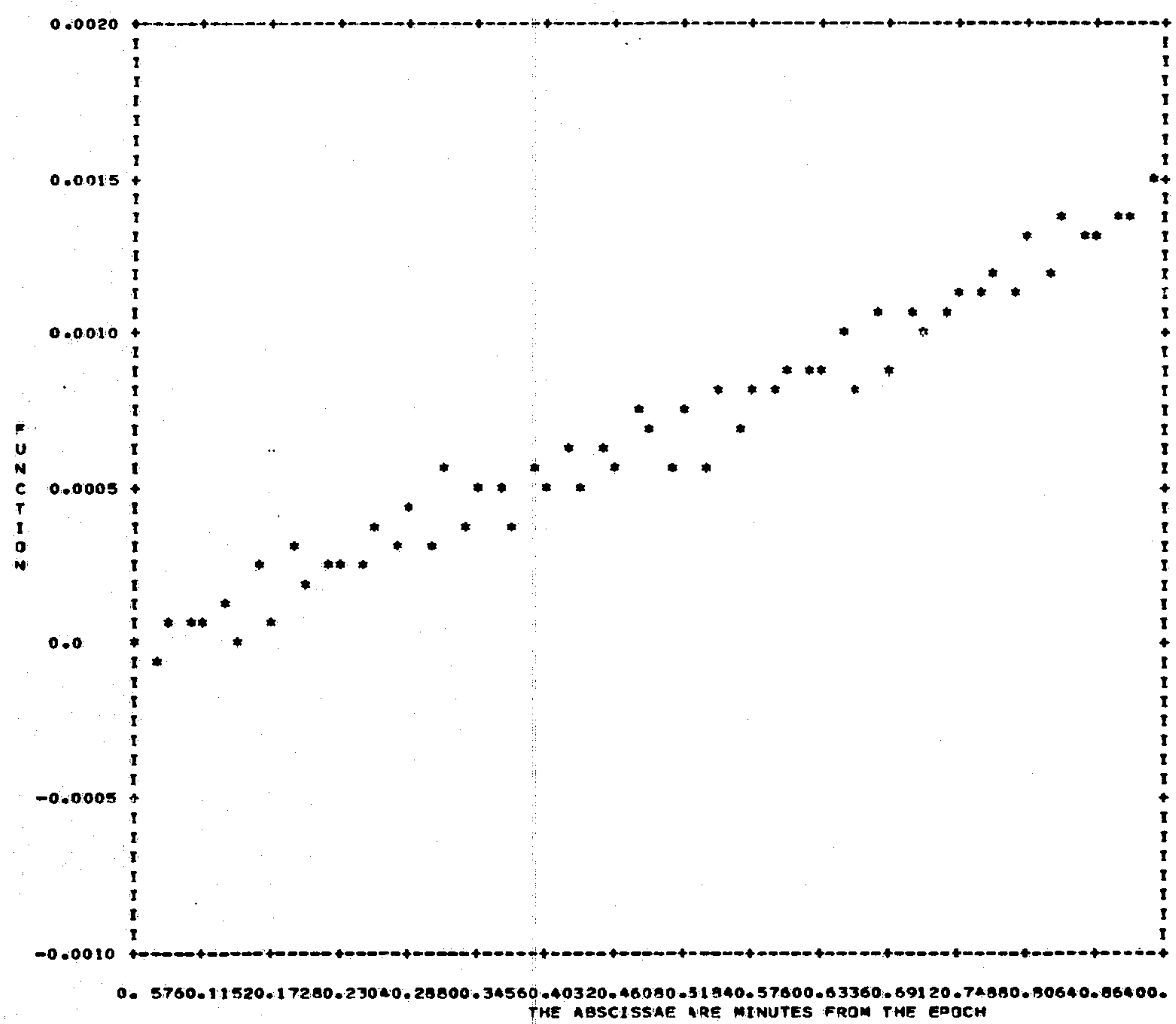

Figure 10d–Plot of Data from Comparison of Orbit 12 Minus Orbit 2 Right Ascension of Ascending Node.

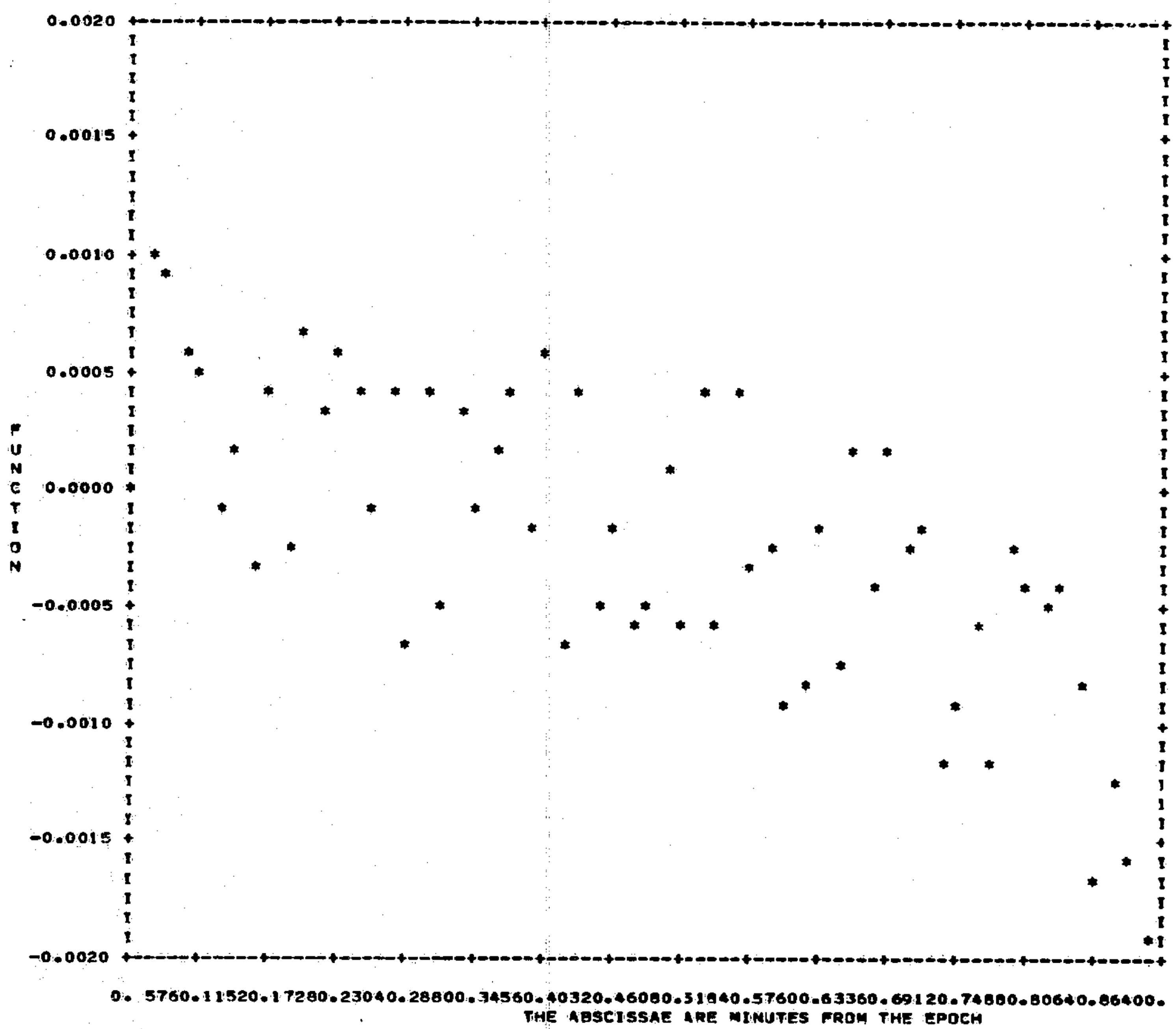

Figure 10e–Plot of Data from Comparison of Orbit 12 Minus Orbit 2 Argument of Perigee.

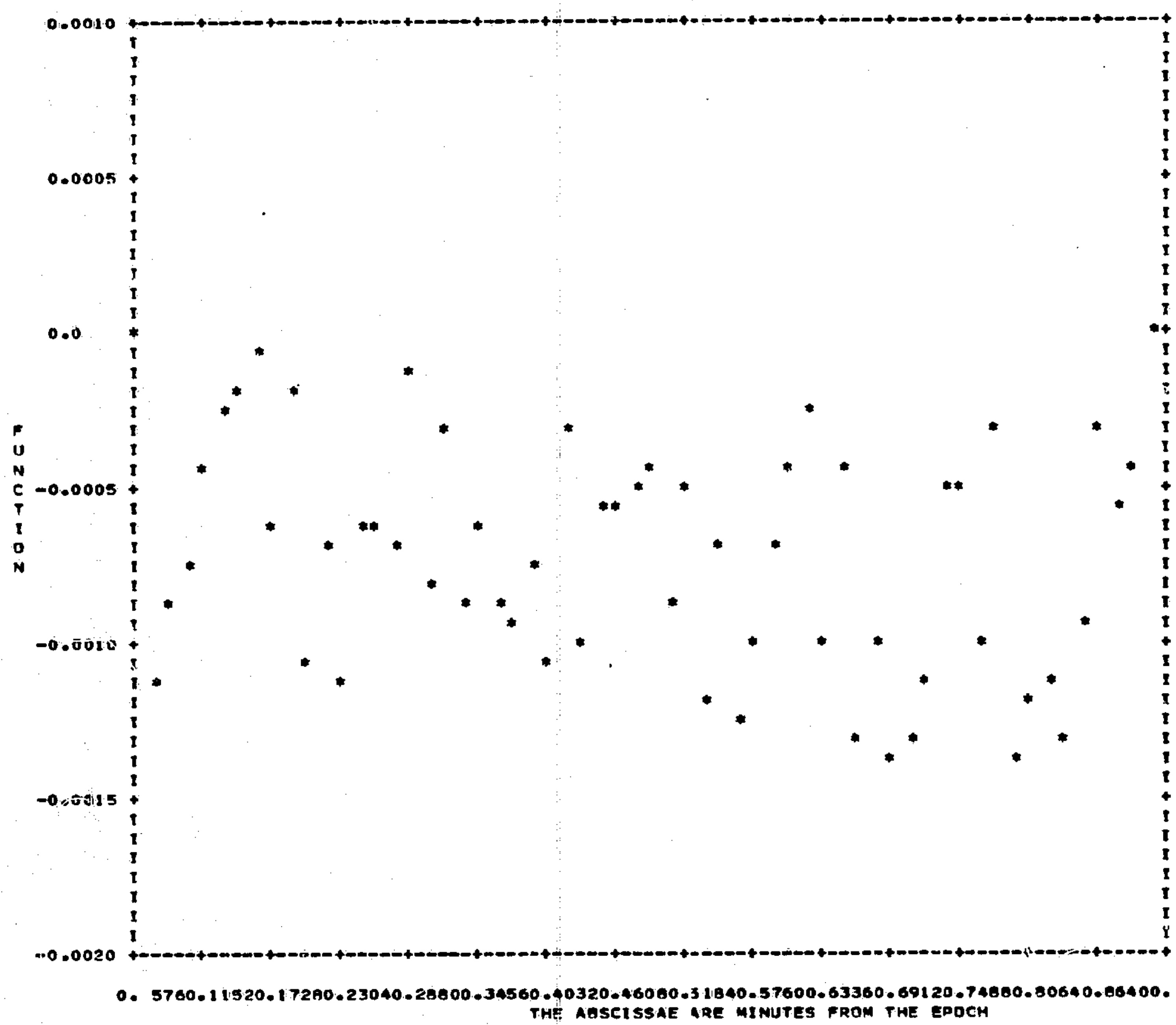

Figure 10f–Plot of Data from Comparison of Orbit 12 Minus Orbit 2 Mean Anomaly.

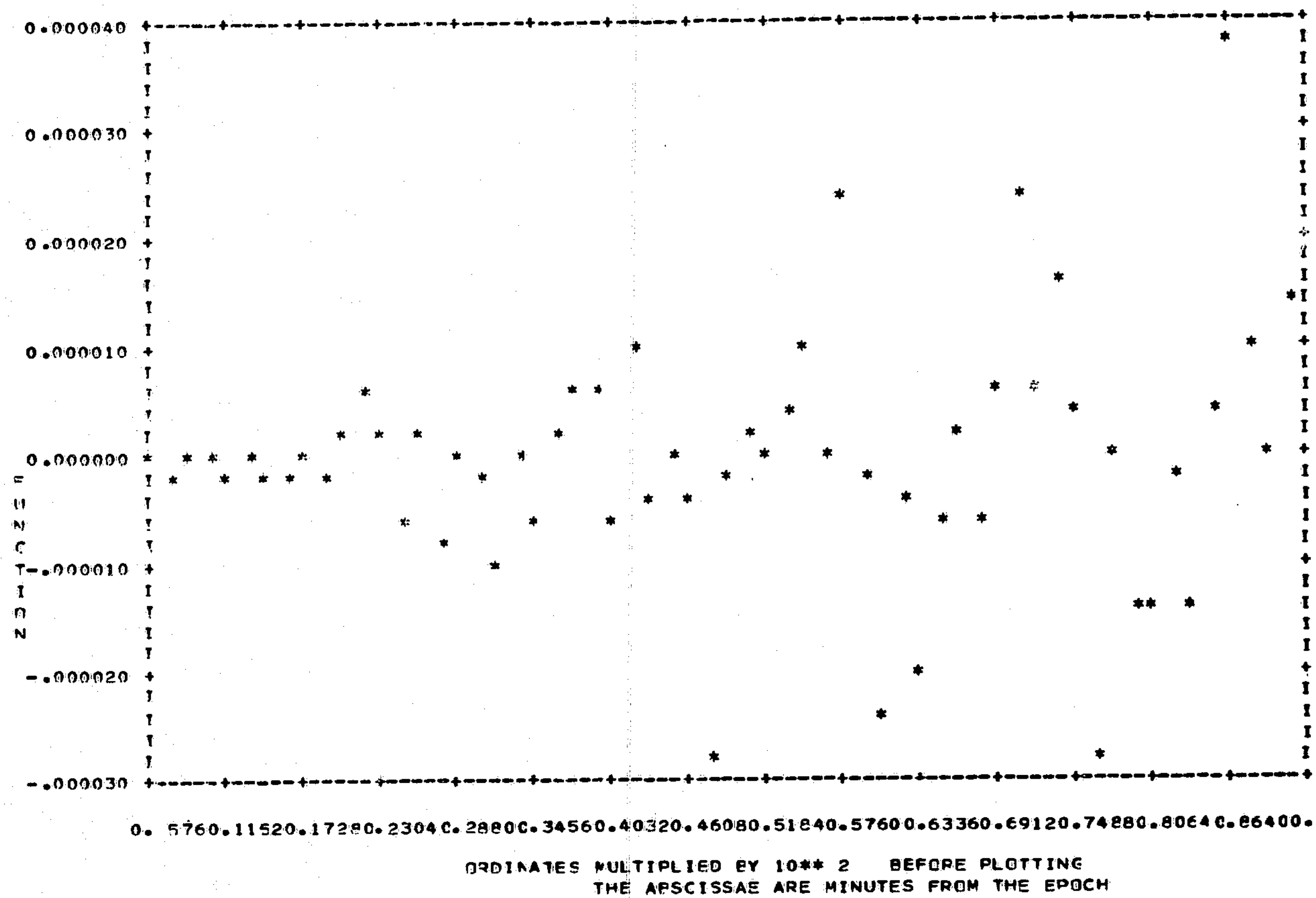

Figure 11a-Plot of Data from Comparison of Orbit 14 Minus Orbit 2 Semi Major Axis.

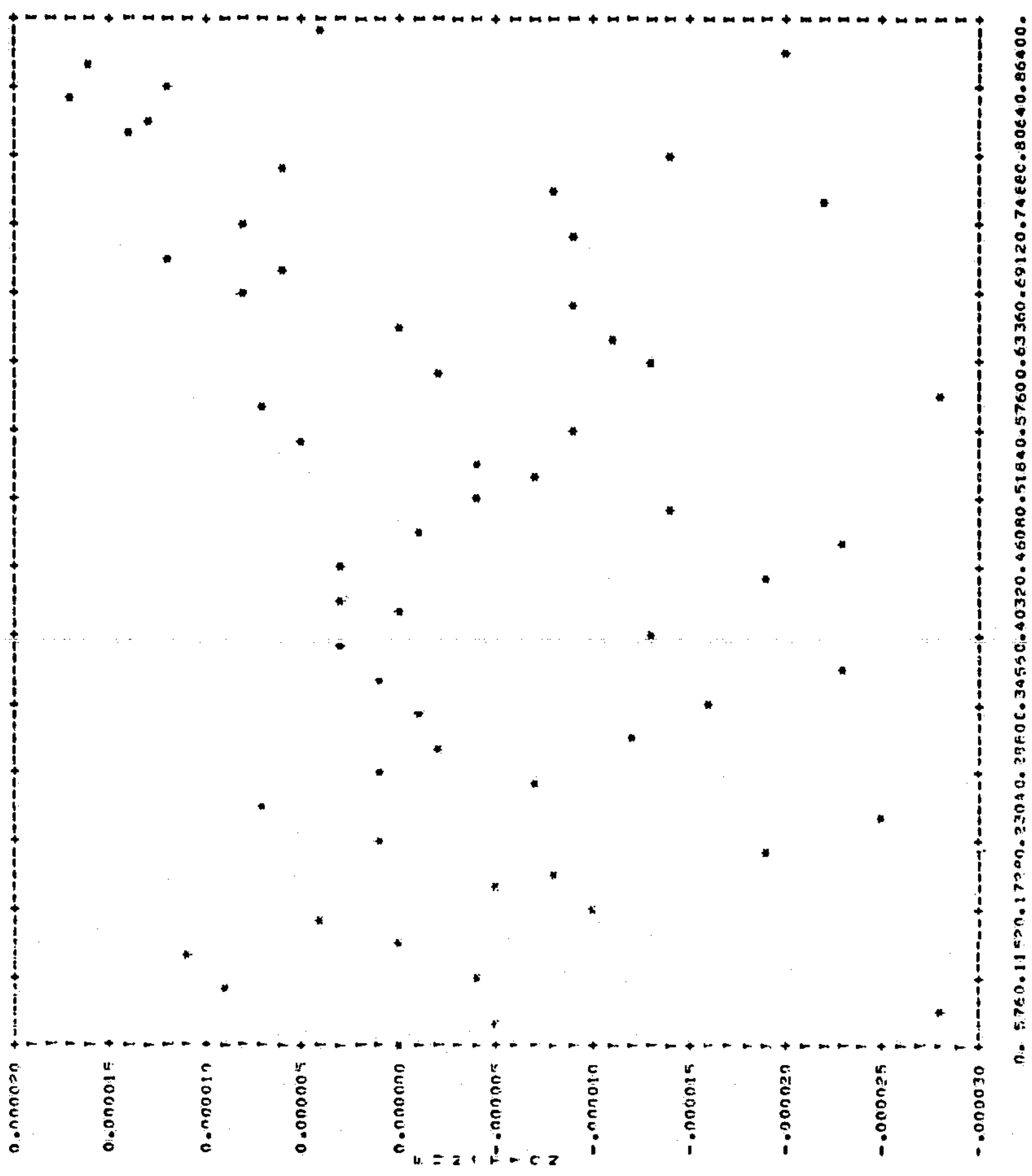

Figure 11b-Plot of Data from Comparison of Orbit 14 Minus Orbit 2 Eccentricity.

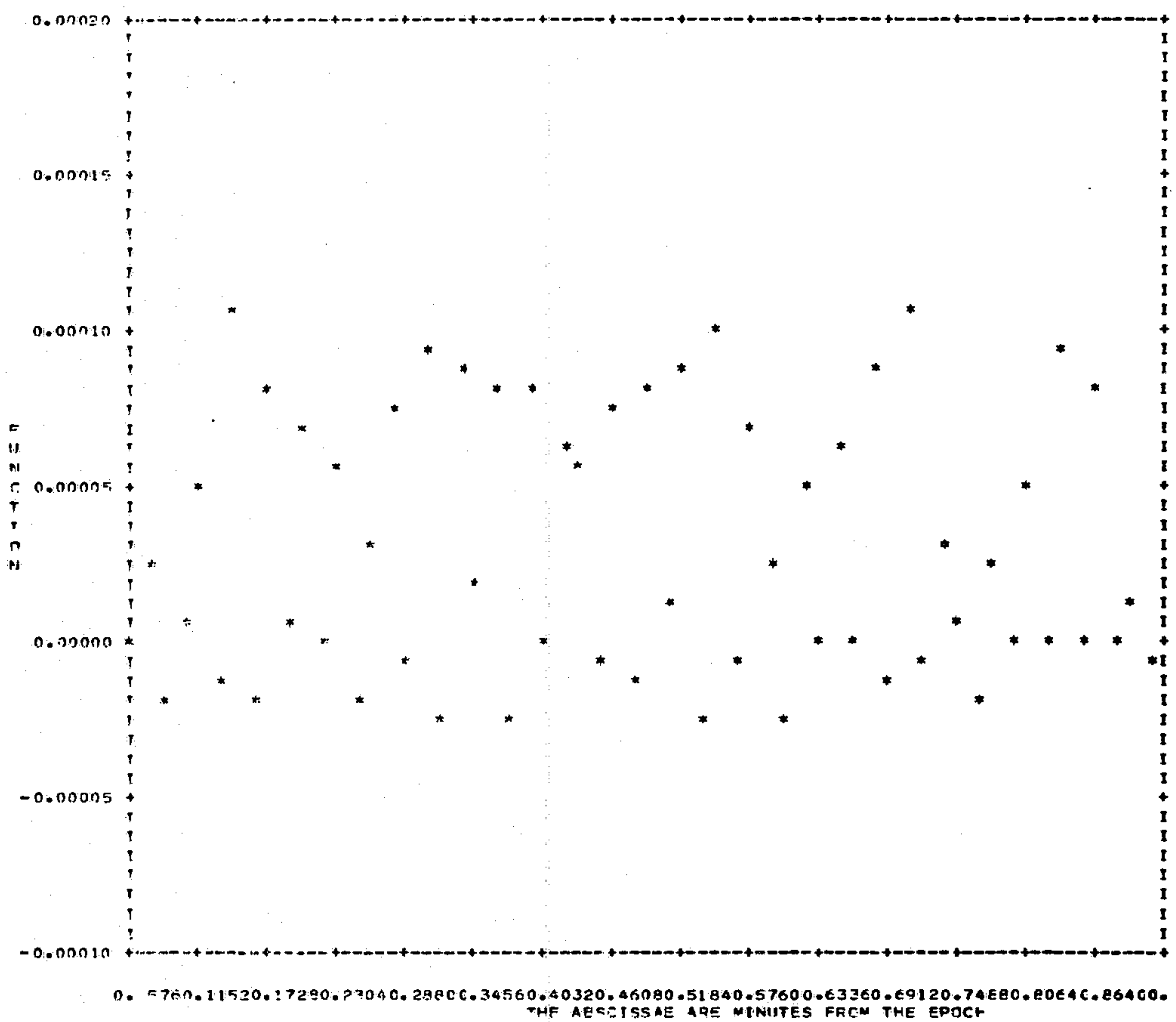

Figure 11c–Plot of Data from Comparison of Orbit 14 Minus Orbit 2 Inclination

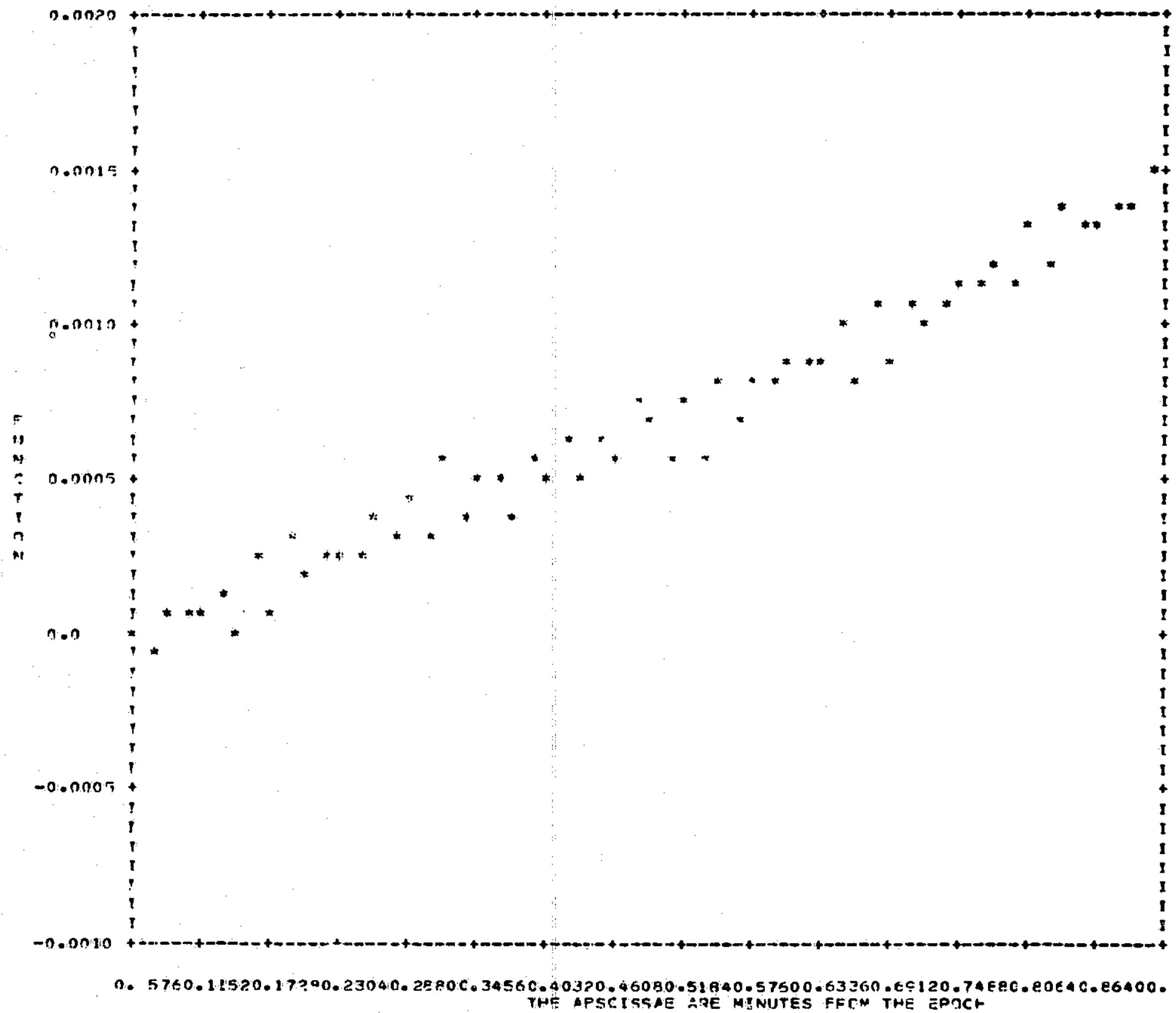

Figure 11d–Plot of Data from Comparison of Orbit 14 Minus Orbit 2 Right Ascension of Ascending Node.

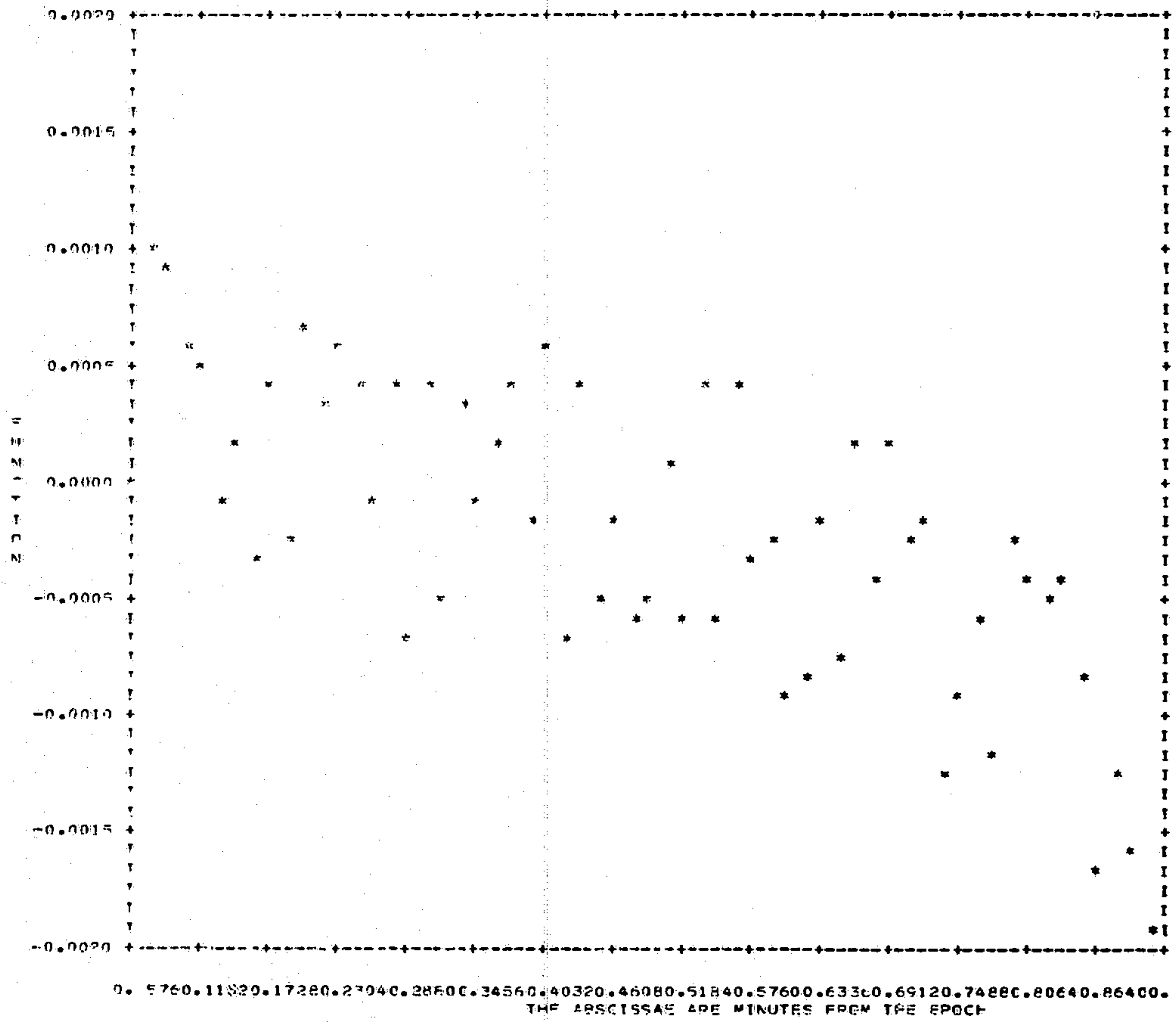

Figure 11e–Plot of Data from Comparison of Orbit 14 Minus Orbit 2 Argument of Perigee.

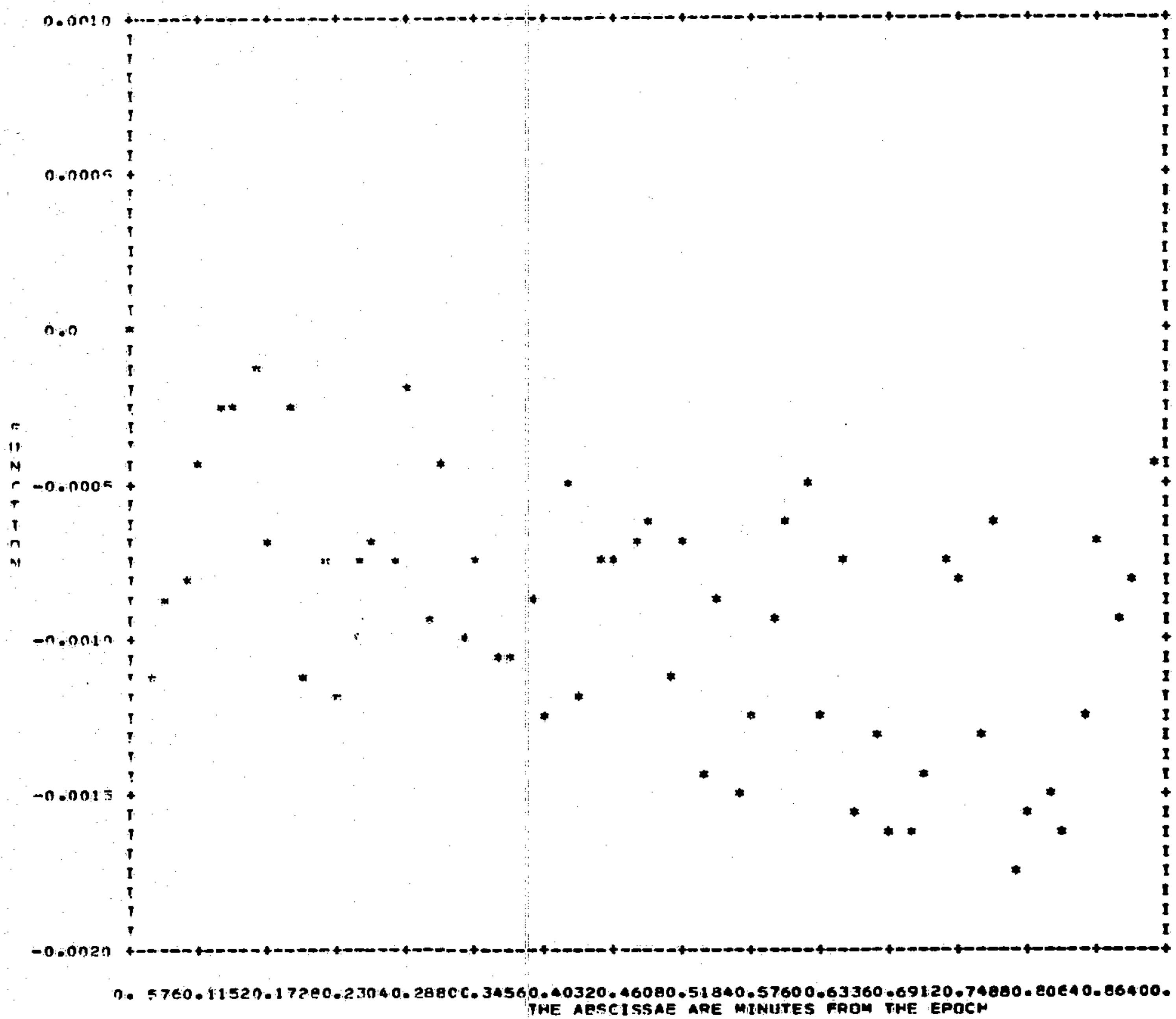

Figure 11f–Plot of Data from Comparison of Orbit 14 Minus Orbit 2 Mean Anomaly.

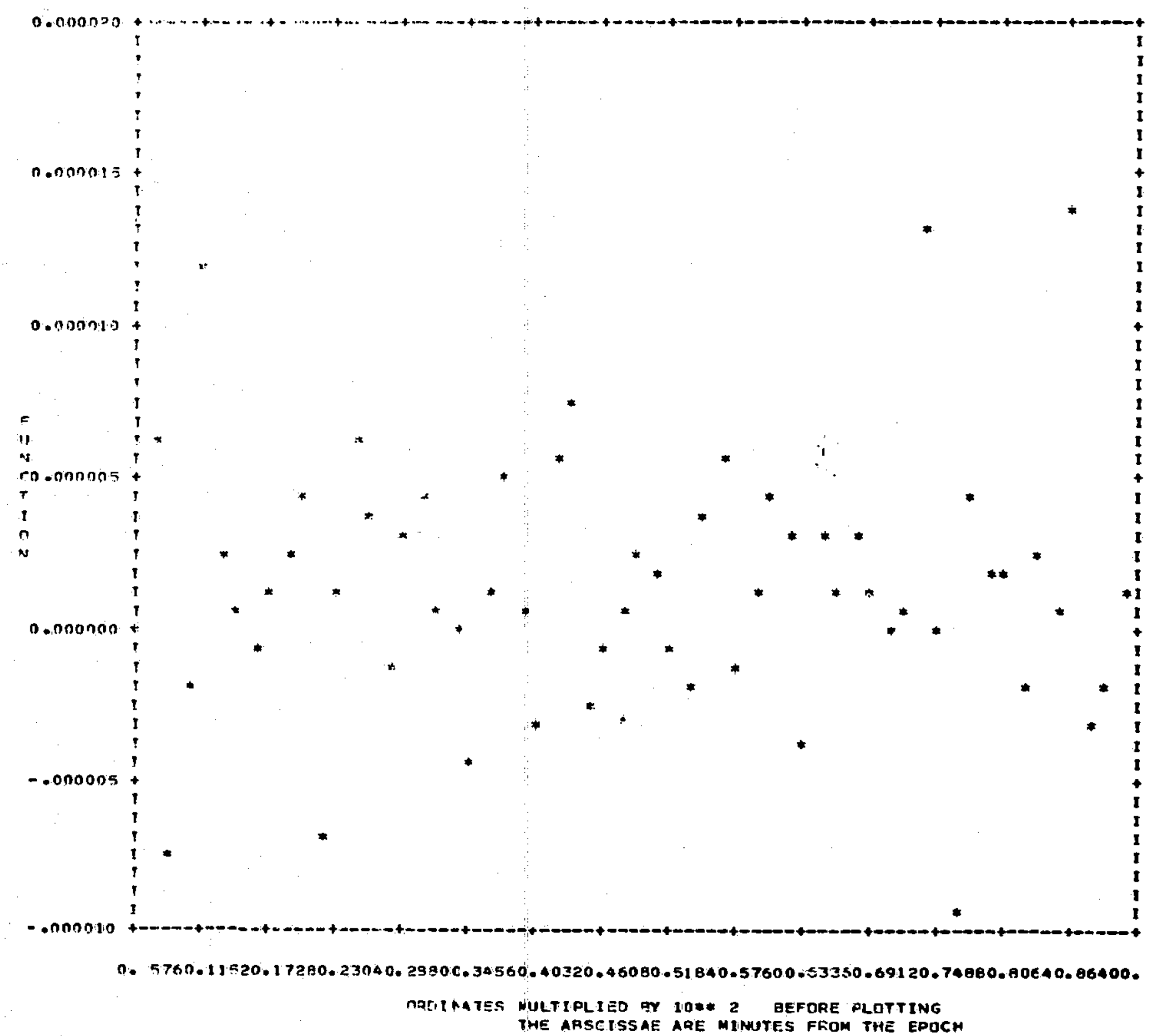

Figure 12a–Plot of Data from Comparison of Orbit 16 Minus Orbit 2 Semi Major Axis.

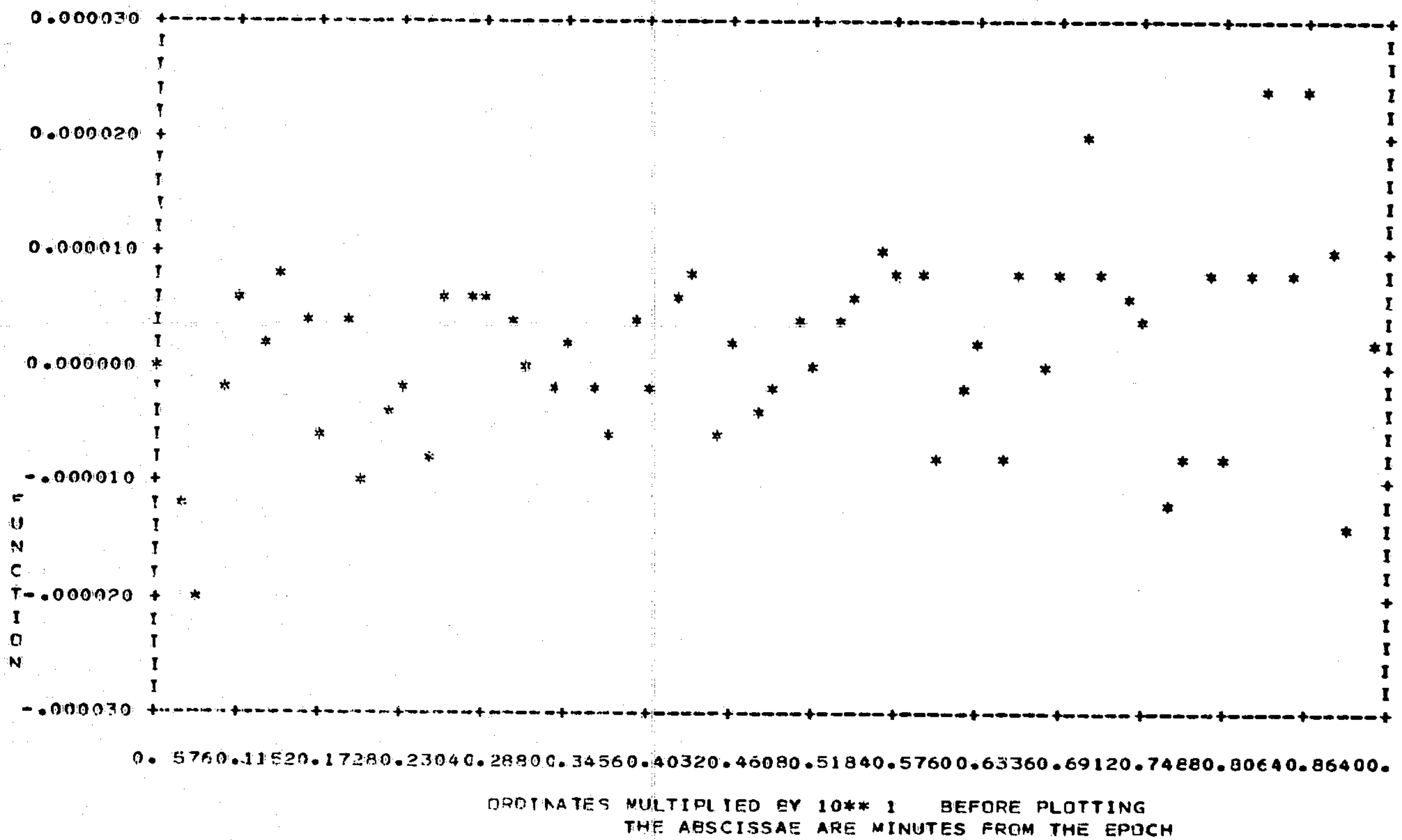

Figure 12b–Plot of Data from Comparison of Orbit 16 Minus Orbit 2 Eccentricity.

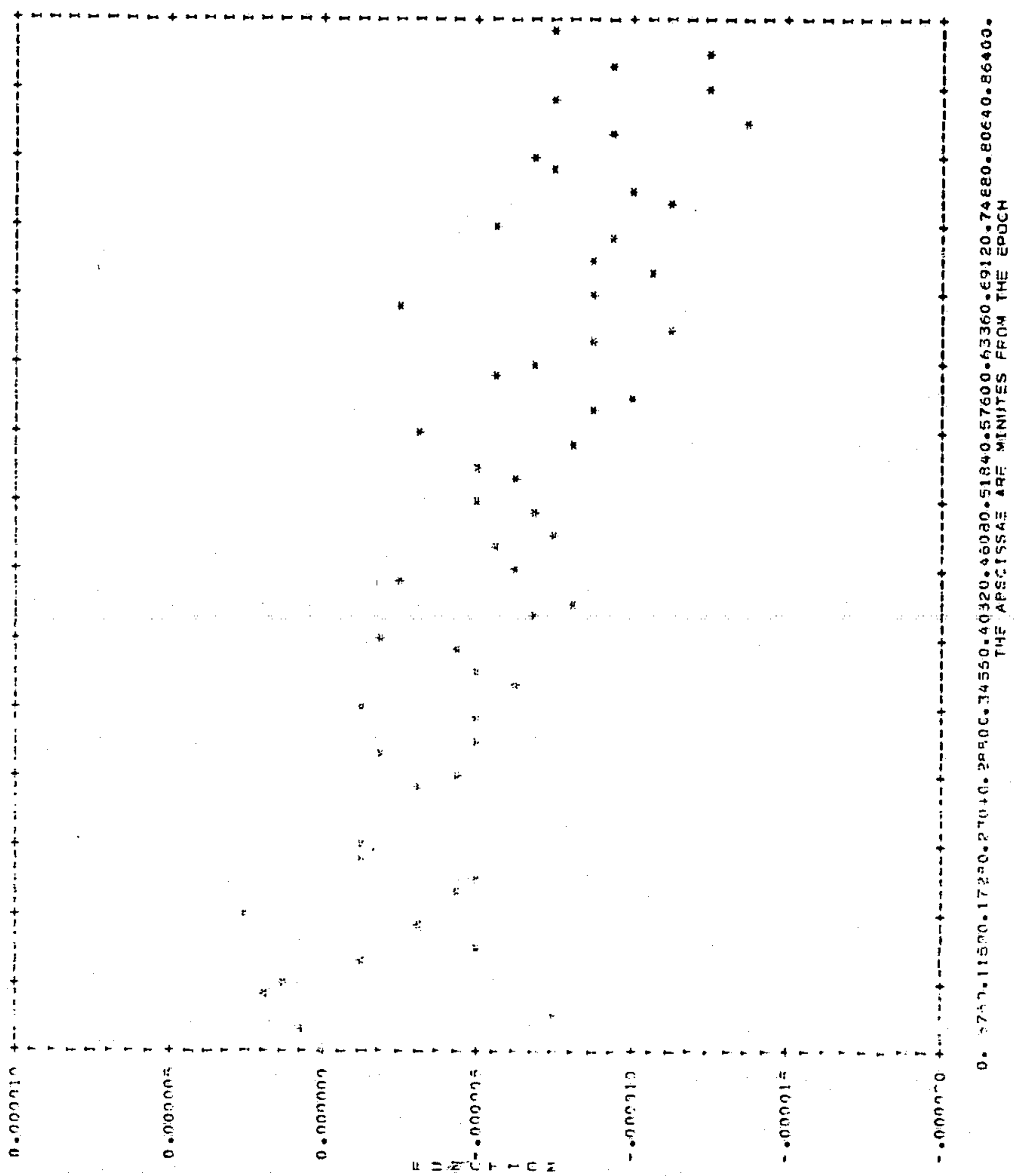

Figure 12c–Plot of Data from Comparison of Orbit 16 Minus Orbit 2 Inclination

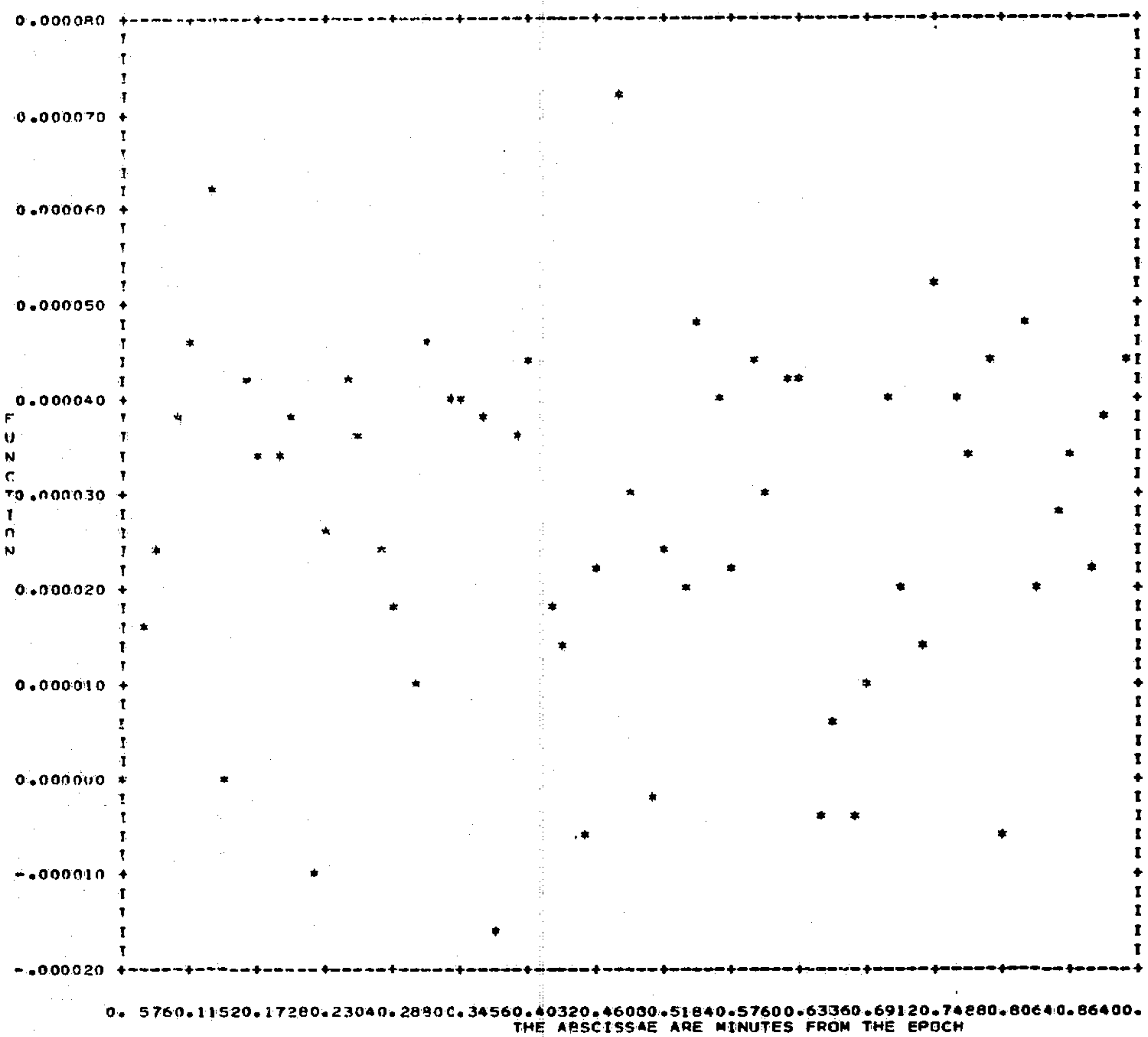

Figure 12d–Plot of Data from Comparison of Orbit 16 Minus Orbit 2 Right Ascension of Ascending Node.

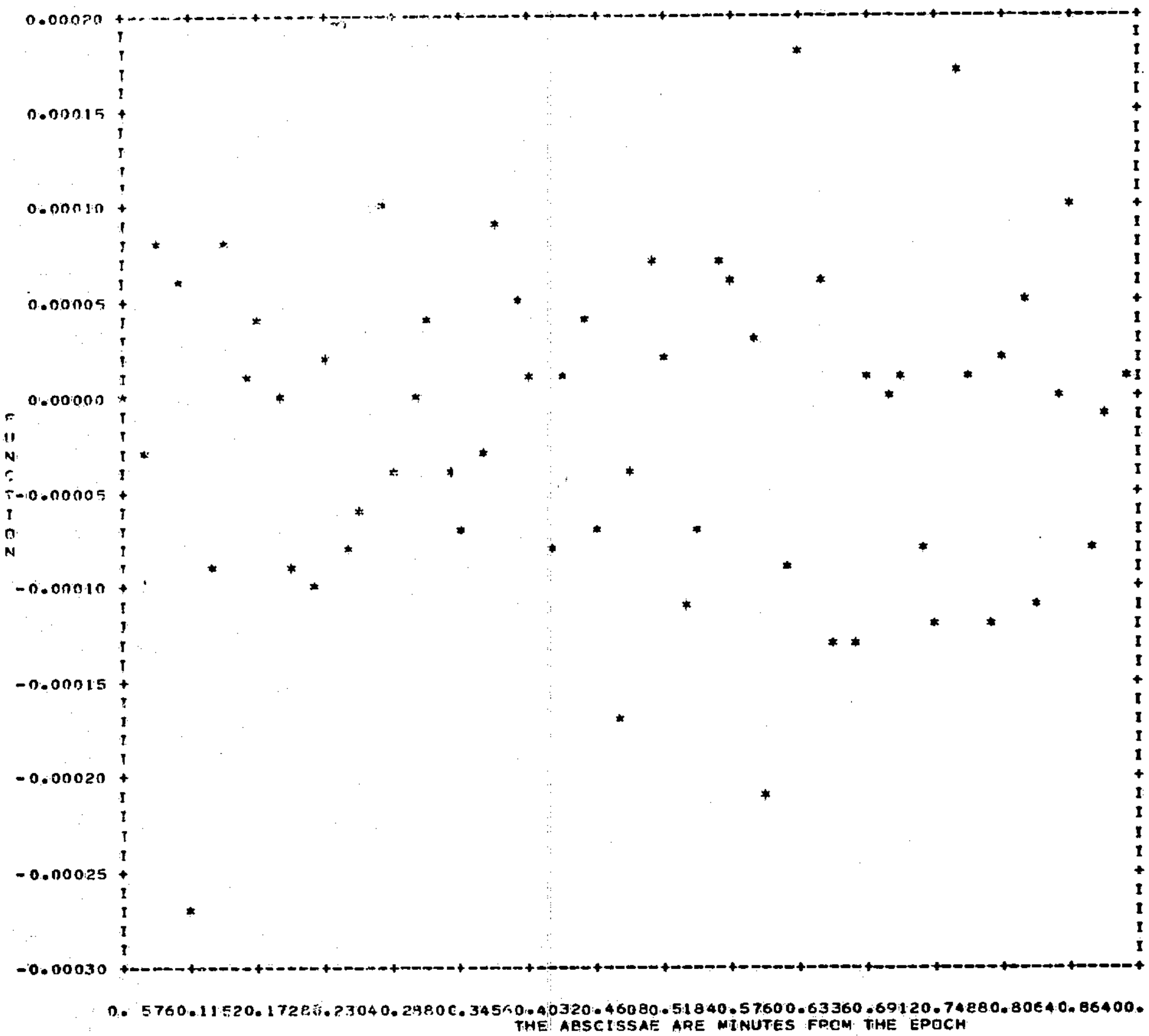

Figure 12e–Plot of Data from Comparison of Orbit 16 Minus Orbit 2 Argument of Perigee.

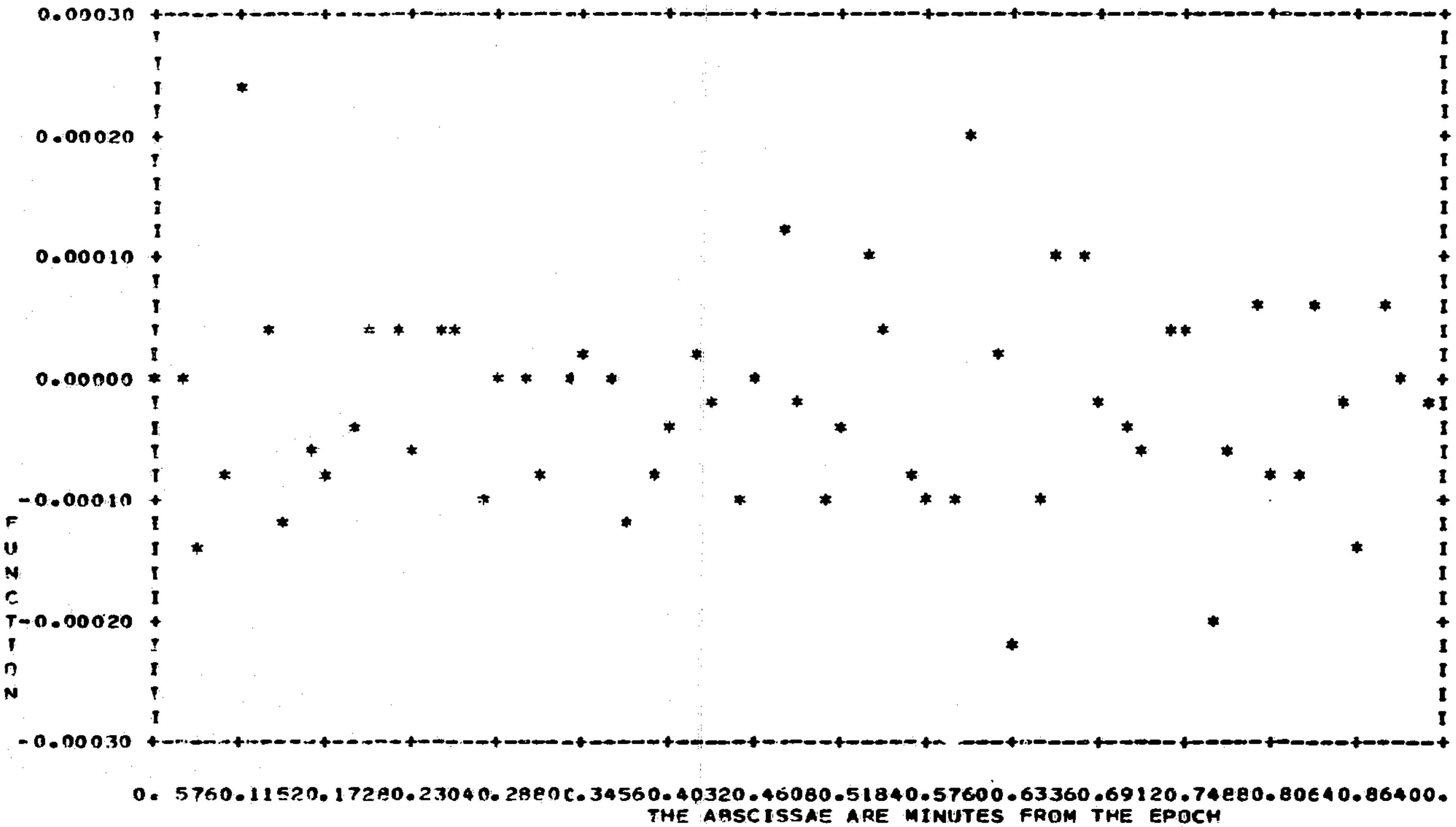

Figure 12f–Plot of Data from Comparison of Orbit 16 Minus Orbit 2 Mean Anomaly.